Durham E-Theses

Heavy quark fragmentation models

Nobary, Gomshi

How to cite:

Nobary, Gomshi (1989) *Heavy quark fragmentation models*, Durham theses, Durham University. Available at Durham E-Theses Online: http://etheses.dur.ac.uk/6499/

Use policy

HEAVY QUARK

FRAGMENTATION MODELS

M.A. Gomshi Nobary, BSc. and MSc. (Tabriz)

Department of Physics

Durham

A thesis submitted to the University of Durham

for the Degree of Doctor of Philosophy

April 1989

To the honor and memory of my parents

Batoul and Hussein

'The nice thing is that we must be content with the acknowledgement of the wonder. . .'

Einstein

ACKNOWLEDGEMENTS

ABSTRACT

We discuss the process of quark fragmentation placing a particular emphasise on the change of the fragmentation spectrum due to kinematical effects when light quarks are replaced by heavy ones. After investigating different methods of data extraction, we compile the data on heavy quark fragmentation from various collaborations. These data are compared with various models of heavy quark fragmentation for charm and bottom quark fragmentation. In our comparison we first separate the fragmentation models into two categories in accordance with their behaviour at large values of the fragmentation parameter. Models that are in agreement with the dimensional counting rules have a softer behaviour than some popular models which are not in agreement. This point is crucial in the case of heavier quarks. However, due to the large errors in experimental data, it is hard to make a firm judgement about the merits of these models.

We study the spin properties of heavy quark fragmentation and obtain the fragmentation functions for different polarisation states. The fragmentation function for an unpolarised state is then taken to be a combination of the longitudinal and the transverse fragmentation functions.

We also give a model in which the transverse momentum of the constituent quarks is taken into account. The effect of the increase in the constituent transverse momentum is to soften the fragmentation by a limited amount, since there is a small probabability that the constituents of a bound state will have a large relative momentum.

Finally we give a rather detailed Monte Carlo study of the effect of different fragmentation models on the momentum spectrum of heavy mesons, and the final state leptons resulting from heavy quark production in hadron colliders at CERN and FNAL. We find that the effect on the lepton spectrum is more significant.

CONTENTS

CHAPTER 1

INTRODUCTION

CHAPTER 2

EXPERIMENTAL STUDIES OF HEAVY QUARK FRAGMENTATION

CHAPTER 5

WAVEFUNCTION APPROACH TO
HEAVY QUARK FRAGMENTATION

CHAPTER 6

HEAVY MESON PRODUCTION AND THEIR
SEMILEPTONIC DECAYS

CHAPTER 7

SUMMARY

Appendix

LIST OF FIGURES

CHAPTER 1

CHAPTER 2

CHAPTER 3

CHAPTER 4

CHAPTER 5

CHAPTER 1

INTRODUCTION

A naive explanation of the quark-gluon structure of hadrons, confinement and hadronisation is given in this chapter. After introducing the process of quark fragmentation in electron-positron collision we give the definition of the fragmentation functions and a short explanation of their properties. It is emphasised that the process of fragmentation is one of the major problems of QCD, the best candidate for the theory of strong interactions. It is now clear that the soft and statistical behaviour of light quark fragmentation changes into a much harder process in the case of heavy quarks.

1.1 Quark-Gluon Structure of Hadrons

It was conjectured long ago that the observed 'elementary' particles are not really elementary at all. Already in the late forties Fermi and Yang[1] suggested that the the pion is a composite system of a nucleon and an antinucleon. In the early fifties the discovery of the K-meson and the hyperons give rise to models in which some particles were considered to be fundamental while others were regarded as composite systems. The best known model of this kind was that of Sakata[2] in which the proton, the neutron and the Λ-hyperon were chosen as fundamental particles. The Sakata model, and the scheme of unitary symmetry SU(3) which was built up on the basis of the fundamental p, n, Λ fields, led to a proper classification of the pseudoscalar and vector mesons, but faced difficulties with the description of baryons. The *Eightfold Way* which was suggested by Gell-Mann[3] and Ne'eman[4] provided the possibility of describing both the mesons and baryons. A splendid verification of this symmetry was the

1

experimental discovery of the Ω^- hyperon in 1964.

The idea of the quark structure of hadrons appeared first in the papers of Gell-Mann[5] and Zweig[6]. It was shown that the SU(3) octet symmetry may be realised on the basis of a fundamental triplet of some hypothetical particles, called 'quarks' by Gell-Mann, carrying fractional electric charge. We now have several compelling reasons to believe in this new layer of matter.

Firstly the large cross sections observed in deeply inelastic lepton-hadron scattering indicate that there is important structure at distance scales of less than 10^{-16} cm, whereas the overall proton electromagnetic radius is of order of 10^{-13} cm. It is found that, in processes involving large momentum transfer (e.g. $e^+e^- \rightarrow$ hadrons, ep $\rightarrow$eX, νp$\rightarrow$ νp, pp$\rightarrow$X, $p\bar{p}$ $\rightarrow$X, πp$\rightarrow$X, where X denotes an inclusive sum over final states), the hadrons appear to be made up of constituent 'partons' which are almost free. The angular dependence observed in these experiments suggests that the underlying charged constituents carry half-integer spin. These studies have raised the question of whether it is theoretically possible to have pointlike objects in a strongly interacting theory. Asymptotically free non-Abelian gauge interactions, of which QCD is an example, offer this hope (Perkins,1977).

Secondly, as we mentioned above, it was the success of the Eightfold Way which originally motivated the quark model. We now believe that the existence of two 'flavours' of low mass quarks coincides with the isospin symmetry of nuclear physics. Adding a somewhat heavier 'strange' quark to the theory gives rise to the multiplet structure in terms of representations of the group SU(3).

Thirdly, there is further evidence for compositeness in the excitations of the low-lying hadrons. Particles differing in angular momentum fall neatly into place on the famous 'Regge trajectories' (Collins and Squires, 1968). In this

way families of states group together as orbital excitations of some underlying system. The sustained increase of these trajectories with increasing angular momentum points toward strong long-range forces between the constituents.

Finally the idea of quarks became incontrovertible with the discovery of charmonium, the 'hydrogen atom' of elementary particle physics. The spectroscopy of the charmonium and upsilon families is admirably explained by non-relativistic potential models for their bound states of heavy quarks (Eichten *etal.* 1980).

Thus it seems that the quarks, originally introduced to construct the representations which describe hadronic spectra, have a deeper role as the actual constituents of hadrons. The established quarks are listed in Table (1.1).

Table(1.1) Quark flavours.

Flavour	Effective Mass	Charge
Up(u)	$0.3\ (GeV/c^2)$	+2/3
Down(d)	$0.3\ (GeV/c^2)$	–1/3
Strange(s)	$0.5(GeV/c^2)$	–1/3
Charm(c)	$1.5\ (GeV/c^2)$	+2/3
Bottom(b)	$5.0\ (GeV/c^2)$	–1/3
Top(t) ?	?	+2/3

Despite these successes of the quark model, an isolated quark has never been observed. Certainly these basic constituents of matter do not appear copiously as free particles emerging from present laboratory experiments. They manifest themselves only through their bound states, the baryons and mesons. The difficulty in producing individual quarks has led to the speculation that

they are completely confined. But how can we ascribe any reality to an object which cannot be produced? It is argued that gauge theories potentially possess a simple mechanism for giving constituents infinite energy when in isolation. In this picture a quark-antiquark pair will experience an attractive force which remains non-vanishing even for asymptotically large separations. This linearly rising long distance potential energy forms the basis of essentially all the models of quark confinement.

The confinement phenomenon makes the theory of the strong interactions qualitatively different from the theories of the electromagnetic and weak forces. The fundamental fields of the Lagrangian do not manifest themselves in free hadronic spectra. In the usual quark model baryons are bound states of three quarks. Because we do not observe free quarks, we are led to the conjecture that all the observable strongly interacting particles are colour singlet bound states of these fundamental constituents. Thus the gauge group should permit singlets to be formed from three objects in the fundamental representation. This motivates the use of colour SU(3) as the underlying group of the strong interactions.

1.2 QCD Lagrangian

To make a theory from the quark model it is necessary to describe how quarks interact and how they bind together. It is believed that quantum chromodynamics (QCD) is the unique theory able to explain these facts. QCD is a non-Abelian Yang-Mills (1954) gauge field theory, for the strong interactions, in which the gauge group is $SU(3)_c$ acting on the colour quantum number of the quarks. QCD implies that quarks interact through the 8 massless vector bosons of $SU(3)_c$. These are called 'gluons' and their interaction with the quarks is specified by the gauge principle. Each flavour of quark is taken to transform as

the fundamental representation, a triplet under SU(3)$_c$. The QCD Lagrangian is given by:

$$\mathcal{L} = \overline{\psi}(i\gamma^\mu \mathcal{D}_\mu - m)\psi - \frac{1}{2}tr(G_{\mu\nu}G^{\mu\nu}), \qquad (1.1)$$

where the spinor for the colour triplet quark of mass m is

$$\psi = \begin{pmatrix} q_{red} \\ q_{blue} \\ q_{green} \end{pmatrix}. \qquad (1.2)$$

The covariant derivative is

$$\mathcal{D}_\mu = \partial_\mu + igB_\mu, \qquad (1.3)$$

where g is related to the coupling constant by $\alpha_s = g^2/4\pi$ and B_μ is a three-by-three matrix in colour space formed from the eight colour gauge fields b_μ^l and the generators $\lambda^l/2$ of the SU(3) guage group as

$$B_\mu = \sum_{l=1}^{8} \frac{1}{2}\lambda^l b_\mu^l = \frac{1}{2}\lambda.b_\mu. \qquad (1.4)$$

The λ matrices are familiar from the study of flavour-SU(3) symmetry. These matrices satisfy

$$\left[\lambda^j, \lambda^k\right] = 2if^{jkl}\lambda^l, \qquad (1.5)$$

where f^{jkl} are structure constants of the SU(3) group. The field-strength tensor is

$$G_{\mu\nu} = \sum_l \frac{1}{2}G_{\mu\nu}^l \lambda^l = \frac{1}{2}G_{\mu\nu}.\lambda$$

$$= (ig)^{-1}\left[\mathcal{D}_\nu, \mathcal{D}_\mu\right] = \partial_\nu B_\mu - \partial_\mu B_\nu + ig\left[B_\nu, B_\mu\right]. \qquad (1.6)$$

5

It may be written in component form as

$$G^l_{\mu\nu} = \partial_\nu b^l_\mu - \partial_\mu b^l_\nu + g f^{jkl} b^j_\mu b^k_\nu. \tag{1.7}$$

The quark-gluon interaction term in the QCD Lagrangian is

$$\mathcal{L} = -\frac{g}{2} b^l_\mu \overline{\psi} \gamma^\mu \lambda^l \psi \tag{1.8}$$

which leads at once to the Feynman rules for the quark-antiquark-gluon vertex.

1.3 Asymptotic Freedom and Confinement

In the theory of strong interactions a fundamental difficulty exists in describing the behaviour of quarks and gluons at large distances (or low energies). Here the confinement is strong and so perturbation theory is no longer applicable and non-perturbative models must be introduced to describe the processes of quark or gluon conversion into hadrons (called 'hadronisation'). Thus in the process $e^+e^- \to$ hadrons the cross-section for e^+e^- annihilation into quarks and gluons is calculated using an appropriate order of perturbative QCD, but the subsequent transformation into hadrons at large distances has to be described by a phenomenological model. A commonly accepted mechanism for the latter process is that the coloured quarks and gluons which are created at small distances fly apart stretching the colour lines of force between them. Through the colour polarisation of the vacuum they then transform into jets of colourless hadrons, which have only a restricted transverse momentum with respect to the hadronisation direction, and with a flavour dependent distribution of longitudinal momentum (see figure (1.1)).

The situation is well demonstrated by looking at the momentum (or,
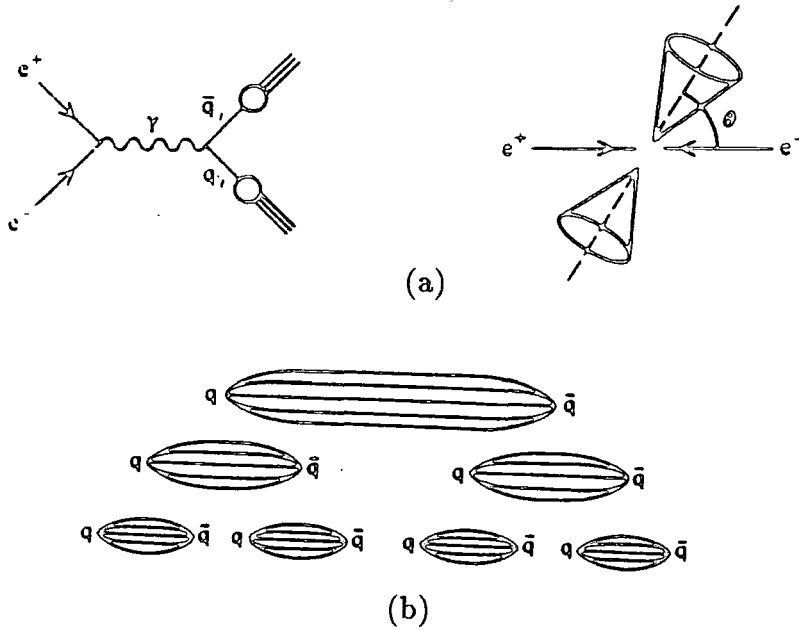
Figure (1.1) . a) Conversion of e^+e^- into two jets of hadrons, and b) lines of force between a quark and an antiquark. When the quarks move away from each other, the breaking of the string is accompanied by further quark-antiquark pair production.

equivalently, position) dependence of the running coupling of the theory.

In the leading log approximation of perturbation theory the running coupling is given by[7]

$$\alpha_s(Q^2) \simeq \frac{1}{(\frac{b_0}{2\pi})\log\left[\frac{Q^2}{\Lambda^2},\right]} \qquad (1.9)$$

with

$$\Lambda^2 \equiv \mu^2 \exp(-4\pi/(\alpha_s b_0)),$$

where μ^2 is the value of Q^2 at which $\alpha_s(Q^2)$ is measured, and $b_0 \equiv \frac{11}{3}N_c - \frac{2}{3}N_f$, where N_c is the number of colours and N_f is the number of flavours of the quarks.

Equation (1.9) has the important consequence that $\alpha_s(Q^2) \to 0$ as $Q^2 \to \infty$ which means that quarks and gluons appear like almost free particles when probed by high momentum transfer. This is known as 'asymptotic freedom' (see figure (1.2)). The other important consequence of (1.9) is that when $Q^2 \to \Lambda^2$, it is seen that $\alpha_s(Q^2) \to \infty$ and so the perturbation series breaks down at small Q^2. Taking the Fourier transform of (1.9) it follows that

$$\alpha_s(r) \simeq \frac{1}{\frac{b_0}{2\pi} \log\left[\frac{1}{\Lambda r}\right]}. \qquad (1.10)$$

As we can see from (1.10), the coupling becomes stronger as the separation between quarks increases and the perturbation series breaks down as $r \to \Lambda^{-1}$. This is because of the gluon self-coupling which implies that the exchanged gluons will attract each other and so the colour lines of force are constrained to a tube-like region between the quarks (see figure (1.2)).

If this tube has a constant energy density per unit length, then the potential energy of the interaction will increase with the separation, $V(r) \sim \lambda\, r$, and so the quarks and gluons can never escape from the hadrons. This 'infarared slavery' is believed to be the origin of the confinement of quarks and gluons inside colour-less hadrons and explains why we do not observe free quarks (Feynman 1972, Dokshitzer 1980). Now we can explain what happens to the quarks in a hadron after they have been struck hard, by say an electron in a typical deep inelastic scattering event. The struck quark attempts to leave the hadron, but then the colour lines of force get stretched into a tube until the potential energy of the colour field is sufficient to create a $q\bar{q}$ pair which serve as the ends of shorter flux tubes. The out-going quark continues on its way, stretching the lines of force, and further $q\bar{q}$ pairs are produced, until eventually all of its kinetic
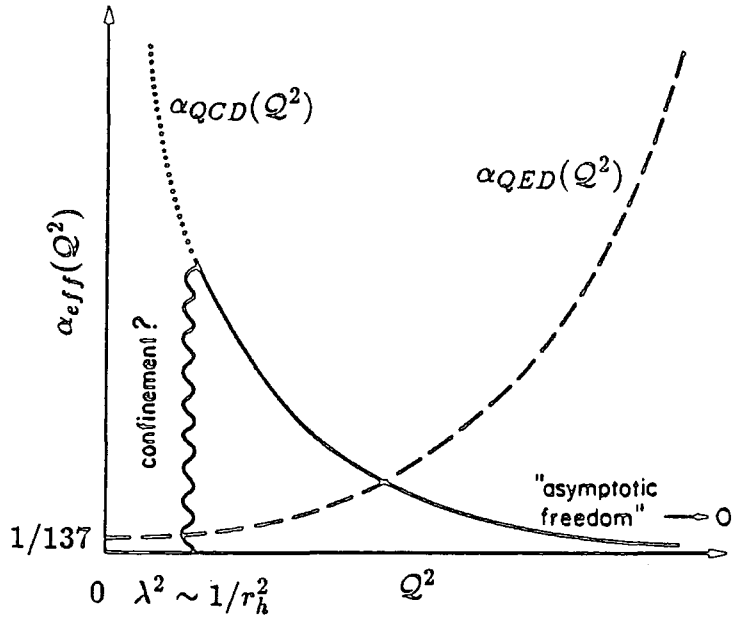
Figure (1.2) . Q^2 *dependence of the effective (running) coupling shown for QED and QCD. Confinement occurs as $Q^2 \rightarrow \Lambda^2 \approx 1/r_h^2$ where r_h is the hadronic radius.*

energy has been changed into clusters of quarks and gluons, each of which has zero net colour and low internal momentum. These clusters can form hadrons since now $\alpha_s(Q^2) \geq 1$, and so the energy given to the struck quark finally manifests itself as a 'jet' of hadrons travelling more or less in the direction of the original struck quark.

1.4 Colliding Beams: $e^+e^- \rightarrow$ Hadrons

In a colliding beam reaction one first of all presumes that the e^+e^- system annihilates through a virtual photon into a quark-antiquark pair. Then just after the collision, one has a free quark and antiquark which begin to recede from each other. What happens next is less clear, but at much later times the quark and antiquark have been replaced by a system of hadrons. At large Q^2 one can write

9

$$\sigma(e^+e^- \to \text{hadrons}) = \sum_{i=udsc...} \sigma(e^+e^- \to q_i\bar{q}_i)$$

$$= 3\sum_i e_i^2 \sigma(e^+e^- \to \mu^+\mu^-) \qquad (1.11)$$

where e_i is the charge of quark i (in units of e) and 3 represents the number of colours. Hence

$$R \equiv \frac{\sigma(e^+e^- \to \text{hadrons})}{\sigma(e^+e^- \to \mu^+\mu^-)} = 3\sum_i e_i^2. \qquad (1.12)$$

As $\sigma(e^+e^- \to \mu^+\mu^-)$ is well known, a measurement of the total e^+e^- annihilation cross section into hadrons therefore directly counts the number of quarks, their flavours, as well as colours.

Equation (1.11) is based on the process $\sigma(e^+e^- \to q\bar{q})$ in leading order. However, one should also include the contributions from diagrams where quarks and antiquarks radiate gluons. To $O(\alpha_s)$ the result in (1.12) is then modified to

$$R = 3\sum_i e_i^2 \left(1 + \frac{\alpha_s(\mathcal{Q}^2)}{\pi}\right) \qquad (1.13)$$

That is to say, the scaling result (1.12), according to which R is independent of $\mathcal{Q}^2$, is violated logarithmically through the $\log \mathcal{Q}^2$ behaviour of α_s.

1.5 Fragmentation Functions

Consider the hadronisation of a quark into a particular hadron h in e^+e^- annihilation. In the parton model the corresponding differential cross-section can be written as

$$\frac{d\sigma}{dz}(e^+e^- \to hX) = \sum_q \sigma(e^+e^- \to q\bar{q})\left[D_q^h(z) + D_{\bar{q}}^h(z)\right],$$

$$= \left(\frac{4\pi\alpha^2}{3s}\right) 3 \sum_q e_q^2 \left[D_q^h(z) + D_{\bar{q}}^h(z) \right] \qquad (1.14)$$
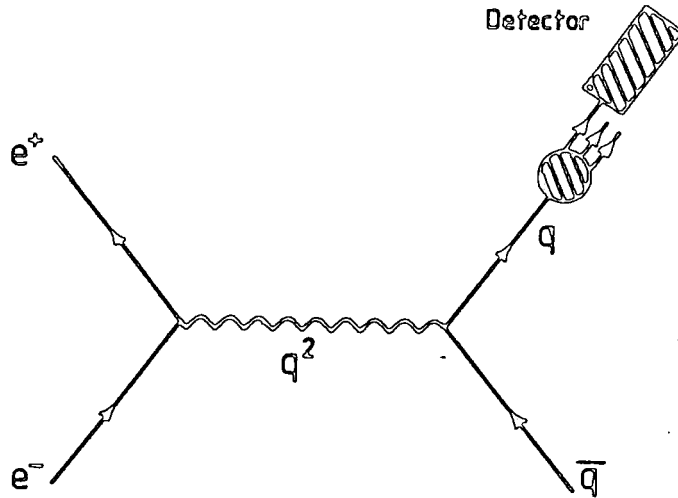
Figure (1.3) . *A hadron h observed with a fraction z of the quark's energy momentum.*

which describes figure (1.3) as two sequential events;

a) Production of a $q\bar{q}$ pair, followed by

b) Hadronisation of either the q or $\bar{q}$ to produce the detected hadron h. The D functions therefore represent the probability that the hadron h is produced by q (or $\bar{q}$), and carries a fraction z of its energy-momentum. In general z is defined as

$$z \equiv \frac{(E + p_{\parallel})_{meson}}{(E + p_{\parallel})_{quark}}, \qquad (1.15)$$

where $p_{\parallel}$ represents the longitudinal momentum along the jet axis.

The fragmentation functions are subject to constraints imposed by momentum and probability conservation:

11

$$\sum_h \int_0^1 z D_q^h(z) dz = 1 \qquad . \qquad (1.16)$$

$$\sum_q \int_{z_{min}} \left[D_q^h(z) + D_{\bar{q}}^h(z) \right] dz = n_h, \qquad (1.17)$$

where z_{min} is a measure of the threshold energy for producing a hadron of mass m_h and n_h is the avarage multiplicity of hadrons of type h. Charge conservation requires that

$$\sum_h e_h \int_0^1 \left[D_q^h(z) - D_{\bar{q}}^h(z) \right] dz = e_q. \qquad (1.18)$$

Equation (1.16) simply states that the sum of the energy of all hadrons is the energy of the parent quark. Clearly the same relation holds for $D_{\bar{q}}^h(z)$. Equation (1.17) says that the number n_h of hadrons of type h is given by the sum of probabilities of obtaining h from all possible parents, namely from q or $\bar{q}$ of any flavour.

Taking the ratio of (1.14) and (1.11) we find

$$\frac{1}{\sigma} \frac{d\sigma}{dz}(e^+ e^- \to hX) = \frac{\sum_q e_q^2 \left[D_q^h(z) + D_{\bar{q}}^h(z) \right]}{\sum_q e_q^2}. \qquad (1.19)$$

So the inclusive cross section $\frac{d\sigma}{dz}$, divided by σ the total annihilation cross section into hadrons, is predicted to scale. Note that σ and $\frac{d\sigma}{dz}$ depend on the annihilation energy.

The picture of a quark (q) fragmenting into a hadron (h) is illustrated in figure(1.4) in terms of perturbation theory. Therefore in higher order QCD the $D_q^h(z)$ functions are scale dependent. In leading log approximation the scale dependence of the fragmentation functions is obtained from the following expression,
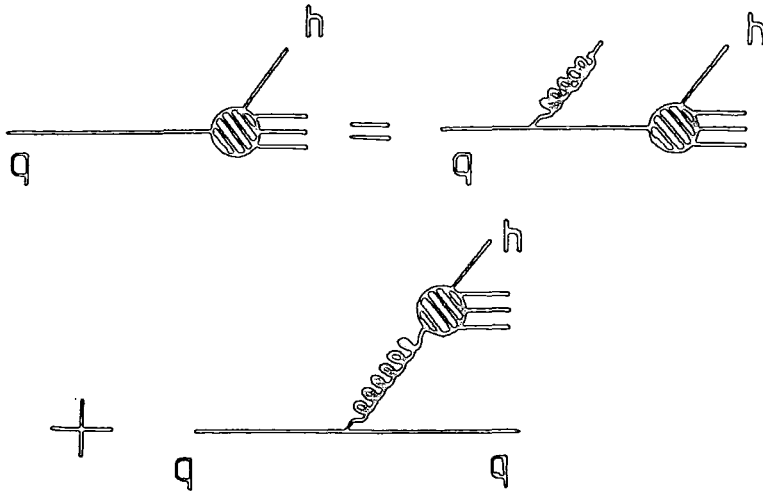
Figure (1.4) . *Quark fragmentation with the final hadron coming either from the further fragmentation of the original quark after gluon emission or from the fragmentation of the emitted gluon.*

$$\frac{\partial}{\partial t} D_q^h(z,t) = \frac{\alpha_s(t)}{2\pi} \int_z^1 \frac{d\eta}{\eta} \Big[P_{q\to q}(\eta) D_q^h(\frac{z}{\eta},t) + P_{q\to G}(\eta) D_G^h(\frac{z}{\eta},t) \Big], \qquad (1.20)$$

where $t \equiv \ln \; \mathcal{Q}^2/\Lambda^2$ and there is an implicit sum over quark flavours. The functions $P_{q\to q}$ and $P_{q\to G}$ describe how the momentum is shared amongst the quark and the gluon. However, since we are interested in heavy meson production through heavy quark fragmentation, the second step in figure (1.4) is automatically disregarded. The effect of initial gluon radiation will be considered separately in chapter 3. Unless otherwise stated, the fragmentation functions in this work will only contribute to the production of the hadron which contains the original heavy quark.

1.6 Reciprocity

In certain limits one can establish a relation between the structure and

the fragmentation functions. Consider the fragmentation of a hadron h from a quark q, with the probability of $D_q^h(z)$ (see for example figure (1.3)). This process could be related to the diagram of figure (1.5) by crossing. Therefore the probability of the transition $q \to h$ with $p_h = z p_q$ is equal to the probability of hadron h containing q with $p_q = x p_h$ (x being the Feynman parameter). This requires
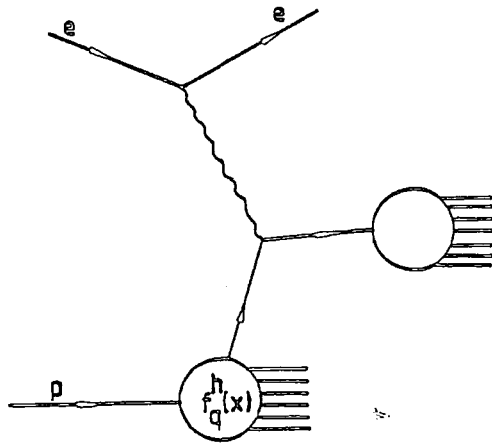
Figure (1.5) . *Deep inelastic electron scattering.*

$$D_q^h(x) \sim x f_q^h(1/x), \qquad (1.21)$$

with

$$x = 1/z. \qquad (1.22)$$

As D's and f's are probabilities, this procedure ignores interference effects but it is expected that the contribution of other diagrams will be small as x and z approach unity.

1.7 Dimensional Counting Rules

The dimensional counting rules describe the behaviour of a cross section at large Q^2. In the limit of $x \to 1$ (x is the usual Feynman parameter) one would have a single parton carrying all the momentum of the hadron, but this is clearly impossible and so the structure function must vanish. As this limit is approached all the other spectator quarks must have vanishing momentum and hard gluon exchanges are needed to transfer their momentum to the fast quark. In the case of a proton for example the structure function behaves like

$$f(x) \sim Q^2 \left[G(Q^2) \right]^2 \sim (1-x)^{4-1} \simeq (1-x)^3, \qquad (1.23)$$

since $Q^2 \sim 1/(1-x)$. Here $G(Q^2) \sim Q^{-4}$ is the form factor of the proton. This result is the dimensional counting rule for the behaviour of the structure functions and is expressed more generally as [8]

$$f(z) \sim (1-z)^{2n_s - 1} \qquad (1.24)$$

in the limit of $z \to 1$, where n_s is the minimum possible number of spectator partons. Thus for a quark q fragmenting into a meson M we have $n_s = 1$ if M contains q and $n_s = 3$ if it does not; see figure (1.6).

As $z \to 1$ the hadron takes all of the parton's momentum so any other partons which are left behind in the hadronisation must have negligible momentum. Hence

$$D_q^h(z) \sim (1-z)^{2n_s - 1}, \qquad (1.25)$$

in the limit $z \to 1$.

Similarly as $z \to 0$ the essentially massless hadron take none of the par-
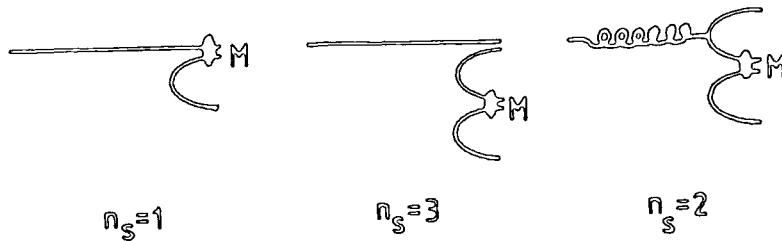
Figure (1.6) . *The minimum number of spectators, n_s, accompanying the fragmentation of partons into a meson M.*

ton's momentum and so we expect $D(z) \sim z^{-1}$, which gives a logarithmic increase of n_h in (1.17). Thus we may expect that

$$D_q^h(z) \sim z^{-1}(1-z)^{2n_s-1}. \tag{1.26}$$

1.8 Quark Fragmentation Models

There are three main types of fragmentation models. We will describe them in order of increasing sophistication starting with independent jet fragmentation. The more sophisticated models, the string and the parton shower models, have more physical insight built into them, and consequently have fewer arbitrary parameters.

a) Independent Jet Fragmentation

The model of Field and Feynman [9] is the prototype of the Independent Jet Model. This model has been one of the most successful and frequently used approaches to jets. It is assumed that each individual parton fragments independently (Figure (1.7)). All the energy of the parton is used up so no more hadronisation can occur. Although the model accomodates a wide range

of data, it has some inherent problems.

i) The basic property of colour confinement is not even conceptually included in the model. The single parton although coloured, has no relation to its compensating partner.

ii) Energy and momentum are not conserved. The primary parton with a typical mass of 300 MeV evolves into jets with masses of 4-5 GeV.

iii) The result is not Lorentz invariant since the fragmentation depends on the energy of the quark.

Some of these flaws can be overcome by joining the individual jets and reshuffling their energy, momentum and quantum numbers. There have been attempts to extend this model to $e^+e^- \rightarrow q\bar{q} \, g$ [10], to baryon production [11] and to implement hard QCD corrections.
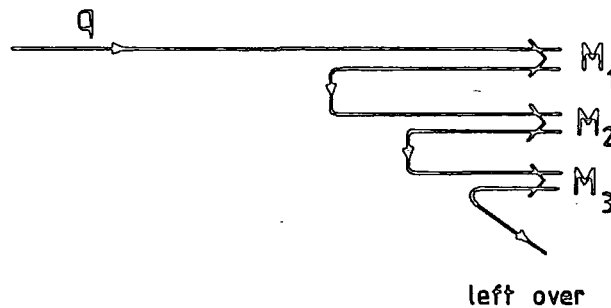
Figure (1.7). *Independent jet fragmentation.*

b) Colour String Model

This was first described by Artru and Mennessier in a (1+1) dimensional model[12]. It has turned out to be a most successful and popular description of jet properties. Through originally developed for e^+e^- interactions it has been

applied to jets in various types of processes like leptoproduction or hadron-hadron collisions. The string concept has evolved into a large system of computer programs mainly due to the work of the Lund group [13]. In contrast to the Independent Jet Model it is not the individual partons that fragment but a colour neutral system stretching between the partons. Hadronisation is viewed as the break up of a string built up by the colour fields as the two quarks fly apart. As we have seen, the linearity of the Regge trajectories, the potentials of quarkonia, and other measurments, suggest a linear rise of the colour potential with increasing distance between sources.

Compared to the Independent Jet Model the string approach has some attractive features.

i) Although not calculable from the fundamental theory its basic assumptions agree better with the general ideas of QCD and quark and gluon couplings.

ii) Energy, momentum and flavour are conserved at each step of the fragmentation process. This conservation is more easily included in the string scheme since at each step the whole massive system is considered whereas in the Independent Jet Model only part of it is treated. Only the last step requires a special procedure for conserving energy and momentum to ensure that the particles acquire the correct mass.

iii) Related to this is the smooth joining of the two jets. Whereas in the Independent Jet Model the energy, momentum, and flavour of each jet are not required to. fulfill the conservation laws at the end of the fragmentation, they are naturally conserved in the Lund Model. Thus no artificial procedure has to be applied to join the final partons to form a hadron.

In spite of these conceptual differences of the two approaches they lead to very similar results for events of the type $e^+e^- \rightarrow q\bar{q}$ since their parameters

can be suitably adjusted.

c) QCD Cascade Models

If the parton which starts the jet formation has a large momentum, and is also far off its mass shell (Q^2 large), then initially perturbative QCD is applicable. The partons branch repeatedly via QCD vertices producing many partons of lower momentum which are less far off mass shell; whose momentum and distance from mass shell decrease with each successive branching. Eventually, a point $Q^2 = Q_o^2$, related to Λ^2, is reached where QCD running coupling constant is no longer small and one needs a non-perturbative model for hadronisation. These two stages of jet evolution are shown in figure (1.8).

1.9 Light and Heavy Quark Fragmentation

Light and heavy quarks are distinguished by comparing their masses with the scale of the strong interaction, Λ. The approximate masses of the quarks are given in table (1.1). The fact that Λ lies within the range of 0.1 and 0.5 GeV, makes it clear that while u, d and presumably s quarks may be accounted as light quarks, c, b and t quarks must be treated as heavy.

The fragmentation of light and heavy quarks exhibit quite different features. There are two reasons for this. First, a charmed meson, for example, can only come from a leading c quark and not from further down the fragmentation chain because the production of a heavy $Q\overline{Q}$ pair in the vaccum is very improbable. Secondly, the fragmentation $c \rightarrow Dd$, for instance, puts a much greater fraction of the quark's energy into the meson that does the fragmentation $u \rightarrow \pi d$. The π and ρ mesons, for example, are made of light quarks and their hadronisation exhibits a statistical behaviour. Figure (1.9) shows the

jet initiating

Parton

Hadronization Process

Hadrons

$Q^2 > Q_o^2$

$Q^2 < Q_o^2$
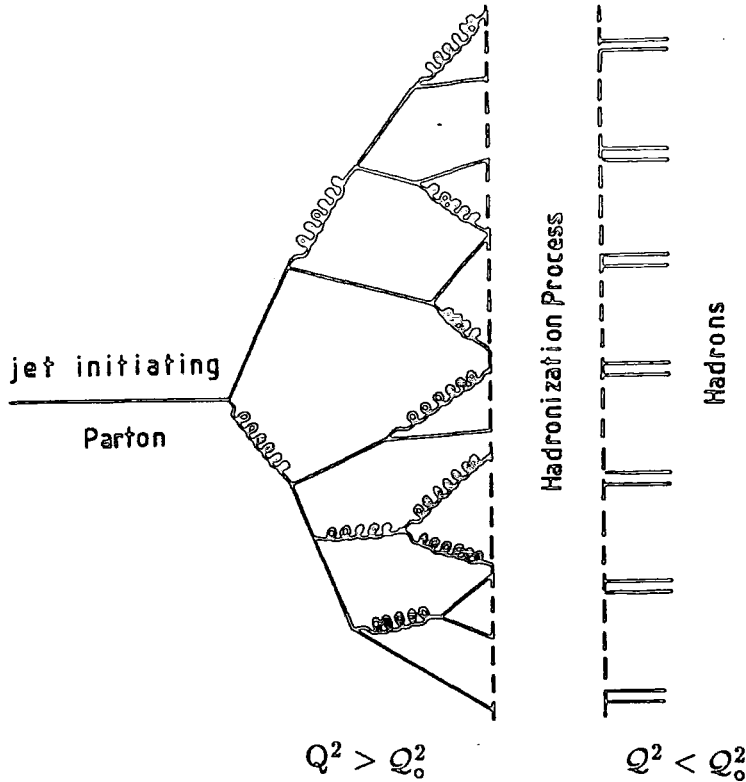
Figure (1.8). *The perturbative $(Q^2 > Q_o^2)$ and non-perturbative $(Q^2 < Q_o^2)$ stages of jet evolution.*

differential cross-section for the production of π^o and ρ^o and of K^o and K^{*o} mesons[14]. (The curves are due to the Lund group[15]). The softness of the fragmentation process is striking. As we shall see the case of charm and bottom quark fragmentation is quite different.

The first theoretical attempt to explain the enormous difference in hadronic production by a heavy quark was made by Bjorken[16]. Bjorken used the naive quark parton model to describe the production and decay dynamics of a very heavy quark Q in $e^+e^- \rightarrow Q\overline{Q}$ two jet system. He deduced that the inclusive distribution (dn/dz) of the produced hadron containing Q should be
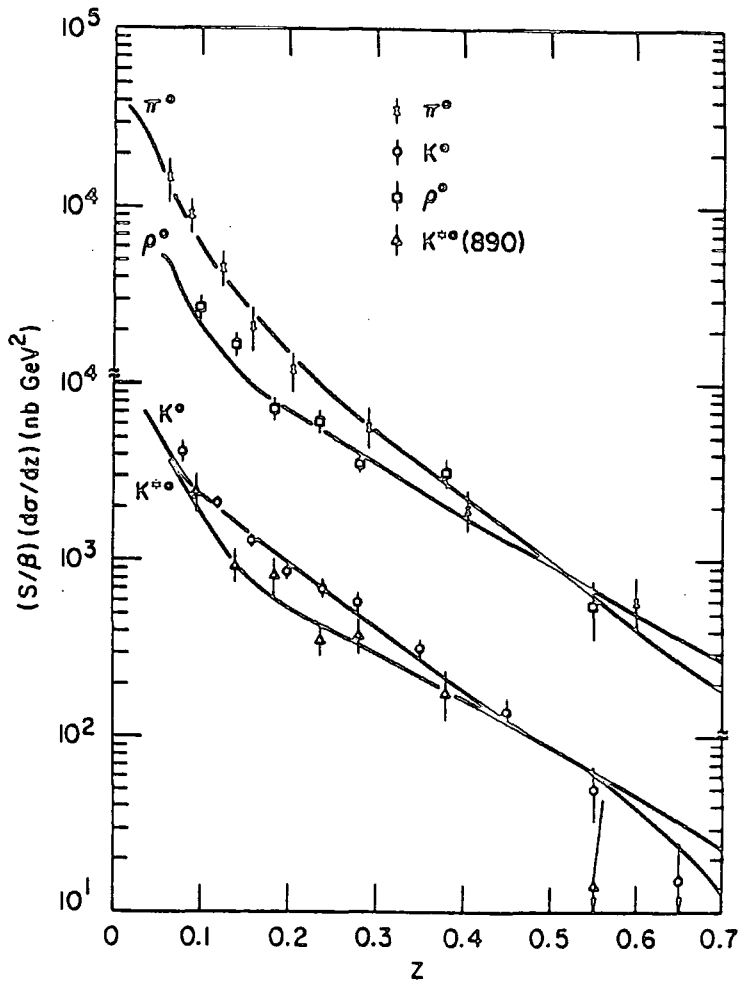
Figure (1.9) . *Vector and pseudoscalar, $\pi^\circ, \rho^\circ, K^\circ$ and $K^{*\circ}$ fragmentation.*

peaked near $z = 1$ (here $z \equiv p/p_{max}$).

Another early attempt to describe the situation where a heavy hadron carries away most of the parton's momentum leaving behind a spectrum of light hadrons (such as π's or K's) was made by Suzuki [17]. The distribution function dn/dx (here x is defined as the ratio of the energies of the produced hadron to that of the beam) is calculated using statistical assumptions. Taking the center of mass energy $\sqrt{s} = 2E$ to be much larger than any of the quark or hadron masses involved, the following result is obtained:

$$D(x) = dn/dx = C \exp\left[-\frac{1}{2}\kappa M_q(x + \frac{m_h^2}{M_q^2}\frac{1}{x})\right], \qquad (1.27)$$

where C is a constant, κ is related to temperature as $\kappa = (kT)^{-1}$, M_q is the invariant mass of the fireballs containing q and $\bar{q}$ $(M_q = m_q + Q)$ and m_h are the quark and hadron masses respectively. $D(x)$ is identified with the fragmentation function. The distribution given by (1.27) has a peak at $x = m_h/M_q$, and falls rapidly as $x \to 0$ and 1. The temperature is taken to be of the order of m_π as is deduced from various lepton-hadron and hadron-hadron collisions. The behaviour of (1.27) for π and K meson production, and also for the production of D and π from a charm quark, and π from u and d quarks, is shown in figure (1.10). These diagrams, together with the figure (1.9), demonstrate the change of the nature of the fragmentation as one increases the quark mass. It is generally accepted that this change is mainly for kinematical reasons.

1.10 Conclusion

Although the quark model seems to be quite successful in explaining the strong interaction phenomena, the mechanism of quark and gluon fragmentation is far less well understood. It is only possible to describe the situation through fragmentation functions, which are mainly calculated from phenomenological models. The most sophisticated model, and the one which has the most physical insight, is the QCD cascade model. However, as the early works of Suzuki and Bjorken show, in the hadronisation process a heavy hadron tends to carry away most of the quark's momentum leaving the light hadron spectrum softer than that which is obtained from light quarks. Naturally this changes the final hadron production spectrum dramatically and opens a new door to the investigation of heavy quark fragmentation.
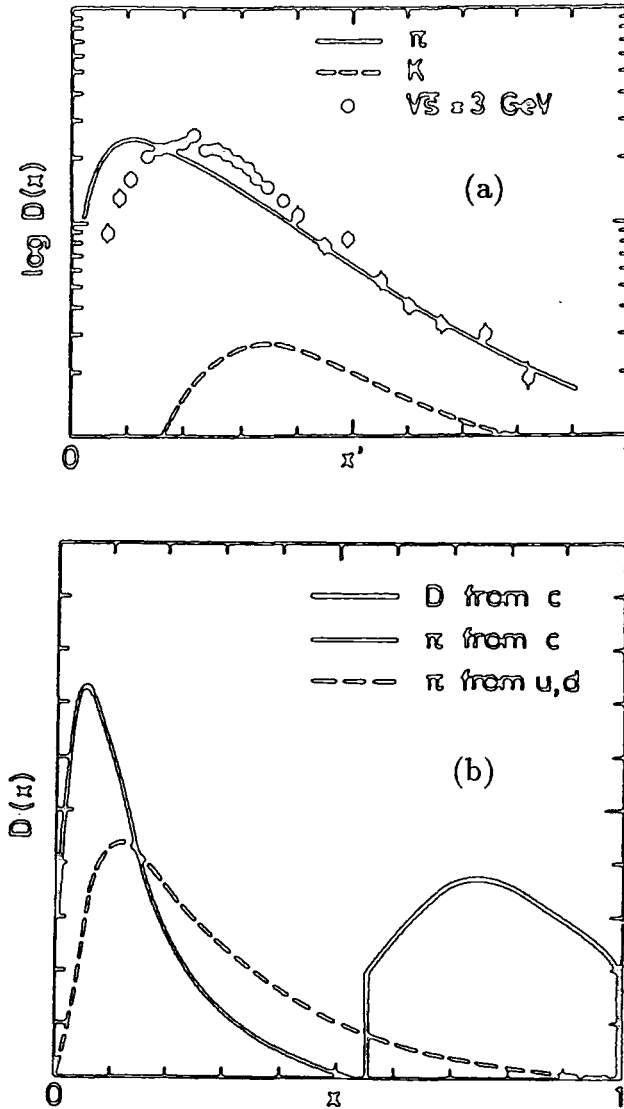
Figure (1.10) . *The fragmentation function (1.27) for (a) π and K meson fragmentation, (b) for D mesons coming from charm, and π meson from c, u and d quarks, respectively*[17] .

23

CHAPTER 2

EXPERIMENTAL STUDIES OF HEAVY QUARK FRAGMENTATION

During the last few years a number of e^+e^- annihilation experiments have reported results on the fragmentation of heavy quarks using a variety of methods. Although a wealth of information has been extracted from these experiments, comparison of the results among themselves, and with the theoretical predictions, is difficult because of the variety of experimental techniques employed and the different definitions of the fragmentation parameters which have been used. Therefore it is necessary to explore the experimental procedures and particularly to appreciate the experimental uncertainities and the influence of QCD effects such as radiative corrections.

In this chapter we explain the use of different fragmentation parameters and review the main experimental procedures employed to establish the relationship between the fragmentation mechanism and the experimentally observed quantities. Having explored these procedures, we evaluate their outcome for charm and bottom fragmentation, both in terms of the mean value of the fragmentation parameters and the fragmentation functions themselves. We summarise these results and look at different sources of errors and discuss the possible outlook for improving them.

2.1 Background and Definitions

Elementary particle reactions at high energies often involve the hard scattering of quarks, leptons and gauge bosons. But whereas the electroweak bosons appear as free particles in high energy experiments, thus allowing detailed stud-

ies of the electroweak forces, quarks and gluons materialise as jets of hadrons due to the strong 'confinement' of coloured objects.

As mentioned in chapter 1, so far only phenomenological models exist to describe the fragmentation of quarks and gluons to the observed particles. It is believed that the coloured quarks and gluons which are created at small distances polarise the vaccum to produce jets of colourless hadrons which have only a restricted transverse momentum with respect to the fragmentation direction and have a flavour dependent distribution of longitudinal momentum. Usually the transverse momentum distribution is parametrised by a Gaussian distribution with a width of only a few hundred MeV. The longitudinal momentum distribution is described by a scaling function $D(z)$ where z is the fraction of available momentum (or energy) carried by a given produced hadron. $D(z)$ represents the probability that a hadron is produced with a given value of z.

Originally it was assumed that $D(z)$ for heavy quarks would be similar to that for light quarks which fragment principally into pions and kaons with a z distribution which falls steeply as z increases. However, our discussion in section 1.8 suggests that in the case of a fragmenting heavy quark a large fraction of the available energy is likely to be carried by the hadron which contains that heavy quark[18]. This is different from the case of light quarks which fragment principally into low momentum hadrons. In practice, a jet originating from a charm quark at high energies looks much the same as any other jet when the decay products of the charmed meson are included. The difference is that the energy fraction transferred to the charmed meson is substantially higher than for light quarks and mesons. However, after the charmed meson has branched off there is again no difference between the remainder of the cascade and a light-quark jet of the same energy. This kinematical difference between heavy and light quark fragmentation leads to fragmentation functions peaked towards high

values of z (said to be 'hard fragmentation'). This is the observed behaviour of charmed and bottom hadrons produced from leading c and b quarks.

The determination of $D(z)$ has been the subject of many recent theoretical and experimental studies. One of the experimentally favoured models is the form proposed by the Lund group[19]. The fragmentation function in this model is written as

$$D(z) \propto \frac{1}{z}(1-z)^A \exp\left(\frac{-Bm_T^2}{z}\right), \qquad (2.1)$$

where $m_T = m^2 + k_T^2$ is the transverse mass of the produced hadron and the parameters A and B are to be determined experimentally. However, although the above parametrisation has been used by various experimentalists, the most popular functional form is that proposed by Peterson et al. [20]. This fragmentation function has the following form

$$D(z) \propto \frac{1}{z\left[1 - \frac{1}{z} - \frac{\epsilon_Q}{(1-z)}\right]^2}, \qquad (2.2)$$

in which ϵ_Q is the only free parameter which is to be determined experimentally for each heavy quark. It is inversely proportional to the square of the fragmenting heavy quark mass forming the leading hadron.

Although the Peterson model has been adopted for most experimental and theoretical purposes for c and b quark fragmentation, interpretation of the variable z, which we shall replace by ξ from now on, is different in different models. At least five different definitions for this quantity has been used in the literature, namely

$$\xi = z \equiv \frac{(E + p_\parallel)_{hadron}}{(E + p)_{quark}} \qquad (2.3)$$

$$\xi = z_E \equiv \frac{E_{hadron}}{E_{quark}} \approx z \qquad (2.4)$$

26

$$\xi = x_E \equiv \frac{E_{hadron}}{E_{beam}} \tag{2.5}$$

$$\xi = x_p \equiv \frac{p_{hadron}}{\sqrt{E_{beam}^2 - m_{hadron}^2}} \tag{2.6}$$

$$\xi = x_\gamma \equiv \frac{2E_{hadron}}{\sqrt{s_{eff}}}, \tag{2.7}$$

where E_{beam} is the energy of the e^+e^- beam, $\sqrt{s_{eff}}$ is the energy of the virtual photon produced in e^+e^- collision after accounting for initial state radiation, and E_{quark} is the energy of the quark after further accounting for the emission of the one or more gluons. $(E + p_{\parallel})_{hadron}$ is the energy and the momentum component parallel to the fragmentation direction carried by the primary hadron. It is quite clear that these quantities will differ from each other when the quark and hadron masses and the effects of gluon emission and initial state radiation are considered. These effects are depicted schematically in figure(2.1) and lead to the following inequalities

$$E_Q \leq \frac{1}{2}\sqrt{s_{eff}} \leq E_{beam}, \tag{2.8}$$

and therefore by definition

$$x_E \leq x_\gamma \leq z. \tag{2.9}$$

The various definitions of ξ originate from the methods employed in extracting information from the fragmentation of the heavy quark in an experiment. Usually the energy of the produced hadron is accurately determined and since the beam energy is an accurately known quantity, the fractions x_E and x_p given by (2.5) and (2.6) are readily accessible. On the other hand the fractions z and z_E, cannot be measured directly since the heavy quark's energy is not known directly.
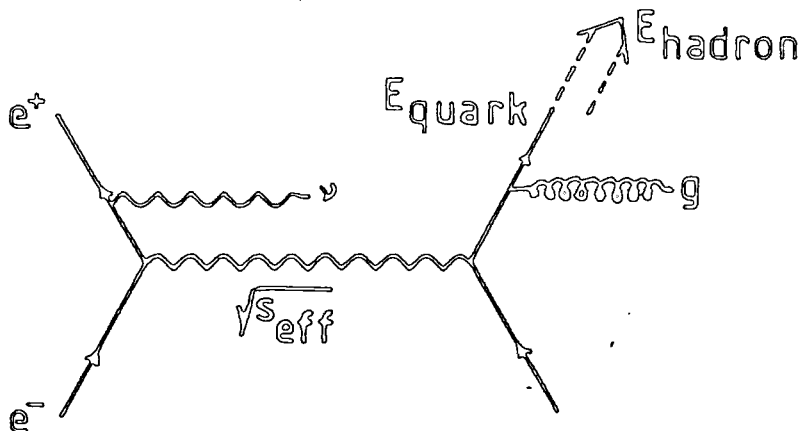
Figure (2.1) *The effect of initial state radiation and gluon emission leading to $E_Q \leq \frac{1}{2}\sqrt{s_{eff}} \leq E_{beam}$.*

2.2 Heavy Quark Fragmentation From Multiplicity Measurement

There is little reason to assume that there is much difference between hadronic jets from up, down and strange quarks because their masses are not large compared to the QCD scale $\Lambda_{QCD} \approx 200$ MeV. But the relatively large rest masses of the charm and bottom quarks suggests that the decay multiplicity of heavy hadrons containing heavy quarks should be higher than light quark states.

Experimental results on the mean charmed multiplicity of multi-hadronic events containing heavy quark jets, $\langle n \rangle_Q$, can be used to provide information on heavy quark fragmentation. One should distinguish between the contribution to $\langle n \rangle_Q$ from the decay of the two primary hadrons, i.e. the leading multiplicity $\langle n_l \rangle_Q$, and the reminder of the fragmentation process, i.e. the non-leading multiplicity $\langle n_{nl} \rangle_Q$. The latter can be related to a corresponding average non-leading energy, $\langle E_{nl} \rangle_Q$. By using the measured variation of the mean charged

multiplicity as a function of the center of mass energy, E_{cm}, in $e^+e^- \rightarrow q\bar{q}g$ events, the mean value of the fragmentation variable, x_E given in (2.5), can be obtained from the relation

$$\langle x_E \rangle_Q = 1 - \frac{\langle E_{nl} \rangle}{E_{cm}}. \qquad (2.10)$$

A typical measurement of the charged particle multiplicities in hadronic events deriving from bottom or charmed quarks has been performed by Rowson et al. [21], in the Mark-II detector at PEP in e^+e^- annihilation at 29 GeV. The results are listed in Table (2.1).

Table(2.1)Charged multiplicities of $b\bar{b}$ and $c\bar{c}$.

	$b\bar{b}$	$c\bar{c}$
One S and one H*	$15.2 \pm 0.5 \pm 0.7$	$13.0 \pm 0.5 \pm 0.8$
Nonleading mixture	$16.1 \pm 0.5 \pm 1.0$	$13.2 \pm 0.5 \pm 0.9$
Nonleading	$5.2 \pm 0.5 \pm 0.9$	$8.1 \pm 0.5 \pm 0.9$

*(S = Semi − leptonic, H = Hadronic)

This report reveals various facts about c and b quark fragmentation. In the first place, the lower nonleading multiplicity for $b\bar{b}$ relative to $c\bar{c}$ provides independent evidence that b fragmentation is harder than c fragmentation. Secondly, using this information (and also (2.10)) it is found from the nonleading multiplicities that bottom and charmed hadrons fragment with mean energy fractions $0.79^{+0.10}_{-0.05}$ and $0.60^{+0.09}_{-0.011}$ respectively.

Another report[22] of multiplicity measurements in heavy quark jets tagged by a D^* yields $\langle z_{rec.} \rangle_c = 0.58^{+0.05+0.05}_{-0.03-0.04}$, where $z_{rec.}$ stands for the reconstructed value of the parameter z.

2.3-Heavy Quark Fragmentation From Hadronic Decays

Measurements of the differential cross section in inclusive charged and neutral meson production and multi-hadronic decays can reveal precise information about heavy quark fragmentation.

In the case of charm quark fragmentation, charged D^* production is studied through the decay mode

$$D^{*+} \longrightarrow D^\circ \pi^+, \qquad (2.11)$$

in this procedure. Due to the special decay kinematics and the good mass resolution of the HRS (High Resolution Spectrometer) detector at PEP, a D^* signal shows up clearly in the distribution of the mass difference

$$\Delta M = M(D^\circ \pi) - M(D^\circ). \qquad (2.12)$$

D° is reconstructed in the decay modes

$$D^\circ \longrightarrow K^- \pi^+, \qquad (2.13)$$

$$\longrightarrow K^- \pi^+ \pi^- \pi^+, \qquad (2.14)$$

$$\longrightarrow K^- \pi^+ \pi^\circ, \qquad (2.15)$$

together with the charge conjugate states. Although in this technique the signals appear quite clearly, further reduction of the background is achieved by application of the D° mass constraint, and also by requiring that $|\cos \theta_K^*| < 0.8$, where $\cos \theta_K^*$ is the decay angle of the $K^- \pi^+$ system in its helicity frame.

The JADE collaboration[23] has measured the differential cross section for $D^{*\pm}$ production, in $e^+ e^-$ annihilation at $\sqrt{s}$=34.4 GeV from combination of decay channels (2.13) and (2.14). This is shown in figure (2.2). They have also
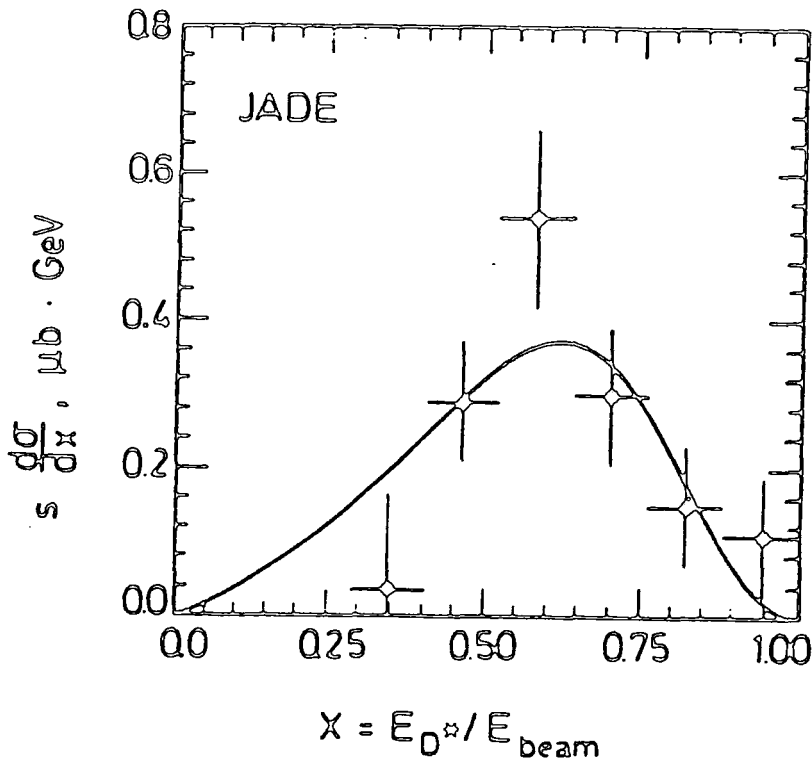
Figure (2.2) *The scaled differential cross section $s\frac{d\sigma}{dx}$ for inclusive $D^{*\pm}$ meson production together with Peterson's fragmentation function.*

evaluated the average value of the fragmentation parameter for $x_E > 0.4$ which comes out to be $\langle x_E \rangle = 0.64 \pm 0.05$.

2.4 Heavy Quark Fragmentation From Inclusive Lepton Production

While the hadronisation of charmed quarks into charmed mesons and baryons has been successfully measured by multiplicity measurements and hadronic decay studies, the fragmentation of b quark in to b flavoured hadrons is much less well explored by these techniques due to the small cross section and the very inefficient reconstruction of the b flavoured hadrons.

Significant progress towards an understanding of both b and c fragmen-

tation has been made by studies of inclusive lepton production. Such processes are described by the fragmentation of a heavy quark into a heavy hadron which subsequently undergoes a semi-leptonic decay. This is shown in Figure (2.3) where a b quark is produced with energy E_b by the reaction $e^+e^- \to b\bar{b}g$. Then the b quark fragments into a B meson of energy $E_B = zE_b$ with probability $D(\xi)$. The B meson subsequently decays semi-leptonically, $B \to l\nu_l X$.
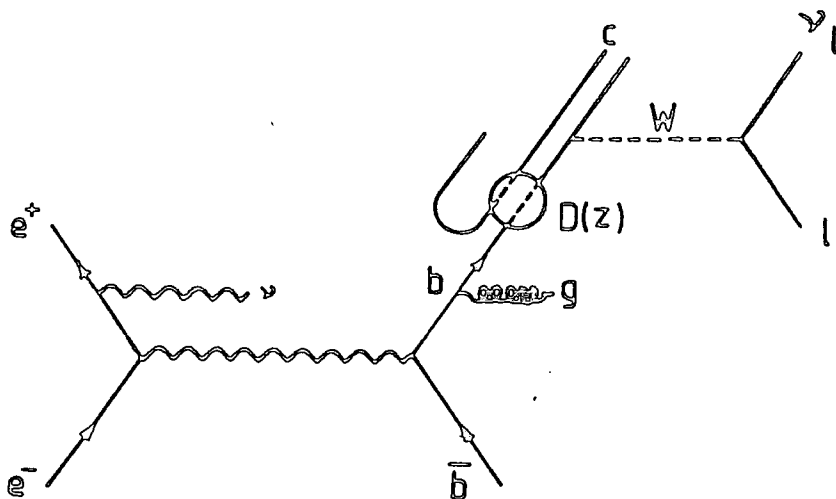
Figure (2.3) *The fragmentation and semi-leptonic decay of a bottom quark.*

The lepton momentum, p_l, being dependent upon the momentum of the parent hadron, contains information about the fragmentation of the heavy quark.

2.4a Flavour Separation

To distinguish between the contributions from different quark flavours, a variable sensitive to the quark mass is used. A universal choice is the lepton

momentum transverse to the thrust axis (p_T). Its mean value is quite different for c and b quarks although this difference depends not only on the quark mass, but also on the extent of the jet broadening due to gluon radiation. The definition of the thrust axis and lepton momentum components are illustrated in Figure (2.4).
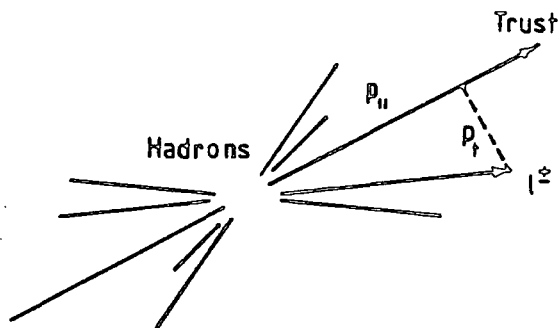
Figure (2.4) *The definition of the event axis and lepton parallel $p_\parallel$ and transverse p_T momenta in $e^+e^- \to l^\pm$ +hadrons.*

To achieve further separation between the quark flavours, a variable which indicates the topology of the event, such as thrust or sphericity, is sometimes used. In this respect the *transverse jet mass* variable, M[24], is particularly useful. M is defined as

$$M \equiv \frac{E_{cm}}{E_{vis}} \sum_n |p_T^{out}|, \qquad (2.16)$$

where p_T^{out} is the magnitude of the momentum components of the particle out of the event plane, and the sum runs over all charged and neutral tracks. E_{vis} is the total visible energy of the event. In addition to providing information on the heavy quark fragmentation functions, the production rate of prompt leptons yields valuable knowledge of the weak semi-leptonic branching ratios of

heavy quarks. Usually the production of the prompt leptons is described by the spectator parton model. (This model will be discussed in greater detail in chapter 6). This model predicts equal semi-leptonic branching ratios for charged and neutral charmed mesons, and likewise for bottom mesons. Although there are indications of different measured lifetimes and branching ratios, the above mentioned model is widely used by experimentalists. Recently the contribution of nonspectator diagrams was investigated in a report by the Crystal Ball Collaboration [25] on B meson decay.

While it would be possible to obtain an efficient flavour separation by using simple cuts in p_T and/or thrust, it turns out that an increase in the statistical significance of the results can be obtained by a multi-dimensional analysis. For that purpose the MARK-J group subdivide this sample into various bins in the variables p_T, $p_{\parallel}$, and T and thereby measure $\frac{d^3\sigma}{dp_T dp_{\parallel} dT}$. The TASSO group bins the distribution in p_T and $p_{\parallel}$, and thus measures $\frac{d^2\sigma}{dp_T dp_{\parallel}}$.

2.4b Analyses of inclusive lepton production

Typical analyses proceed by deducing the prompt lepton momentum and transverse momentum (and sometimes thrust) distributions of the quark flavours as a function of ξ using a sample of simulated data. Then, by fitting to the corresponding distributions of the experimental data, experiments are able to obtain information on the ξ distribution of the fragmenting heavy quark. Here the choice of the definition of ξ is not restricted as all the variables in the Monte Carlo model are known *a priori*. This freedom in defining ξ (within the limits imposed by the use of a Monte Carlo model) is a major factor contributing to the use of so many different ξ's. Although (2.3) is theoretically preferred, (2.4), (2.5), and (2.7) have also been used in analyses of inclusive leptons. These various definitions of ξ manifest themselves in different results for parameter

ϵ_Q of the Peterson function, which in turn give different values for $\langle \xi \rangle$. This is a crucial factor which has to be accounted for before drawing conclusions and comparing results between experiments.

The most recent data on lepton production is reported by the JADE collaboration[26]. They have used muon detection in e^+e^- annihilation at 34.6 GeV and binned the data in $p(\mu)$, $p_T(\mu)$ and M space. The fit to the muon inclusive data sample is performed by using the Peterson fragmentation function and weighting the spectra of the above mentioned parameters for the c and b quarks. Two definitions of ξ, namely z and x_E of (2.4) and (2.5), are investigated in this experiment. The results for $\langle z \rangle$ and $\langle x_E \rangle$ are summarised in Table (2.2). The fact that $\langle x_E \rangle$ is lower than $\langle z \rangle$ by the order of 10-15% is attributed to the expected softening due to gluon emission.

Table(2.2) Avarage of ξ with different definitions for c and b quarks.

ξ	ϵ_c	ϵ_b	$\langle \xi_c \rangle$	$\langle \xi_b \rangle$
z	$0.015^{-0.006}_{+0.009}$	$0.0035^{-0.002}_{+0.004}$	0.77 ± 0.03	0.86 ± 0.04
x_E	$0.088^{-0.023}_{+0.032}$	$0.020^{-0.007}_{+0.012}$	0.64 ± 0.03	0.76 ± 0.03
x_E	0.25	$0.015^{-0.006}_{+0.010}$	0.54	0.77 ± 0.03
x_E	$0.109^{-0.024}_{+0.033}$	$0.019^{-0.007}_{+0.012}$	0.62 ± 0.02	0.76 ± 0.03

The quantities $\langle z_{c,b} \rangle$ are also determined by dividing the z regions into several intervals and weighting these intervals without assuming any functional form. The results of this treatment provide data on the fragmentation functions. These data together with others, have been compiled into a table which appears later in this chapter.

2.5 Comparison of Data and Discussion

The experimental procedures which we have explained so far have revealed a wealth of information about the production, fragmentation and decay of heavy quarks and the related heavy hadrons.

Because of the problems of reconstructing the bottom hadrons, the data from charged multiplicity measurements and hadronic decays are limited and mainly concern charm quark fragmentation. We gave typical examples of the average values of ξ, the fragmentation parameter which are obtained by the procedures introduced in sections (2.2) and (2.3). However, there have been plenty of reports on fragmentation of both charmed and bottom quarks using inclusive lepton production. As we explained earlier in this chapter, the characteristic parameters used in this procedure, namely p, p_T and T of the prompt lepton, are distinctively different for charm and bottom quarks and therefore provide a more sophisticated way to extract the data.

We have listed the measured values of the average fragmentation parameters from the different collaborations in table (2.3). The main fragmentation function that has been used to extract data is the Peterson fragmentation function. It is necessary to emphasise that the derivation of Peterson fragmentation function is relatively naive and it would indeed be surprising if it were to provide the ultimate description of the data. However, within the limited statistics available, the cross section is in accordance with the Peterson form when fitted as a function of z rather than x_E[27]. The fact that $\langle x \rangle$ must be lower than $\langle z \rangle$, because of radiative corrections, is confirmed by Table (2.3).

Finally we have compiled data on the fragmentation functions for charm and bottom fragmentation in Figures (2.5) and (2.7). Due to large error bars in figure (2.5), it is hard to make a firm judgment about the fragmentation models using such compilation. Therefore we choose the sets of data with smallest error bars and use for this purpose [28] which we give in figure (2.6).

The source of error in the extraction of the data is the low statistics. Since a consistent data set is only obtained by proper adjustment of the parameter(s) of the model used in the fitting procedure, a good knowledge of the parametrisation of the quark fragmentation functions [29] may reduce the systematic errors in many analyses. Further contributions to the systematic error arise from the uncertainties in the final state lepton detection, the background from $\tau^+\tau^-$ and two photon events, and from uncertainities in the shape of the $p(\mu)$ and $p_T(\mu)$ and M distributions of the different quark flavours. The errors in the reconstruction of the thrust axis and the event plane, and from a lack of understanding of the QCD radiation and confinement effects, should also be considered.

Table(2.3) $\langle \xi_b \rangle$ and $\langle \xi_c \rangle$ from semi − leptonic decay.

	Ref.	l	ξ	$\langle\xi_c\rangle\%$	$\langle\xi_b\rangle\%$
TASSO	[30]	μ	z	77^{+5+3}_{-7-11}	85^{+10+2}_{-12-7}
TASSO	[31]	e	z	57^{+10+5}_{-9-6}	85^{+15+15}_{-10-11}
MARK-J	[32]	μ	z	$46 \pm 3 \pm 3$	$74 \pm 2 \pm 5$
JADE	[33]	μ	z	$77 \pm 3 \pm 5$	$86 \pm 4 \pm 5$
MAC	[34]	μ	z	17-67	80 ± 10
MARK-II	[35]	e	z	0.59 ± 0.06	0.79 ± 0.06
CLEO	[36]	e	z	50^{+7+11}_{-4-10}	80^{+3+6}_{-3-6}
HRS	[37]	μ	x_E	47^{+6+8}_{-3-5}	—
DELCO	[38]	e	x_E	59 ± 4	72 ± 5
TPC	[39]	μ	x_E	$60 \pm 6 \pm 4$	$80 \pm 5 \pm 5$
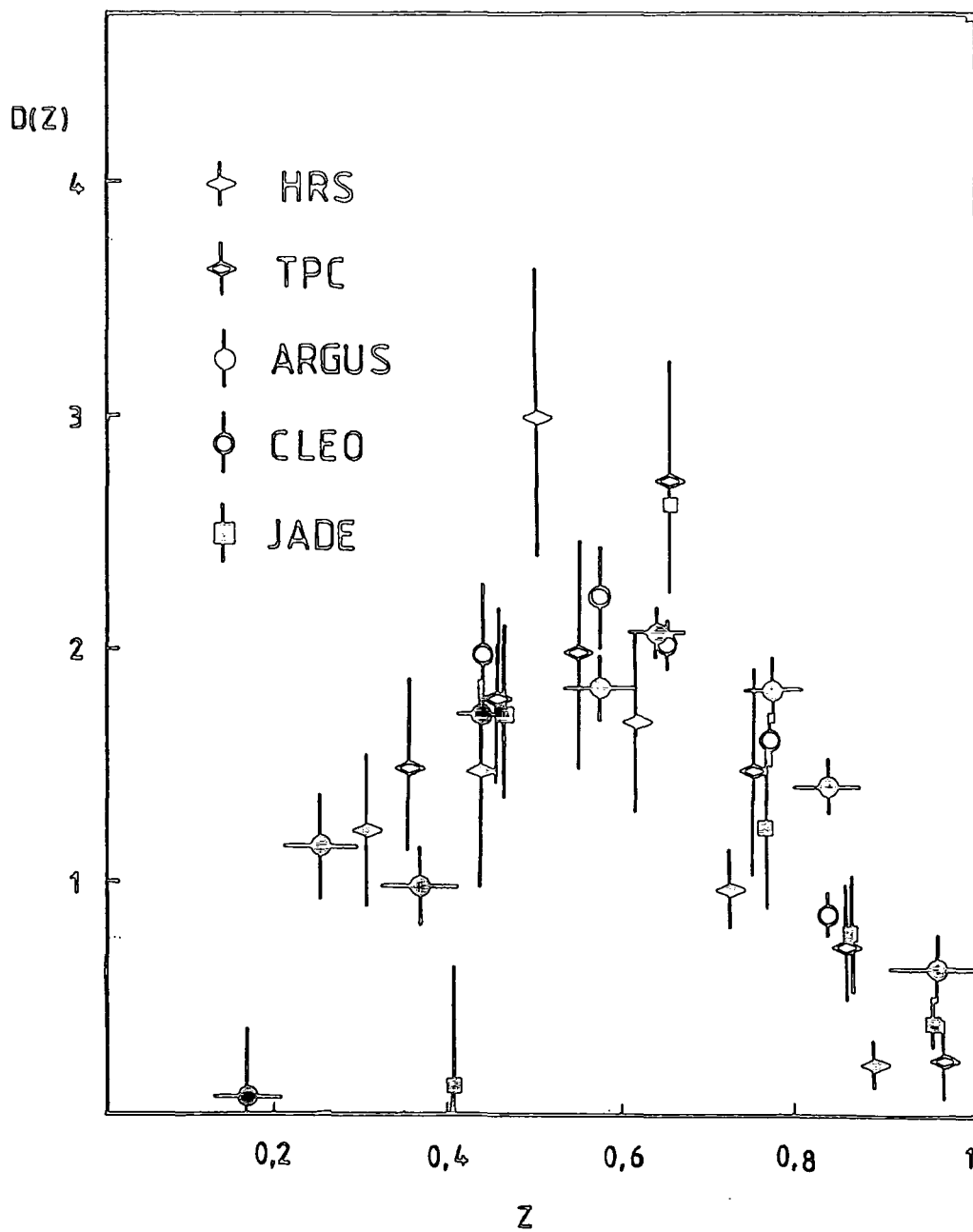
Figure (2.5) *Compilation of data on the charm fragmentation function obtained using D^* production. See [28] and [40].*
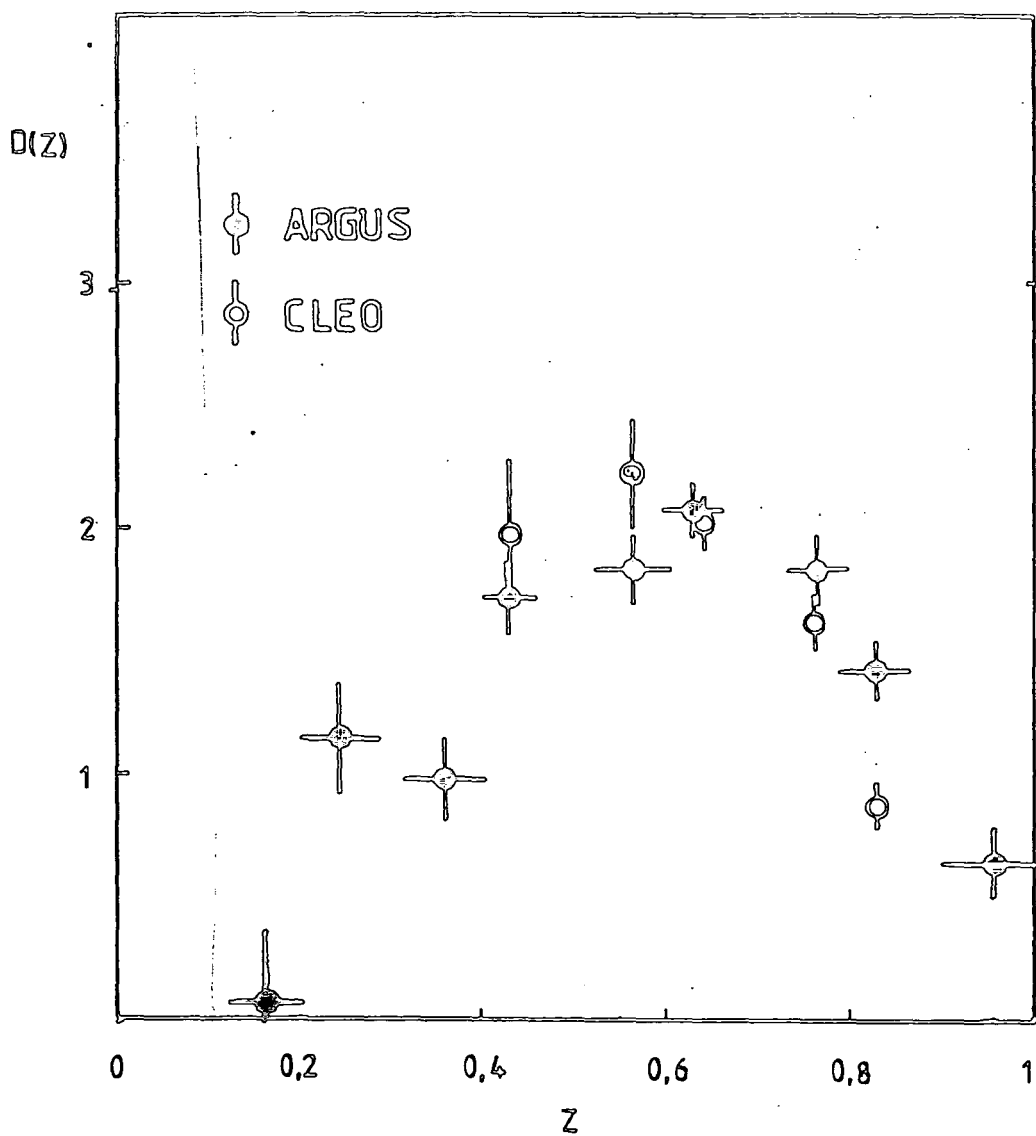
Figure (2.6) *Compilation of data on D^* fragmentation function reported in reference [28].*
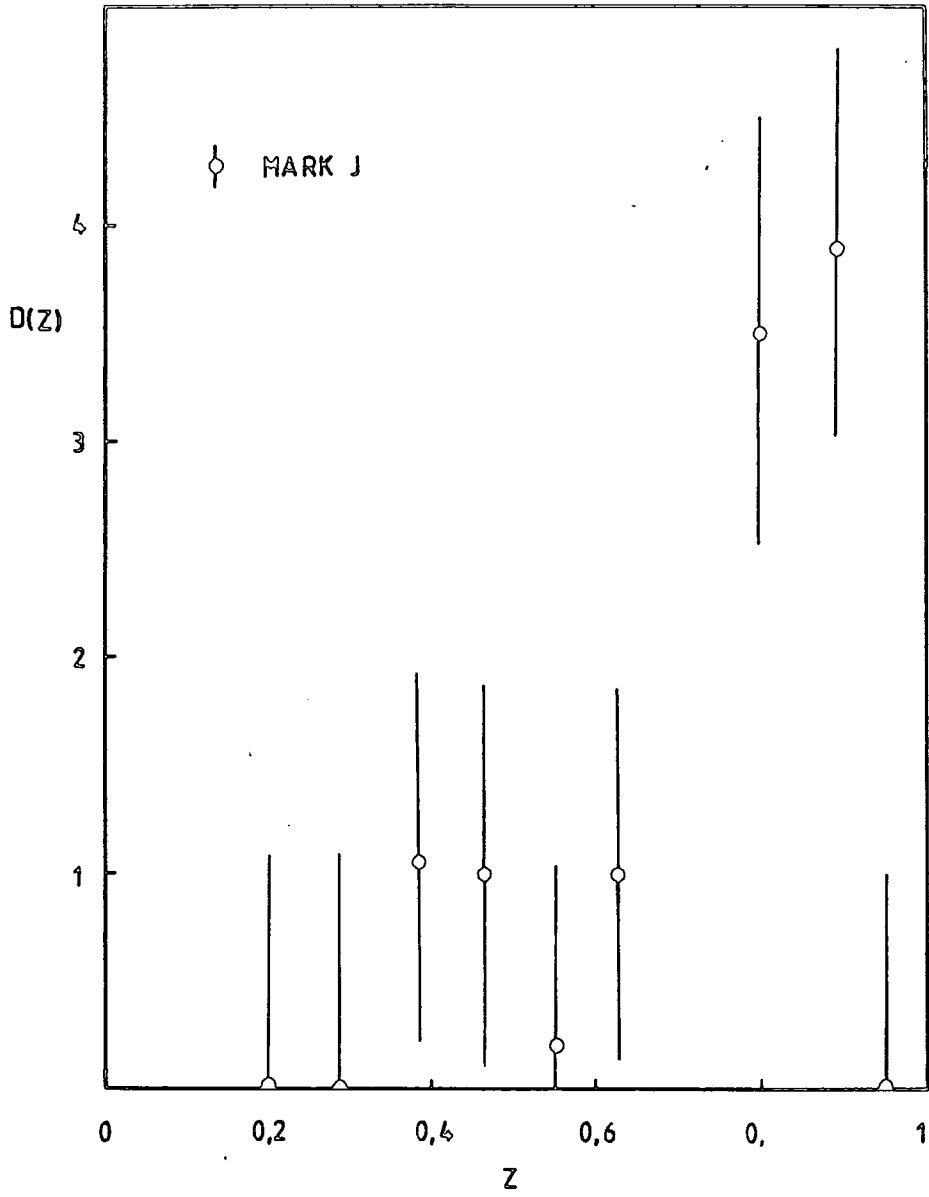
Figure (2.7) *The same as Figure (2.5) using B meson production.* [28]

CHAPTER 3

HEAVY QUARK FRAGMENTATION MODELS

We learned in the previous chapters that in the hadronisation of the heavy quarks, the heavy quark tends to carry away most of the parton's momentum and, unlike the statistical nature of light quark fragmentation, the fragmentation is a hard process. The quark content and the masses of the heavy mesons produced in charm and bottom quark fragmentations are listed in Table(3.1).

Table(3.1) Charmed and bottom mesons.

State	Mass (GeV/c^2)	Quark Content
D^+	1.869	$c\bar{d}$
D°	1.865	$c\bar{u}$
D^{*^+}	2.010	$c\bar{d}$
D^{*°	2.007	$c\bar{u}$
B^+	5.271	$b\bar{u}$
B°	5.274	$b\bar{d}$
B^*	5.323	$b(\bar{u}\ or\ \bar{d})$

In this chapter we review briefly five heavy quark fragmentation models, due to Scott[42], Peterson et al.[43], Collins-Spiller[44], Suzuki[45] and Amiri-Ji[46] respectively. As we have mentioned in the previous chapters, the only important radiative correction to heavy quark fragmentation is the initial gluon radiation by the heavy quark. We shall evaluate the effect of such a correction on the Peterson model later in this chapter. Eventually, we compare the results of these models with one another and also with the experimental data for the production of D, D^*, B and B^* mesons. The predictions for top quark

41

fragmentation are also given.

3.1 The Scott Model

A model of heavy quark fragmentation in e^+e^- annihilation was introduced by Scott [47]. It is based on the study of deep inelastic lepton scattering. The dominant parton model diagram for this process is shown in figure (3.1).
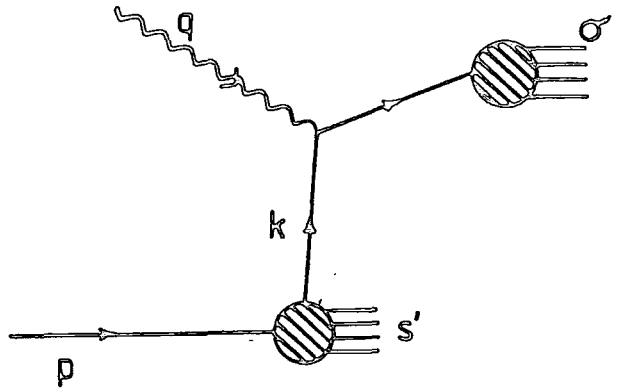
Figure (3.1) *Parton model diagram for deep inelastic lepton scattering.*

The parton k is off-shell, and after it has been struck by the current, it fragments into a system of hadrons whose invariant mass is $\sqrt{\sigma}$. The invariant mass of the hadronic system into which the parent hadron fragments after the parton with momentum k has been removed is $\sqrt{s'}$. Both σ and s' refer to the properties of the hadronic system before any quark confining forces have had time to act. It is assumed that these forces are such that they do not eliminate the normal requirement that both σ and s' be positive. Using the covariant parton model Landshoff and Scott[48] were led to the following structure functions of the hadron.

42

$$F_2(x) = \frac{1}{\gamma} C x \left[\frac{1-x}{\Lambda(x)} \right]^{\gamma}, \tag{3.1}$$

with

$$\langle k_T^2 \rangle = \frac{1}{\gamma - 1} \Lambda(x), \tag{3.2}$$

where

$$\Lambda(x) \equiv x s_0 + (1-x) m_q^2 - x(1-x) m_H^2, \tag{3.3}$$

and where m_q and m_H are the masses of the light quark and the produced hadron respectively. γ is a constant and its value is fixed by the behaviour of the structure function as $x \to 1$. According to dimensional counting rules[49], $\gamma = 1$ for mesons. The value of $\langle k_T^2 \rangle$ in (3.2) has to be recalculated if $\gamma = 1$. In (3.3) s_0 is a constant and corresponds to the invariant mass-squared of light hadrons left behind by the heavy hadron and is of the order of a few GeV^2.

Scott's model is based mainly on the above ideas. Figure (3.2) shows the production of a heavy hadron H from parton k. This is indeed a reciprocal diagram to that of figure (3.1). Now using (3.1) along with (3.2) and the reciprocity relation it is found that

$$D(z) \propto \frac{(1-z)z^2}{z s_0 + (1-z) m_H^2 - z(1-z) m_q^2}. \tag{3.4}$$

This function has the behavior

$$D(z) \sim (1-z), \tag{3.5}$$

as $z \to 1$. The behavior of (3.4) is given for the production of D, D^* and B mesons with $s_0 = 1$ or 4 GeV^2 in figure (3.3). As s_0 increases, the fragmentation function becomes softer. We have chosen $s_0 = 1$ Gev^2 when we compare the results of this model against data and other models. This choice is made because
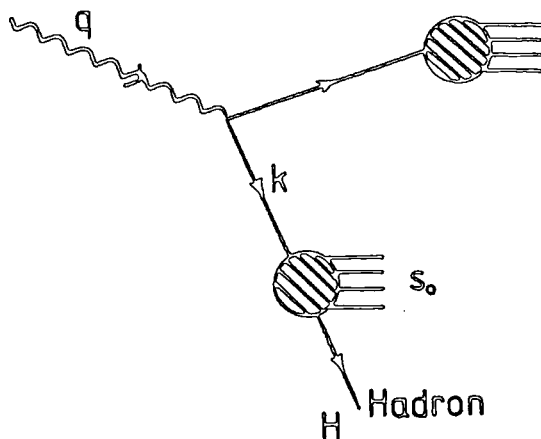
Figure (3.2) *Fragmentation of a heavy hadron H in e^+e^- annihilation. The hadron leaves other light hadrons which are indicated by the constant s_0.*

we do not expect high mass hadronic matter to be produced along with the heavy hadron.

3.2 The Peterson Model

A simple and popular model based mainly on the kinematics of heavy quark fragmentation is given by Peterson *et al.* It is assumed that when a light antiquark $\bar{q}$ attaches to a fast moving heavy quark, the heavy quark Q decelerates only slightly. Thus Q and $(Q\bar{q})$ should carry almost the same energy. Figure (3.4) shows the principle of this model.

Using the quantum mechanical parton model, it is postulated that the dominant part of the amplitude is determined by the value of the energy transfer (the energy denominator),
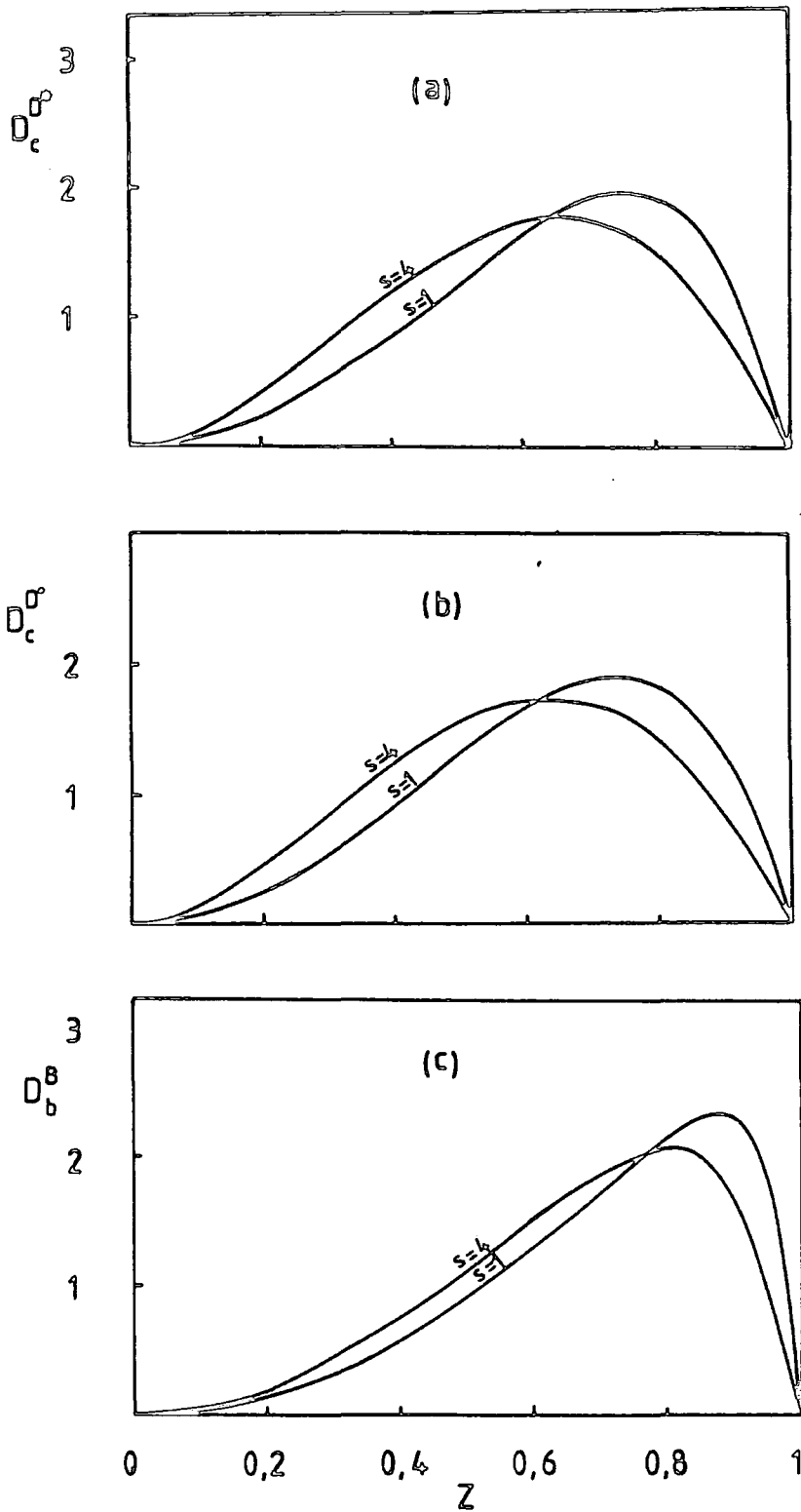
Figure (3.3) *Fragmentation functions of the Scott model a)* $D_c^{D^*}(z)$,

b) $D_c^{D^o}(z)$ *and* $D_b^{B^o}(z)$ *for* $s_0 = 1,4$ *GeV*^{2}.
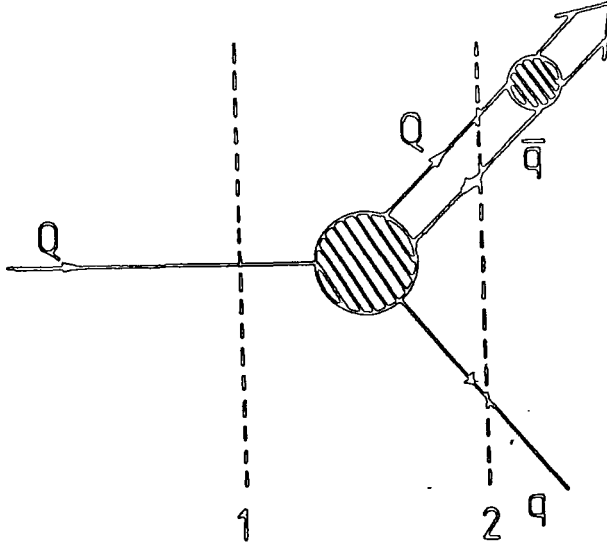
Figure (3.4) *The quantum mechanical basis of heavy quark fragmentation. The dashed lines represent the time slices which are used to drive the fragmentation function.*

$$\Delta E = E_H + E_q - E_Q. \tag{3.6}$$

Defining the fragmentation parameter as in (2.3), one can write (3.6) in the following form

$$\Delta E = (m_Q^2 + z^2 p^2)^{1/2} + (m_q^2 + (1-z)^2 p^2)^{1/2} - (m_Q^2 + p^2)^{1/2}$$

$$\propto \left[1 - \frac{1}{z} - \frac{\epsilon_Q}{1-z} \right], \tag{3.7}$$

where the energies have been expanded about the (transverse) particle masses and $\epsilon_Q \equiv (\frac{m_q}{m_Q})^2$ is the ratio of the effective light and heavy quark masses. Taking

a factor of z^{-1} for the longitudinal phase space, the proposed fragmentation functions take the following form:

$$D(z) = \frac{N}{z\left[1 - \frac{1}{z} - \frac{\epsilon}{1-z}\right]^2}.$$ (3.8)

The normalisation constant N is fixed by summing over all hadrons containing the quark Q, i.e.

$$\sum \int dz D(z) = 1.$$ (3.9)

It is expected that when the quark mass increases, the quantity $\langle z \rangle$ should get very close to unity. However equation (3.8) has the property that

$$D(z) \sim (1 - z)^2,$$ (3.10)

in the limit $z \to 1$. This is in conflict with the dimensional counting rules discussed in section (1.6) which demand a behaviour $\sim (1 - z)$ in this limit. However this simple parametrisation has been widely used by experimentalists to determine the properties of the fragmentation process.

3.3 The Collins-Spiller Model

The next model of interest was introduced by Collins and Spiller. This model is consistent with reciprocity which demands that the fragmentation functions should be related to the hadronic structure functions. It also agrees with the dimensional counting rules, i.e. has $D(z) \sim (1-z)$. Since we will look at the spin properties of fragmentation motivated by this model in the next chapter, we give more details of this model here.

3.3a The model

The model is based on the diagrams of the figure (3.5). Part (a) shows the principle of independent jet fragmentation. The heavy meson takes a fraction z of the initial quark's momentum. In part (b) the forward amplitude for $e^+e^-\overline{M} \longrightarrow e^+e^-\overline{M}$ is shown. This gives the cross-section for $e^+e^- \longrightarrow MX$. A heavy quark is produced in e^+e^- annihilation and fragments into a heavy meson through the vertex indicated by Γ. The four momenta are labelled. The function Γ is chosen to have the following form by Collins and Spiller.

$$\Gamma = Cg(z_M, z_q)G^{1/2}(k_{T_M}^2)G^{1/2}(k_{T_q}^2)\overline{u}_Q(\zeta_Q k_M)v_{\overline{q}}(-\zeta_q k_M) \qquad (3.11)$$

with

$$p_Q = \zeta_Q k_M, \qquad k_q = -\zeta_q k_M, \qquad (3.12)$$

where ζ_Q and ζ_q are the fractions of the meson's four momentum carried by the heavy and light quarks respectively. Momentum conservation requires that $\zeta_Q + \zeta_q = 1$. In (3.11) $\overline{u}_Q$ and $v_{\overline{q}}$ are the quark and antiquark spinors and C is a normalisation constant. The G functions describe the transverse momentum distributions of the meson M and the quark q. These functions are chosen to have a Gaussian form but the final answer is independent of this choice. Finally $g(z_M, z_q)$ is intended to represent the longitudinal momentum distribution of the meson and the light spectator quark along the direction of Q. Again the conservation of momentum requires that $z_M + z_q = 1$. z_M and z_q are the meson and quark light-cone momentum fractions defined respectively by

$$\begin{cases} z_M \equiv \dfrac{k_M^+}{p_Q^+} \equiv z \\[2mm] z_q \equiv \dfrac{k_q^+}{p_Q^+} = (1 - z), \end{cases} \qquad (3.13)$$

48
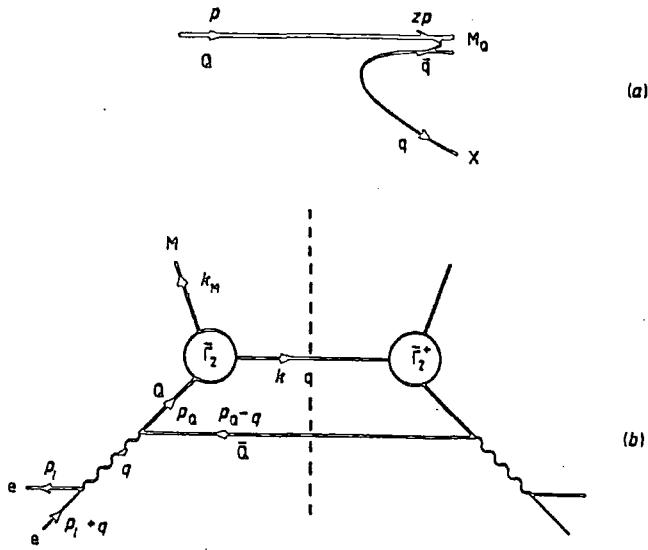
Figure (3.5) . *Heavy Quark fragmentation in* e^+e^- *annihilation.*

where $k_M^+ = k_M^0 + k_M^3$ and so on. To obtain the g function for this case Collins and Spiller consider a single gluon exchange approximation for the meson bound state. The gluon propagator in figure (3.6) has the following behaviour:
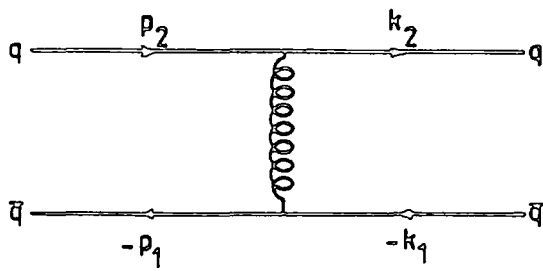
Figure (3.6) . *Single gluon exchange approximation in meson bound state.*

$$\frac{1}{(k_1 - p_1)^2} = \frac{1}{k_1^2 + p_1^2 - \left[x_1 k_M^+ p_1^- + \frac{(k_1^2 + k_{T_1}^2)p_1^+}{x_1 k_M^+} \right]} \bigg|_{x_1 \to 0} \sim x_1. \qquad (3.14)$$

Similarly in terms of the other momenta

$$\frac{1}{(k_2 - p_2)^2} = \frac{1}{k_2^2 + p_2^2 - \left[x_2 k_M^+ p_2^- + \frac{(k_2^2 + k_{T_2}^2)p_2^+}{x_2 k_M^+} \right]} \bigg|_{x_2 \to 0} \sim x_2, \qquad (3.15)$$

Since the propagator appears twice in $|\Gamma|^2$, it is realised that

$$|g(x_1, x_2)|^2 = x_1 x_2. \qquad (3.16)$$

To satisfy reciprocity they choose

$$|g(z_M, z_q)|^2 \equiv -z_M^2 z_q. \qquad (3.17)$$

Although, since we have a hadron and a quark, there is no reason for (3.17) to be symmetric, the fragmentation and the corresponding (reciprocal) structure function should be smooth continuation of each other. The sign change in (3.17) is due to the analytic continuation of x_2 and z_M. Using light cone momentum conservation, $z_M + z_q = 1$, we can write (3.17) as

$$|g(z_M, z_q)|^2 = -z_M^2(1 - z_M), \qquad (3.18)$$

and therefore we can write the following behaviour for $|g|^2$

$$\begin{cases} |g|^2 \big|_{z_M \to 1} \longrightarrow 0 \\ \\ \frac{\partial}{\partial z_M} |g|^2 \big|_{z_M \to 1} \longrightarrow 1. \end{cases} \qquad (3.19)$$

If we rewrite (3.16) using $x_1 + x_2 = 1$, it becomes

$$|g|^2 = x_2(1 - x_2). \qquad (3.20)$$

Using $x_2 = \frac{p_Q^+}{k_M^+}$, and also (3.13), we can write

$$x_2 = \frac{1}{z_M}. \tag{3.21}$$

Therefore (3.21) and (3.20) produce:

$$\begin{cases} |g|^2 \Big|_{z_M \to 1} \longrightarrow 0 \\[3mm] \frac{\partial}{\partial z_M} |g|^2 \Big|_{z_M \to 1} \longrightarrow 1, \end{cases} \tag{3.22}$$

which proves that with the choice of (3.17) the structure and fragmentation functions will indeed join smoothly at $z_M = \frac{1}{x_2} = 1$.

3.3b. Fragmentation Functions

In this section the derivation of a useful form of the fragmentation functions in terms of the discontinuity of the amplitude in the diagram of figure (3.11) is given. We write the defining relation of (1.14) in the following form

$$\frac{1}{\sigma_{tot}} \frac{d\sigma}{dz_M} (e^+ e^- \longrightarrow M X) = \frac{1}{\sum_q e_q^2} \sum_q e_q^2 \left[D_q^M(z_M) + D_{\bar{q}}^M(z_M) \right]. \tag{3.23}$$

If an experiment sets out to measure a fragmentation function of a quark q into a meson M, then what will be measured is

$$D_q^M(z_M) = \sum_j D_q^{M_j}(z_M), \tag{3.24}$$

where $D_q^{M_j}(z_M)$ is defined as the fragmentation function for q going to M and $j - 1$ other partons, $(j \geq 2)$. The summation is not only over j, but all possible sets of partons for each j value as well.

For light quark fragmentation many terms contribute to this summation. However, for a heavy quark fragmenting into a meson which contains that heavy quark, the single term with $j = 2$ will dominate. This is because most of the

quark's momentum is retained by the hadron, due to the large quark and hadron masses.

To obtain the fragmentation functions, Mueller's 'Optical Theorem' is used in the following form

$$16\pi^3 E_M \frac{d^3\sigma}{dk_M^3}(e^+e^- \longrightarrow MX) = \frac{2}{h}\text{Disc}(A_{e^+e^-\overline{M}\longrightarrow e^+e^-\overline{M}}), \qquad (3.25)$$

where h is the flux factor and $\text{Disc}(A)$ is the discontinuity of the amplitude shown in fig(1.b). The derivation of this theorem is explained in figure (3.7b).

Using $z_M = \frac{k_M^+}{p_Q^+}$, it follows that

$$16\pi^3 E_M \frac{d^3\sigma}{d^3 k_M}(e^+e^- \longrightarrow MX) = 16\pi^3 k_M^+ \frac{d^3\sigma}{dk_M^+ d^2 k_{T_M}}(e^+e^- \longrightarrow MX)$$

$$= 16\pi^3 z_M \frac{d^3\sigma}{dz_M d^2 k_{T_M}}(e^+e^- \longrightarrow MX). \qquad (3.26)$$

We use (3.26) to integrate (3.25) over $d^3 k_M$. Then using the parton model relation,

$$\sigma_{tot} \equiv \sigma(e^+e^- \longrightarrow X) = 3\sigma(e^+e^- \longrightarrow \mu^+\mu^-)\sum_Q e_Q^2, \qquad (3.27)$$

in which the factor 3 is due to the summation over the colours of the quarks, the final result is

$$3e_Q^2 D_Q^{M_Q}(z_M)\sigma(e^+e^- \longrightarrow \mu^+\mu^-) = \int \frac{d^2 k_{T_M}}{16\pi^3 z_M} \frac{2}{h}\text{Disc}(A). \qquad (3.28)$$

Finally using (3.28) and the discontinuity of the forward amplitude given in figure (3.5), the Collins and Spiller fragmentation functions are obtained,
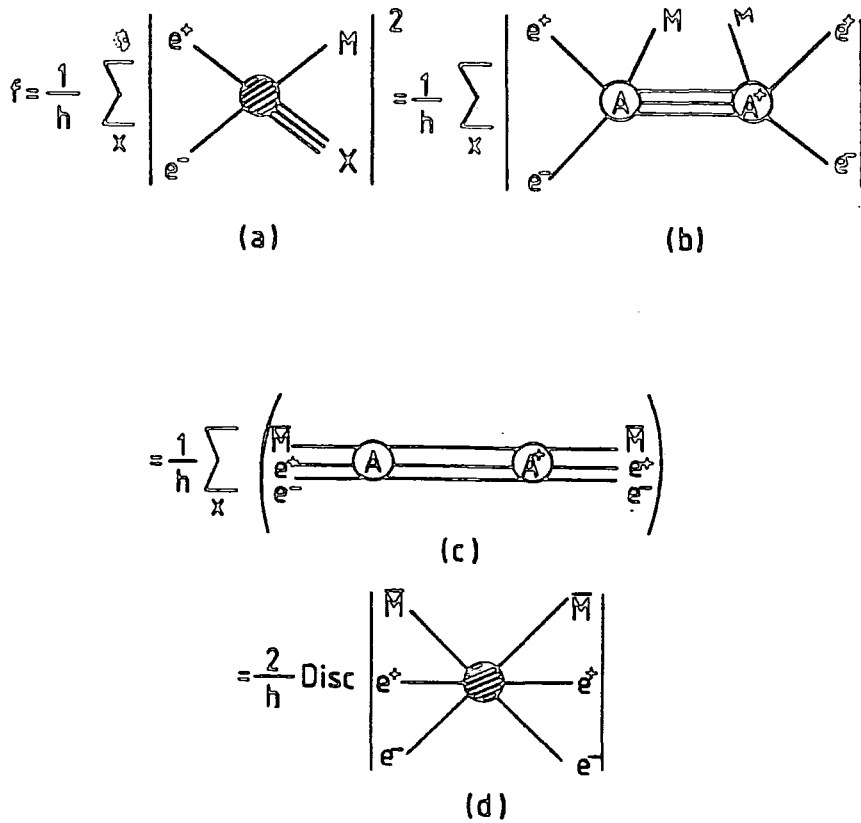
Figure (3.7) . *Derivation of Mueller's theorem. (a) is the definition of the cross-section f, and h is the flux factor. To get (b) the completeness relation is used. (c) is obtained by crossing $\overline{M}$ and $\overline{M}'$, and (d) is the unitarity relation for the $\overline{M}e^+e^- \rightarrow \overline{M}'e^+e^-$ amplitude.*

$$D(z) = Nz\left[\frac{1-z}{z}(m_M^2 + \langle k_T^2\rangle) + \frac{z}{1-z}(m_q^2 + \langle k_T^2\rangle) + 2\langle k_T^2\rangle - 2m_M m_q\right]$$

$$\times\left[\frac{m_M^2 + \langle k_T^2\rangle}{z} + zm_Q + 2m_M M_Q\right]$$

$$\times\left[m_Q^2 - \frac{m_M^2 + \langle k_T^2\rangle}{z} - \frac{m_q + \langle k_T^2\rangle}{1-z}\right]^{-2}, \tag{3.29}$$

where N is a normalisation constant, m_M and m_Q are the heavy meson and the heavy quark masses respectively, and m_q is the light quark mass which is taken

to be negligible. It is clear from (3.29) that the fragmentation function has the behaviour $\sim (1 - z)$ in the limit of $z \rightarrow 1$ in agreement with the dimensional counting rules.

Since the observed meson may not be produced directly from the heavy quark but through a secondary hadronic decay like $D^* \rightarrow D\pi$, the experimental test of (3.29) becomes complicated. To incorprate this fact, Collins and Spiller use an inclusive decay distribution which represents the probability of an excited meson M_Q^* emitting a pseudoscalar meson M_Q, which carries away a fraction of its momentum through decay of the type $M_Q^* \rightarrow M_Q\pi$. The distribution function given by Collins and Spiller has the following form:

$$f_{M^*}^M(z) = \frac{N'}{z(1 - z)\left[\frac{m_{M^*}}{\langle k_T^2 \rangle} - \frac{m_M^2 + \langle k_T^2 \rangle}{z} - \frac{m_\pi^2 + \langle k_T^2 \rangle}{1 - z}\right]^2} \qquad (3.30)$$

Thus the real fragmentation function, which allows for secondary fragmentation, should have the form

$$D_Q^{M_Q}(z, \kappa) = \kappa D_Q^{M_Q}(z) + (1 - \kappa) \int_z^1 \frac{dy}{y} D_Q^{M_Q^*}(y) f_{M^*}^M(\frac{z}{y}), \qquad (3.31)$$

where κ is a parameter which lies between zero and one and determines the fraction of secondary fragmentation. The first term in (3.31) represents the direct fragmentation into the meson M, while the second term is fragmentation through an intermediate M^* meson which carries away a fraction y of the quark's momentum. We have shown this in figure (3.8).

3.4 Spin Properties of Heavy Quark Fragmentation

As we shall see, the models which we have reviewed so far agree with the
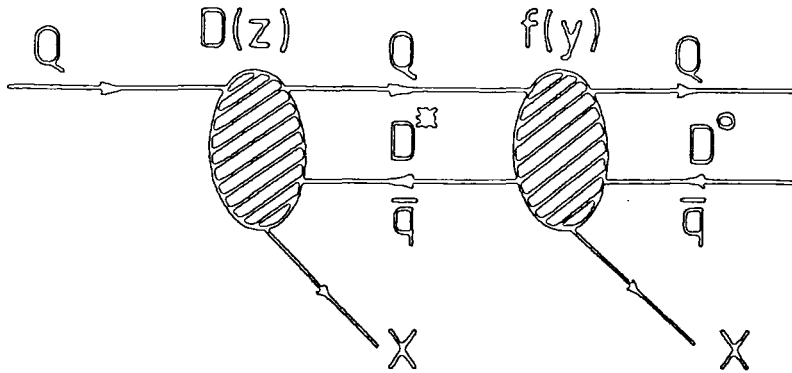
Figure (3.8) . *Explanation of secondary fragmentation used in (3.31).*

experimental data on the fragmentation functions satisfactorily. But if we want to know further details such as the spin properties of the fragmentation, the z dependence of the vector/pseudoscalar ratio, and so on, we need more elaborate models based on a more detailed understanding of the strong interaction dynamics. Suzuki and Amiri-Ji have introduced new models which are a first step in this direction. The transverse momentum of the beam appears as a free parameter in the Suzuki model, but it gives a complete spin picture of the basic fragmentation phenomenon. In the Amiri's model there is no free parameter in the final results and they are a complete second order perturbative calculation, but they are lengthy and complicated, and only in the limit of $\frac{m_{H}^{2}}{s} << 1$ do they reduce to simple forms. Another point about the latter model is that the fragmentation functions are given for pseudoscalar and vector meson production and not in the form of spin components as in the case of Suzuki model. So the evaluation of the z dependence of the decay angular distribution (in the process $D^{*} \to D\pi$ for example) in this model is not possible.

3.5 The Suzuki Model

The basic process of heavy meson fragmentation is illustrated in figure (3.9). A vector gluon interacts with quarks through the non-Abelian guage interaction.
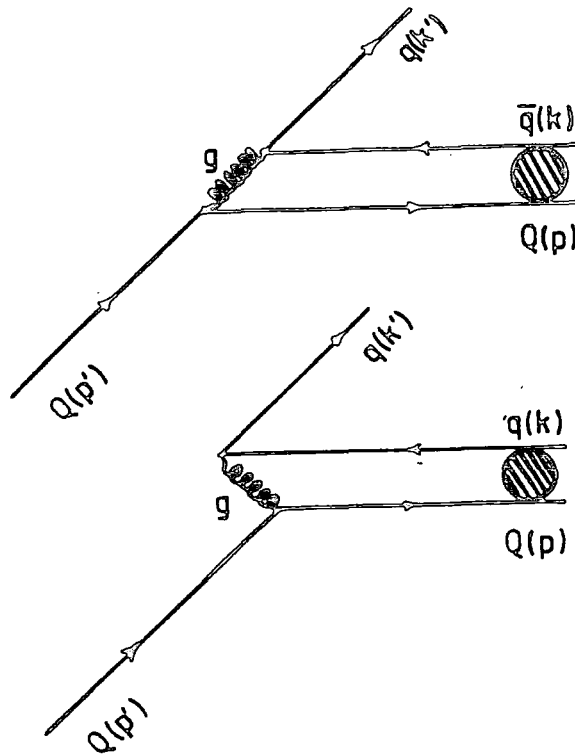
Figure (3.9) *Fragmentation of a heavy meson $Q\bar{q}$. A heavy quark Q forms an S-wave bound state with a light antiquark $\bar{q}$ created by a single vector gluon g.*

It is assumed that Q and $\bar{q}$ in figure (3.9) are emitted collinearly with each other. In other words, the relative motion of Q and $\bar{q}$ is neglected and no mesons with a nonvanishing relative orbital angular momentum are produced. Consequently, whether Q and $\bar{q}$ form a vector meson or a pseudoscalar meson is

determined by the total spin of the $Q\bar{q}$ system at the time when the $\bar{q}$ is created by the gluon. Since the original heavy quark is off its mass shell the method of old fashioned perturbation theory is employed. This theory or, equivalently the so-called light-cone perturbation theory, offers a way of treating an off-shell external fermion line.

While the $^1S_0$ fragmentation function has a single term, the $^3S_1$ fragmentation functions are expressed in the form of a diagonal spin density matrix of the $Q\bar{q}$ vector meson polarisation

$$D_1(z) = \begin{pmatrix} D_{11}(z) & 0 & 0 \\ 0 & D_{oo}(z) & 0 \\ 0 & 0 & D_{-1-1(z)} \end{pmatrix}. \tag{3.32}$$

Since $D_{-1-1(z)} = D_{11(z)}$, the diagonal elements of the D_1 matrix are denoted as

$$D_T(z) \equiv \left[D_{11}(z) + D_{-1-1}(z)\right]/2$$

$$D_L(z) \equiv D_{oo}(z). \tag{3.33}$$

where T and L stand for transverse and longitudinal polarisation, respectively. The final results of the calculation of the fragmentation functions in Suzuki's model are

$$D_o(z) = \frac{N}{zF(z)}\left\{\left[\frac{2m_Q + m_q}{m_Q + m_q} - \frac{m_Q + m_q}{m_Q}\frac{1}{z} - \frac{m_q(m_Q + 2m_q)}{m_Q(m_Q + m_q)}\frac{1}{1-z}\right.\right.$$

$$\left.\left. - \frac{\langle k_T^2 \rangle}{m_Q(m_Q + m_q)}\frac{z}{1-z}\right]^2 \frac{\langle k_T^2 \rangle}{m_Q^2}\frac{z^2}{(1-z)^2}\right\}, \tag{3.34}$$

$$D_T(z) = \frac{N}{zF(z)}\left\{\left[1 - \frac{m_q}{m_Q}\frac{1}{1-z}\right]^2 + \frac{\langle k_T^2 \rangle}{m_Q^2}\left[1 + \frac{1}{(1-z)^2}\right]\right\}, \tag{3.35}$$

57

$$D_L(z) = \frac{N}{zF(z)}\left\{\left[\frac{m_Q + m_q}{m_Q}\frac{1}{z} - \frac{m_Q m_q + \langle k_T^2 \rangle}{m_Q(m_Q + m_q)}\frac{z}{1-z}\right]^2 \right.$$

$$\left. + \left[\frac{m_Q - m_q}{M_Q + m_q}\right]^2 \frac{\langle k_T^2 \rangle}{m_Q^2}\frac{z^2}{(1-z)^2}\right\}, \tag{3.36}$$

where N is a normalisation constant, m_Q and m_q are the heavy and the light quark masses and $\langle k_T^2 \rangle$ is the average value of the squared transverse momentum. $F(z)$ is given by

$$F(x) \equiv \left[1 - \left[\frac{m_Q + m_q}{m_Q}\right]^2 \frac{1}{z} - \frac{m_q^2 + \langle k_T^2 \rangle}{m_Q^2}\frac{1}{1-z}\right]^4. \tag{3.37}$$

Equation (3.34) is used to represent the production of pseudoscalar mesons. For unpolarised vector mesons one uses

$$D(z) = 2D_T(z) + D_L(z). \tag{3.38}$$

Evaluation of the fragmentation functions for different states and also of the vector/pseudoscalar ratio is straightforward. The decay angular distribution of $D^* \to D\pi$ in the rest frame of D^* is

$$d\Gamma/d\Omega = 1 + \alpha(z)cos^2\theta, \tag{3.39}$$

and $\alpha(z)$ is determined as

$$\alpha(z) = \left[D_L(z) - D_T(z)\right]/D_T(z). \tag{3.40}$$

where θ is the emission angle of π(or D).

Like the Peterson model, these fragmentation functions have the behaviour $\sim (1-z)^2$ in the limit of $z \to 1$. In fact if the z dependence of the vertices in the figure (3.9) is ignored, the two models become identical.

3.6 The Amiri-Ji Model

Recently a phenomenological model for the prediction of heavy flavoured meson production was presented by Amiri and Ji. In this work second order perturbation theory is used to calculate the fragmentation functions to predict heavy meson production in e^+e^- annihilation. The essentials of the quark fragmentation in second order perturbation theory is shown in figure (3.10).
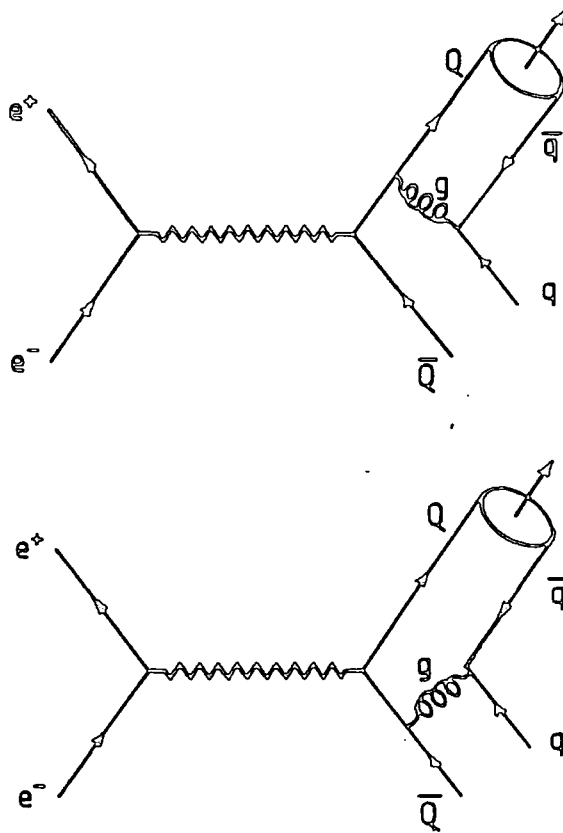
Figure (3.10) *Inclusive production of mesons in e^+e^- annihilation. Two more diagrams can be obtained by exchanging the primary and the secondary quark pair.*

The invariant amplitude $\mathcal{M}$ for the diagrams of fig.(3.10) is obtained from

$$\mathcal{M}(k_i, q_i) = \int [dx] T_H(k_i, q_i, x_i) \phi_M(x_i, q^2), \tag{3.41}$$

where $[dx] = dx_1 dx_2 \delta(1 - x_1 - x_2)$ with x_1 and x_2 being the momentum fractions carried by the constituent quarks of the bound state, T_H is the hard scattering amplitude which can be calculated perturbatively from the quark-gluon subprocesses and ϕ_M is the probability amplitude for finding the quarks inside the bound state (which are collinear up to the scale q^2 in a meson bound state). This amplitude is approximated to the following form

$$\phi(x_i, q^2) = C \delta(x_1 - r), \tag{3.42}$$

where $r = \frac{m_Q}{m_M}$ and C is a constant. This approximation is discussed in greater detail in chapter 5. Using (3.42) in (3.41) it follows that

$$\mathcal{M}(k_i, q_i) = C T_H(k_i, q_i, r). \tag{3.43}$$

The fragmentation functions are obtained from the defining relation

$$D(z) = \frac{1}{\sigma} \frac{d\sigma}{dz}, \tag{3.44}$$

by using the general form of (3.43) for pseudoscalar and vector meson production and integrating over the final state phase space. In the limit of $\frac{m_M^2}{s} << 1$, the final results of this model have the following approximate form:

$$D_0(z) = N_0 z(1 - z)^2 \left[\frac{e_Q^2}{(1 - r)^2} \frac{[1 + (1 - r)z]^2}{(1 - rz)^4} + \frac{e_q^2}{r^2} \frac{(1 + rz)^2}{[1 - (1 - r)z]^4} \right], \tag{3.45}$$

and

$$D_1(z) = N_1 z(1 - z)^2 \left[\frac{e_Q^2}{(1 - r)^2} \frac{[1 + (1 - r)z]^2 + 2z^2}{(1 - rz)^4} \right.$$

$$+\frac{e_q^2}{r^2}\frac{(1+rz)^2+2z^2}{[1-(1-r)z]^4}\Bigg],\tag{3.46}$$

for fragmentation of a singlet and triplet meson respectively, where N_0 and N_1 are normalisation constants and e_Q and e_q are the quark charges. According to the authors the predictions of (3.45) and (3.46) may differ by as much as 20%-50% for D and B mesons depending on the beam energy.

3.7 Radiative Corrections

All the above fragmentation models are parametrised directly in terms of z defined in (2.3). Although this procedure is commonly used it is not correct when the initial QED and QCD radiation of the heavy quark are taken into account. Since the effect of initial photon radiation is smaller than the similar gluon bremsstrahlung by a factor of α/α_s, the major enhancement of the fragmentation spectrum is incorporated by taking just the gluon radiation into account. In the following we will discuss the situation in which a single gluon is emitted by the heavy quark before hadronisation, as displayed in Figure (3.11).
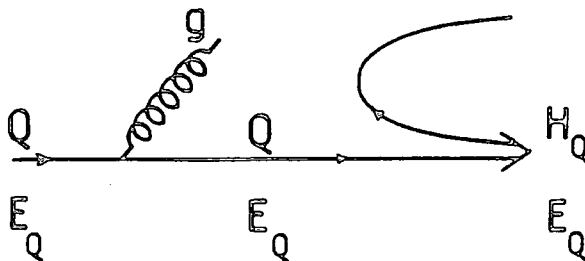
Figure (3.11) *The two step scheme of heavy hadron production from the initial heavy quark Q.*

Here we define

61

$$x_Q = \frac{(E + p_{\parallel})_Q}{(E + p_{\parallel})_{beam}}, \qquad (3.47)$$

and

$$x = x_H = \frac{(E + p_{\parallel})_H}{(E + p_{\parallel})_{beam}}. \qquad (3.48)$$

Following the two steps of the diagram in figure(3.11), we write the corrected fragmentation functions as

$$D_Q^h(x) = N \int_x^1 \frac{dx_Q}{x_Q} P_{qq}(x_Q) D_Q^H(\frac{x}{x_Q}), \qquad (3.49)$$

where N is a normalisation constant and

$$P_{qq} = C_F \left\{ \frac{1 + x_Q^2}{1 - x_Q} \right\}, \qquad (3.50)$$

is the Altarelli-Parisi splitting function [50]. The function $D_Q^h(z = x/x_Q)$ is the usual fragmentation function which satisfies the normalisation condition

$$\int_0^1 dz D_Q^h(z) = 1. \qquad (3.51)$$

In recent studies of heavy flavour physics prompt leptons are used as the signature for heavy quarks. It has been shown by Monte Carlo studies that the mean value of the lepton momentum depends not only on the quark mass but also on jet broadening due to gluon radiation[51]. This effect is particularly significant for the transverse momentum spectrum of leptons from c quark decay.

3.8 Conclusions and Comparison with Data

We have reviewed five different heavy quark fragmentation models in historical order. One important point which puts these models into two different categories, is the behaviour of the fragmentation functions in the limit $z \to 1$, a property that becomes more important for very heavy quarks. As we have seen

the Scott and the Collins-Spiller models behave like $(1 - z)$ in the above limit and therefore show a softer spectrum than the other models which all behave like $(1 - z)^2$ instead and exhibit harder behaviour.

The results of these models for the fragmentation of D, D^* and B mesons from charm and bottom quarks respectively, are shown in figures (3.12), (3.13) and (3.14). If we choose the set of data compiled in figure (2.5), then all models are acceptable. However choice of figure (2.6) makes the judgement more clear. Figure (3.13) shows such a comparison. Apart from the Amiri's model it seems the other models are consistent with the data and one can be hopeful that if we take the effects of the secondary fragmentation, radiative corrections and bound state effects into account the agreement becomes more close. There is a large difference between the Amiri-Ji and the other models in the prediction of D^* meson production. The results of the Amiri-Ji model employed the approximation discussed in section (3.6), which is supposed to affect the results by up to 50 % (according to the authors), so it is hard to understand this inconsistency.

We have applied our results of radiative correction (3.49) to the Peterson model to demonstrate its effect on fragmentation function. A similar behaviour is found with the other models. The effect of such a correction on the production spectrum of D meson is illustrated in figure (3.15).

Another quantity of experimental interest is $\langle z \rangle$. We have calculated this quantity for different models and compared them against experimental data from different collaborations in table (3.2).

The Suzuki and the Amiri-Ji models distinguish between pseudoscalar and vector meson production. This allows one to evaluate the V/(V+P) (vector/pseudoscalar) ratio and study the z dependence of this quantity. Here we compare the results of these two models for the z dependence of the V/(V+P) ratio. The results in the case of charm and bottom fragmentation appear in figure (3.16).

For top quark fragmentation we have chosen to illustrate the cases $m_t =$

40 and 100 GeV. The results of the models for the fragmentation of such a heavy quark are shown in figure (3.17) and (3.18). The fact that the models with the $(1-z)$ behaviour in the limit $z \rightarrow 1$ predict softer fragmentation, becomes much more obvious here. When the mass of the fragmenting quark is large, spin considerations become irrelevant as far as the $^3S_1$ and $^1S_0$ states are concerned. We have checked this for the Suzuki and the Amiri-Ji models. In the case of $m_t = 100$ GeV the difference between vector and pseudoscalar meson fragmentation functions does not exceed a few percent.

Table(3.2) Predictions of $\langle z \rangle$ compared with the data.

	$\langle z \rangle_{D^*}$	$\langle z \rangle_{D^\circ}$	$\langle z \rangle_{B^\circ}$
Scott	0.651	0.649	0.719
Peterson etal	0.627	0.627	0.793
Collins-Spiller	0.680	0.600	0.720
Suzuki	0.631	0.655	0.800
Amiri-Ji	0.783	0.734	0.853
MARK-II	0.59±0.06		
HRS	0.56±0.02		
DELCO	0.60±0.10		
TASSO	0.57±0.08		
CLEO	0.68±0.10		
MARK-J		0.46±0.07	
CDHS		0.68±0.08	
MARK-J			0.75±0.03
MARK-II			0.79±0.06
TASSO			0.84±0.15
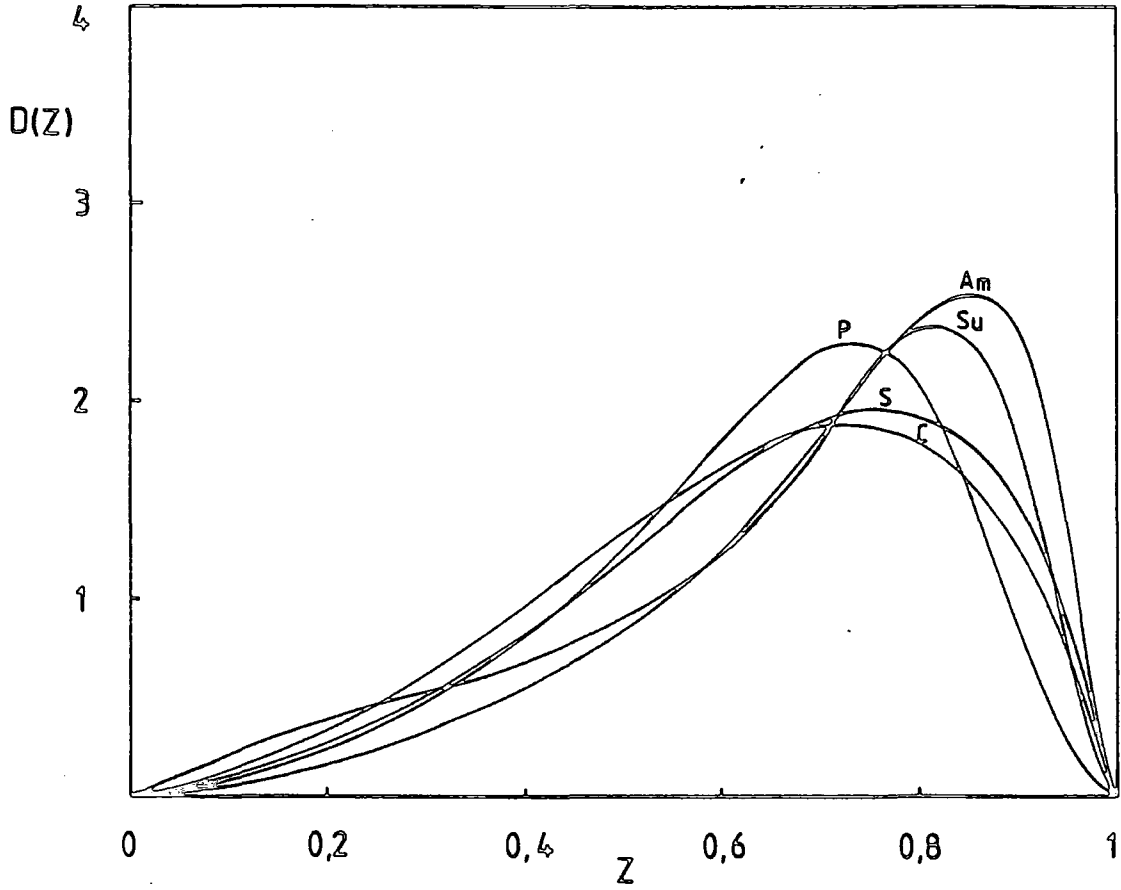
Figure (3.12) *Comparison of the different fragmentation functions for a charm quark fragmenting into a D meson. The models are S: Scott, P: Peterson et al, C: Collins-Spiller, Su: Suzuki and Am for the Amiri-Ji model.*
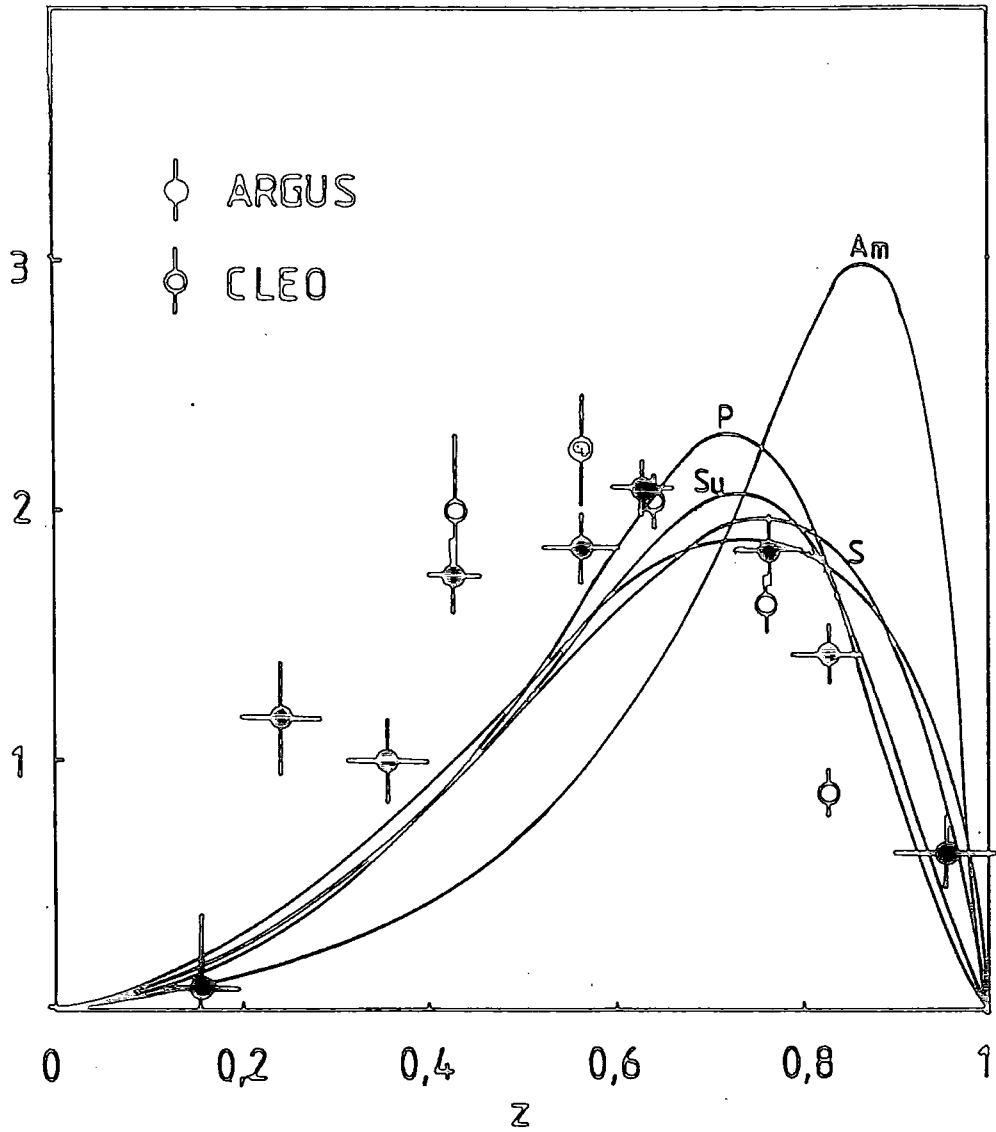
Figure (3.13) *The same as (3.11) for* D^* *fragmentation compared with the experimental data compiled in chapter 2* [24].
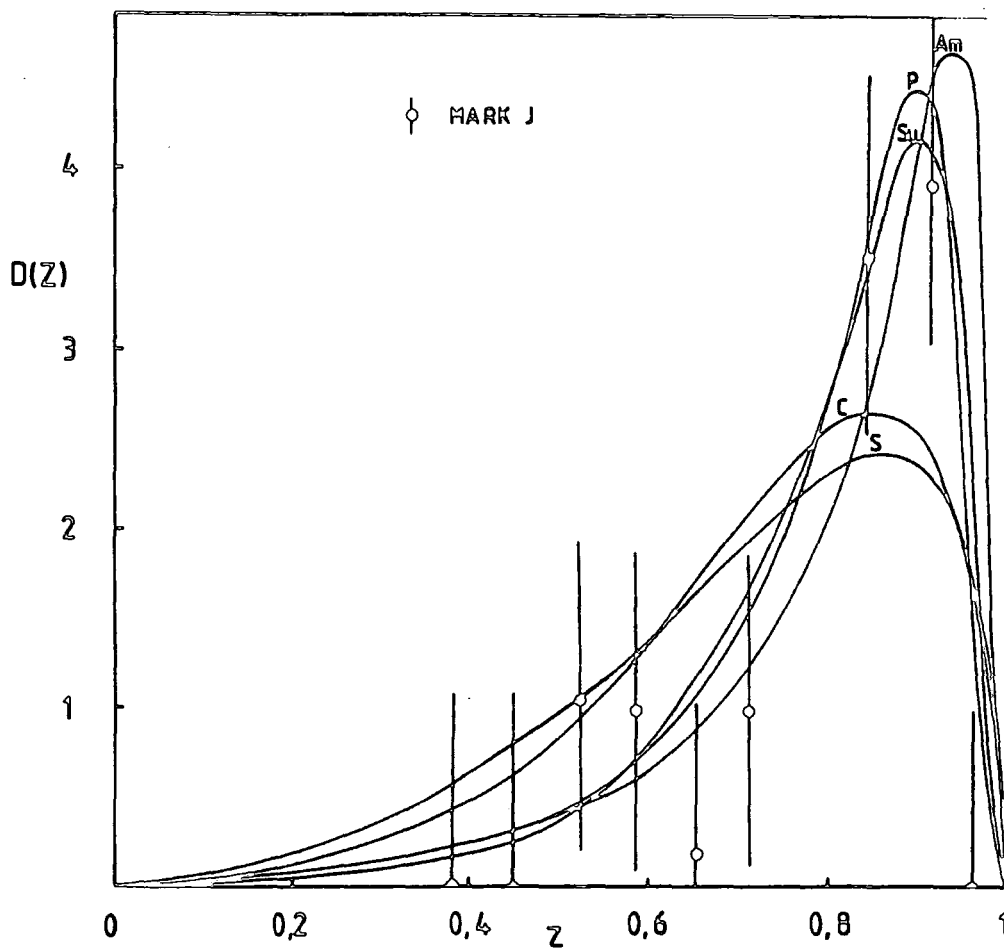
Figure (3.14) *The same as (3.11) for the case of B fragmentation compared with experimental data*[23] .
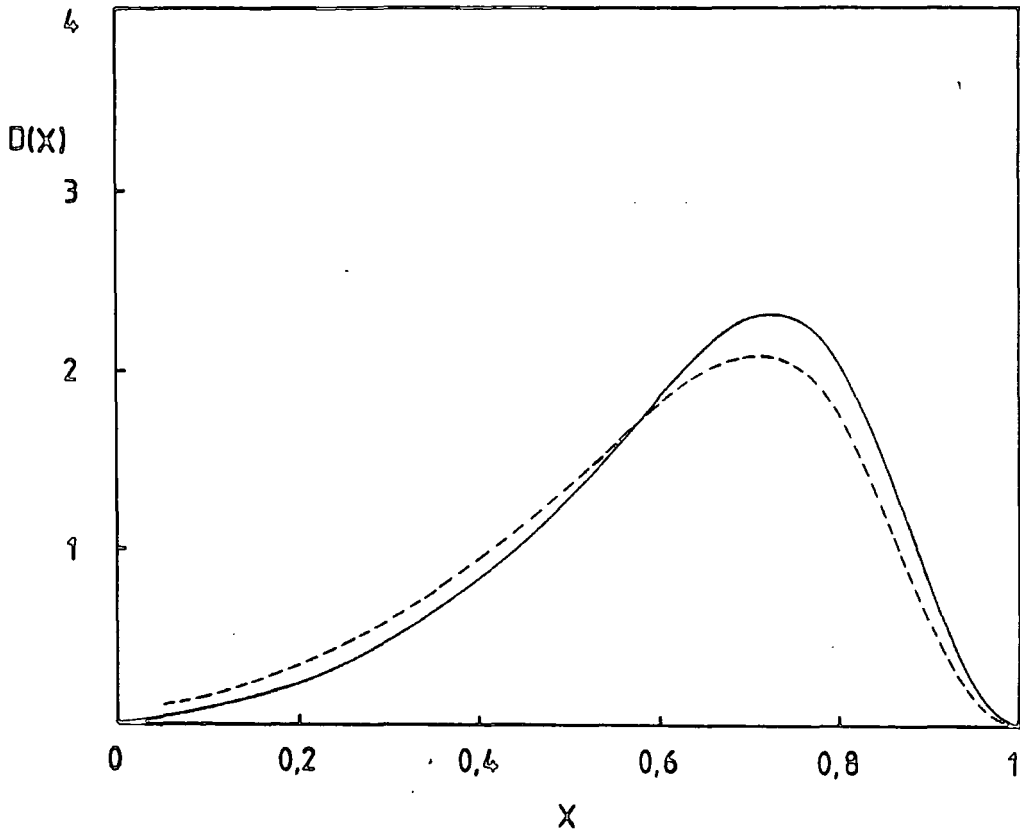
Figure (3.15) *The effect of a single gluon emission before the fragmentation of the charm quark in the Peterson model. the dashed and solid lines represent the model with and without correction respectively.*

68
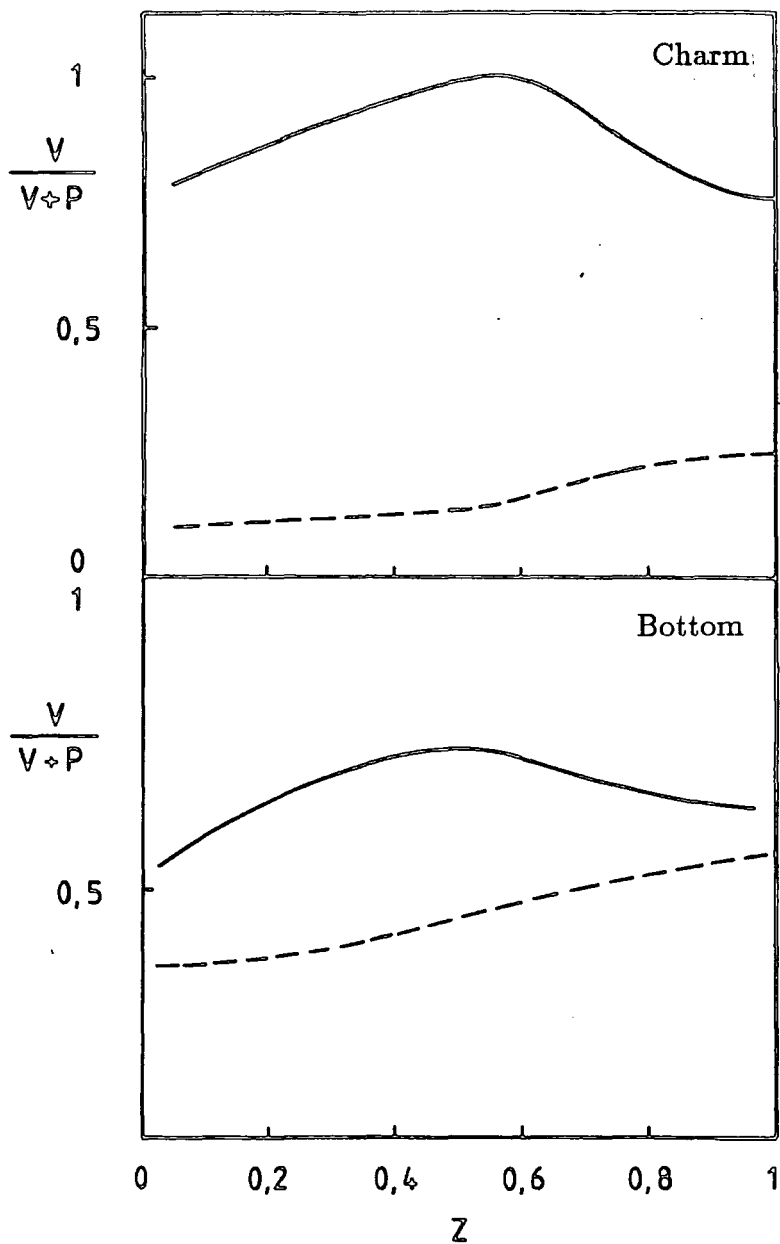
Figure (3.16) *Comparison of the $V/(V + P)$ ratio for Suzuki (solid) and Amiri (dashed) models.*
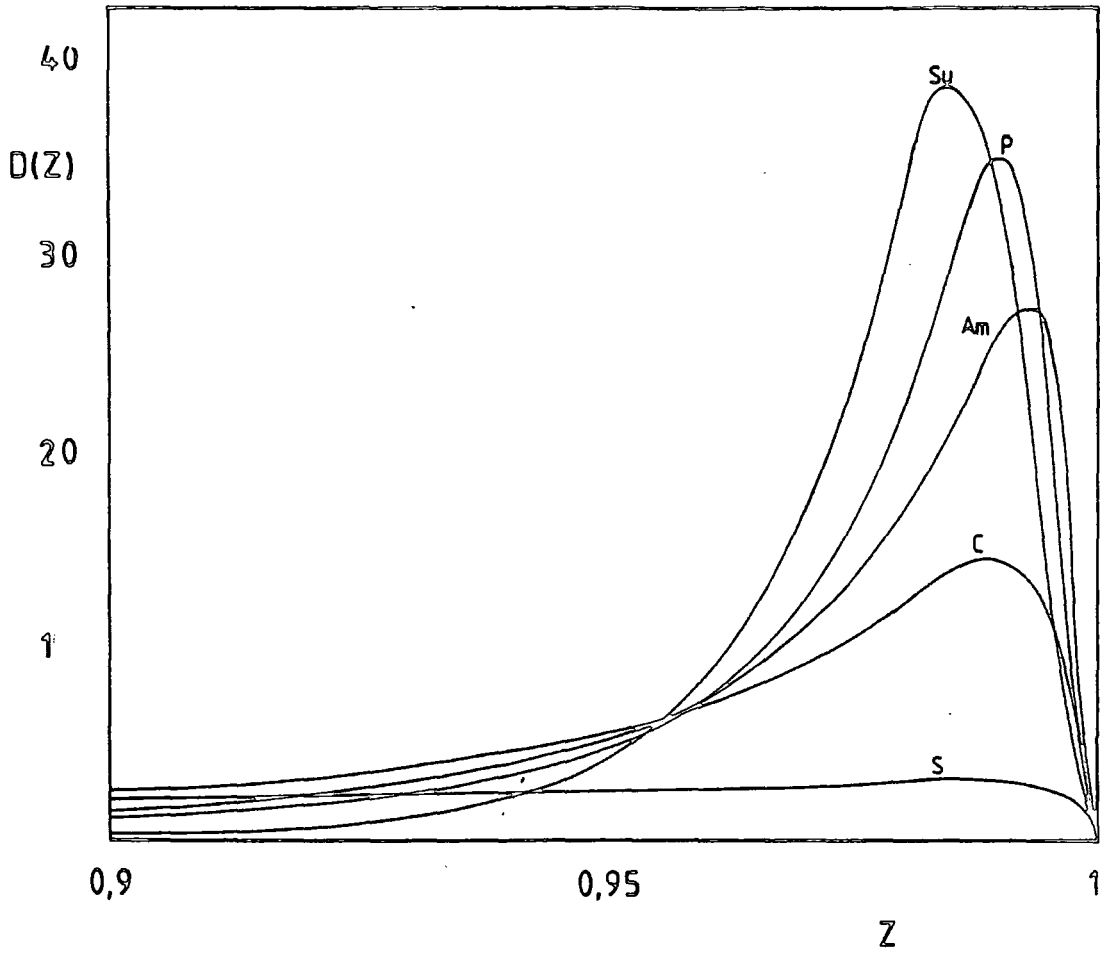
Figure (3.17) *The same as (3.11) for the case of a hypothetical top quark of mass 40 GeV.*
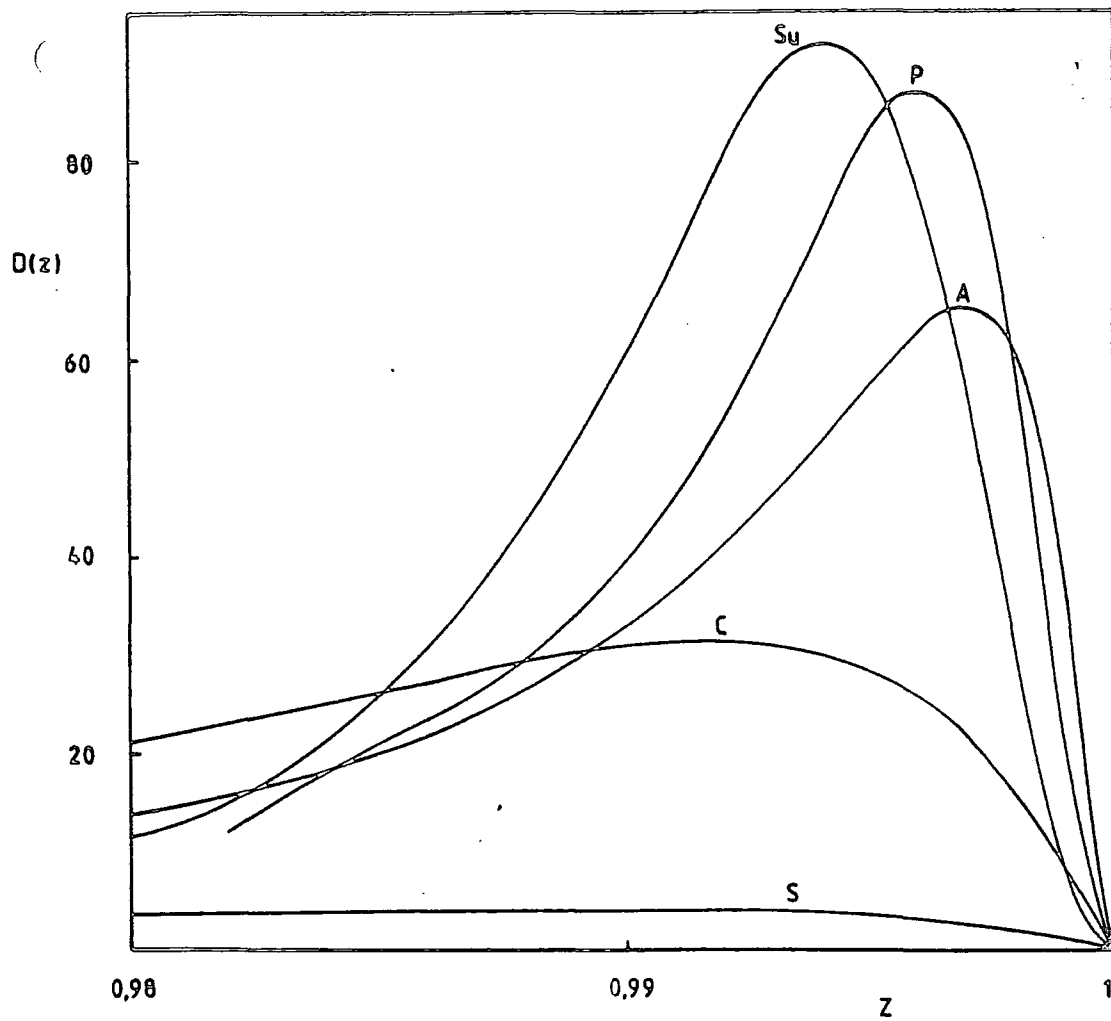
Figure (3.18) *The same as (3.11) in the case of a hypothetical top quark of mass 100 GeV.*

CHAPTER 4

SPIN PROPERTIES OF HEAVY QUARK FRAGMENTATION

The models due to Suzuki and Amiri which we introduced in last chapter, deal with the spin properties of heavy quark fragmentation process and both have the behavior $(1-z)^2$ in the limit $z \to 1$. In this chapter we look at the spin properties of the Collins-Spiller model because this model is consistent with the dimensional counting rules which demand the behavior $\sim (1-z)$ in the same limit.

We repeat their calculation of fragmentation functions for different polarisation states of the produced meson by considering the helicities of the constituents of the bound state when these are probed by a polarised photon. The fragmentation functions for the longitudinal and the transverse polarisation states are obtained by using an appropriate behaviour for these functions consistent with the dimensional counting rules. Like the relevant structure functions, the fragmentation functions for different spin states show different behavior at large z in agreement with the reciprocity relation [52, 53].

As the original Collins-Spiller model, the present model is sensitive to the variation of transverse momentum, and one can expect that the process of secondary fragmentation will soften the fragmentation function. However with $\langle k_T^2 \rangle = 0.3$ GeV^2, which seems quite reasonable, the predictions of this model are satisfactory for both charm and bottom fragmentation. The z dependence of the V/(V+P) ratio in this model is comparable to that of the Suzuki and Amiri models which are given in chapter 3.

4.1 The Model

The basis of this model is the same as the Collins-Spiller model which we

reviewed in section (3.3). We use the same vertex function[54] but distinguish the different spin components. We rewrite the function as

$$\Gamma = Cg(z_M, z_q)G^{1/2}(k_{T_M}^2)G^{1/2}(k_{T_q}^2)\bar{u}_Q(p_Q)v_{\bar{q}}(k_q) \qquad (4.1)$$

To determine the function g, which controls the longitudinal momentum behaviour, we adopt the single gluon approximation to the meson bound state. This approximation has been employed to determine the behaviour of the pion structure function in the limit $x \to 1$ by Gunion, Berger and Brodsky[55]. They obtained

$$\nu W_2(\nu, Q^2) \sim F_2(x) \sim (1 - x)^2 + \frac{2}{9}\frac{\langle k_T^2 \rangle}{Q^2}, \qquad (4.2)$$

in the limits $Q^2 \to \infty$ and $x \to 1$ respectively. The two terms in (4.2) are the contributions to the transverse (scaling) and the longitudinal (nonscaling) parts of the structure functions respectively. Correspondingly, following our discussion in section 3.3a we choose

$$|g_T|^2 \sim -z^3(1 - z)^2, \qquad (4.3)$$

and

$$|g_L|^2 \sim -\frac{2}{9}\frac{\langle k_T^2 \rangle}{Q^2}z^2, \qquad (4.4)$$

which are smooth continuations of the two parts in (4.2) as $z \to 1$. We shall evaluate the spinor part of the vertex function when we calculate the fragmentation functions.

4.2 Calculation of the Fragmentation Functions

First we use the vertex function Γ, given in (4.1), along with the general form of $|g^2|$, to obtain the forward amplitude for the fragmentation of a vector meson. Using the diagram of figure (3.5b), we write this amplitude as

$$A_1 = \frac{ie^2 e_Q^2 |C|^2}{(2\pi)^4} \int \frac{d^4 p_Q d^4 k_q z_M^2 z_q G(k_{T_M}^2) G(k_{T_q}^2) \delta(p_Q - k_M - k_q)}{(p_Q^2 - m_Q + i\epsilon)(p_Q^2 - m_Q - i\epsilon)(q^2 + i\epsilon)(q^2 - i\epsilon)}$$

$$\times \frac{\delta(p_Q - k_M - k_q)}{p_Q^2 - q^2 - m_Q + i\epsilon)(k_q^2 - m_q^2 + i\epsilon)} \bar{u}(p_l)\gamma^\mu u(p_l + q) \sum_\lambda \bar{u}_{Q,\lambda}(p_Q) v_{q,\lambda}(k_q)$$

$$\times (\not{k}_q + m_q)(\not{p}_Q + m_Q)\gamma_\mu(\not{p}_Q + \not{q} + m_Q)\gamma_\nu(\not{p}_Q + m_Q)$$

$$\times \sum_\lambda \bar{v}_{q,\lambda} u_{Q,\lambda}(p_Q)\bar{u}(p_l + q)\gamma^\nu u(p_l), \qquad (4.5)$$

where we have used the previous notation for the momenta and quark masses. Here λ indicates the helicities of Q and $\bar{q}$ and $\sum_\lambda \bar{u}_{Q,\lambda}(p_Q) v_{q,\lambda}(k_q)$ specifies that the $\bar{u}v$ bound state is a vector.

According to the Cutkosky rules[56] the discontinuity of the amplitude A_1 can be written as

$$Disc(A_1) = \frac{ie^2 e_Q^2 |C|^2}{(2\pi)^4} \int \frac{d^4 p_Q d^4 k_q |g|^2 G(k_{T_M}^2) G(k_{T_q}^2) \delta(p_Q - k_M - k_q)}{(p_Q^2 - m_Q + i\epsilon)(p_Q^2 - m_Q - i\epsilon)(q^2 + i\epsilon)(q^2 - i\epsilon)}$$

$$\times \theta(k_q^0)\delta(k_q^2 - m_q^2)\theta[(p_Q - q)^0]\delta[(p_Q - q)^2 - m_Q]$$

$$\times \frac{1}{4}L^{\mu\nu}(p_l, p_l + q)\frac{1}{4}T_{4\mu\nu}(k_M, p_Q, p_Q - q, p_Q)T_2^1(-k_M, k_q) \qquad (4.6)$$

where the θ's are usual step functions. The δ functions put the respective particles on their mass shells. The mass of the electron is neglected for simplicity and the leptonic tensor is defined by

$$L^{\mu\nu}(p_l, p') \equiv tr[\not{p}_l'\gamma^\mu \not{p}_l \gamma^\nu], \qquad (4.7)$$

in which $p' = p_l + q$, while the hadronic tensors are

$$T_{4\mu\nu} = tr[(\not{k}_q + m_q)(\not{p}_Q + m_Q)\gamma_\mu(\not{p}_Q + \not{q} + m_Q)\gamma_\nu(\not{p}_Q + m_Q)], \qquad (4.8)$$

and

74

$$T_2^1(-k_M, kq) = \frac{1}{2}tr[(\rlap{/}{k}_q - m_q)\rlap{/}{\epsilon}(-\rlap{/}{k}_M + m_M)(-\rlap{/}{k}_M + m_M)\rlap{/}{\epsilon}(\rlap{/}{k}_q - m_q)]. \quad (4.9)$$

In (4.9) ϵ is the polarisation vector for the vector meson and $|g|^2$ in (4.6) is either (4.3) or (4.4) for the transverse or longitudinal cases respectively . Next we change (4.6) into light-cone notation using

$$d^4k = \frac{1}{2}dk^+ d^2k_T dk^- = \frac{1}{2x}dx d^2k_T d(k^2) \quad (4.10)$$

and

$$d^4k_n \delta^4\left[k_M - \sum_{i=1}^{n} k_i\right] = dx_n \delta\left[1 - \sum_{i=1}^{n} x_i\right] d^2k_{Tn} \delta^2\left[\sum_{i=1}^{n} k_{Ti}\right]$$

$$\times d(k_n^2)\delta\left[x_n\left[m_M^2 - \sum_{i=1}^{m} \frac{k_i^2 + k_{Ti}^2}{x_i}\right]\right], \quad (4.11)$$

and put the resulting expression back into the equation for the fragmentation function calculated for this model by Collins and Spiller (i.e. eq. (3.28)), so

$$3e_Q^2 D_Q^{Mq}(z_M)\sigma(e^+e^- \longrightarrow \mu^+\mu^-) = \int \frac{d^2k_{TM}}{16\pi^3 z_M} \frac{2}{h} \text{Disc}(A), \quad (4.12)$$

and on cancelling the common factors from both sides, we find

$$D_1^{Mq}(z) = \frac{e^2 e_Q^2 |C|^2}{\sigma(e^+e^- \longrightarrow \mu^+\mu^-)h} \int \frac{dz_q d^2k_{TM} d^2k_{Tq}|g^2|}{(p_Q^2 - m_Q^2 - i\epsilon)(p_Q^2 - m_Q^2 - i\epsilon)}$$

$$\times \frac{\delta^2(\mathbf{k}_{TM} + \mathbf{k}_{Tq})}{(q^2 + i\epsilon)(q^2 - i\epsilon)} G(k_{TM}^2)G(k_{Tq}^2)d(k_q^2)\delta(k_q^2 - m_q^2)$$

$$\times d(p_Q)\delta(p_Q^2 - m_M^2 - k_q^2 - 2k_M.k_q)$$

$$\times \frac{1}{4}L^{\mu\nu}(p_l, p_l + q)\frac{1}{4}T_{4\mu\nu}^1(k_M, p_Q, p_Q - q, p_Q)T_2(-k_M, k_q). \quad (4.13)$$

Next we write $\sigma(e^+e^- \longrightarrow \mu^+\mu^-)$ in the same notation, i.e.

$$\sigma(e^+e^- \longrightarrow \mu^+\mu^-) = \frac{2\pi e^4}{64\pi^3 h} \int \frac{dp^+ d^2 p_T}{q^4 p^+}$$

$$\times \theta\big[(q-p)^\circ\big]\delta\big[(q-p)^2 - m^2\big]L^{\mu\nu}T_{2\mu\nu}(p,p-q), \qquad (4.14)$$

where $L^{\mu\nu}$ is the same as (4.7) and $T_{2\mu\nu}$ is given by

$$T_{2\mu\nu} = tr\big\{(\not p + m)\gamma_\mu(\not p + q + m)\gamma_\nu\big\}. \qquad (4.15)$$

On cancelling the common factors we obtain

$$D_1^{Mq}(z) = -\frac{\zeta_q \zeta_Q |C|^2}{64\pi^3} \int \frac{dz_q d^2 k_{T_M} d^2 k_{T_q}}{z_M z_q} |g^2|\delta(1 - z_M - z_q)$$

$$\times G(k_{T_M}^2)G(k_{T_q})\delta^2(\mathbf{k}_{T_M} + \mathbf{k}_{T_q})\delta(k_q^2 - m_q)$$

$$\times d(p_Q^2)d(k_q^2)\delta(p_Q^2 - m_M - k_q^2 - 2k_M.k_q)$$

$$\times \frac{-2k_M.k_q + 2m_M m_q}{(p_Q^2 - m_Q^2)^2}\big[2k_M.p_Q + 2m_M m_Q - z_M(p_Q^2 - m_Q^2)\big]. \qquad (4.16)$$

Now we use the kinematics of the process to obtain the final result for the fragmentation functions. The original heavy quark is off its mass shell and p_Q^2 is determined by demanding overall momentum conservation in the relevant vertex, i.e.

$$p_Q^2 = (k_M + k_q)^2$$

$$= m_M^2 + m_q^2 + \frac{x_M}{x_q}(k_q^2 + k_{Tq}^2) + \frac{x_q}{x_M}(k_M^2 + k_{TM}^2) + 2k_T^2, \qquad (4.17)$$

where we have used the fact that $\mathbf{k}_{TM} = -\mathbf{k}_{Tq}$. Next we employ the defining relations of z_M and z_q, (3.13), to write

$$p_Q^2 = (m_M^2 + k_T^2) + (m_q^2 + k_T^2)$$

$$+ \frac{z_q}{z_M}(m_M^2 + k_T^2) + \frac{z_M}{z_q}(m_q^2 + k_T^2)$$

$$= \frac{(m_M^2 + k_T^2)}{z_M} + \frac{(m_q^2 + k_T^2)}{z_q}. \qquad (4.18)$$

Other dot products are treated in a similar way. We can perform the transverse momentum integration[57] and do the delta function integration by imposing the condition that $z = z_M = 1 - z_q$. Finally to obtain the transverse and the longitudinal fragmentation functions we use the appropriate form of $|g^2|$, (4.3) or (4.4), and find

$$D_T(z) = N' z^2 (1 - z) F(z), \qquad (4.19)$$

and

$$D_L(z) = N'' z F(z)/(1 - z), \qquad (4.20)$$

where

$$F(z) \equiv \left[\frac{1 - z}{z}(m_M^2 + \langle k_T^2 \rangle) + \frac{z}{1 - z}(m_q^2 + \langle k_T^2 \rangle) + 2\langle k_T^2 \rangle + m_M m_q \right]$$

$$\times \left[\frac{(m_M^2 + \langle k_T^2 \rangle)}{z} + z m_Q^2 + 2 m_M m_Q \right]$$

$$\times \left[m_Q^2 - \frac{(m_M^2 + \langle k_T^2 \rangle)}{z} - \frac{(m_q^2 + \langle k_T^2 \rangle)}{1 - z} \right]^{-2}. \qquad (4.21)$$

Since $F(z) \sim (1 - z)$, it is clear that (4.19) and (4.20) have different limits as $z \to 1$. These limits are the same as the respective structure functions in (4.2) in agreement with reciprocity.

4.3 Charm and Bottom Quark Fragmentation

Fragmentation into a pseudoscalar or an unpolarised vector meson are represented by $D(z) = D_L(z) + 2D_T(z)$ in this model, where D_L and D_T are

the longitudinal and the transverse fragmentation functions given by equations (4.19) and (4.20). We have also examined the fragmentation functions for a polarised vector meson state namely D_T and D_L for different values of $\langle k_T^2 \rangle$. They are as sensitive to the transverse momentum as the original model but for $\langle k_T^2 \rangle = 0.3$ GeV^2 they look quite satisfactory. We have sketched D_T, D_L and $(2D_T + D_L)$ for charm and bottom fragmentation in figure (4.1) and (4.2). The longitudinal fragmentation function is an increasing function with its maximum at $z = 1$. This is reflected in the predicted fragmentation functions for pseudoscalar and vector meson production. The curves are drawn with the transverse fragmentation function normalised to one. The prediction of this model for the V/(V+P) ratio is shown in figure (4.3). This is comparable to figure (3.16) in which the same results for the Suzuki and the Amiri fragmentation models are shown. Finally we compare the prediction of this model with data on charm and bottom fragmentation in figure (4.4).

4.4 Conclusions

In the original model the spin averaged fragmentation function $D(z) \sim (1 - z)$ in accordance with the dimensional counting rules. However if the structure functions have the behaviour (4.2) then the transverse and the longitudinal fragmentation functions $\sim (1 - z)^2$ and $\sim$ constant respectively, as is clear from (4.19) and (4.20).

The prediction of the V/(V+P) ratio in this model is somewhat lower than other models. Although one can employ the process of secondary fragmentation to give more softening of the fragmentation functions, the results of this model for charm and bottom fragmentation are in good agreement with the data.
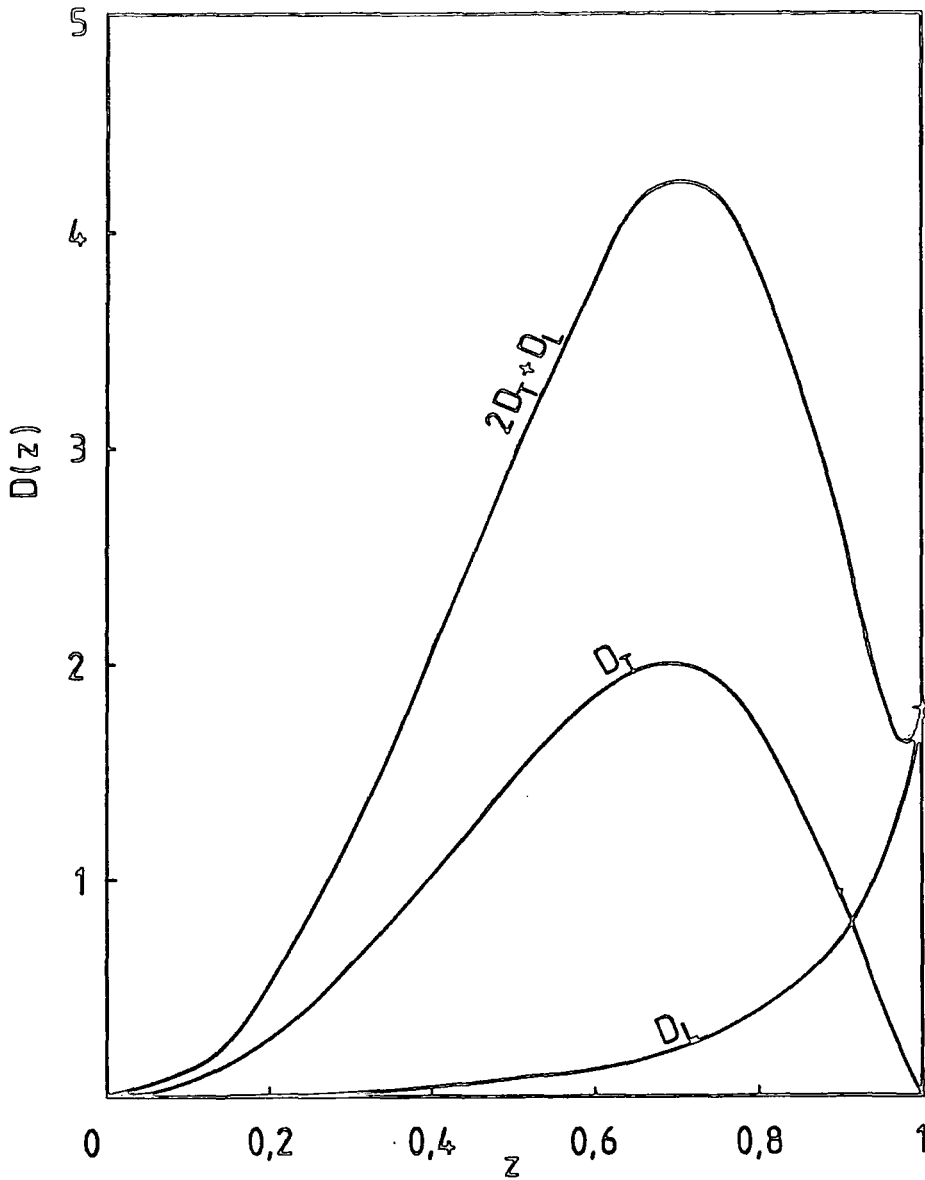
Figure (4.1) . *Figure shows the behavior of DT and D_L and $(2D_T + D_L)$ fragmentation functions in terms $\langle k_T^2 \rangle = 0.3$. The D^* fragmentation function is normalized to one.*
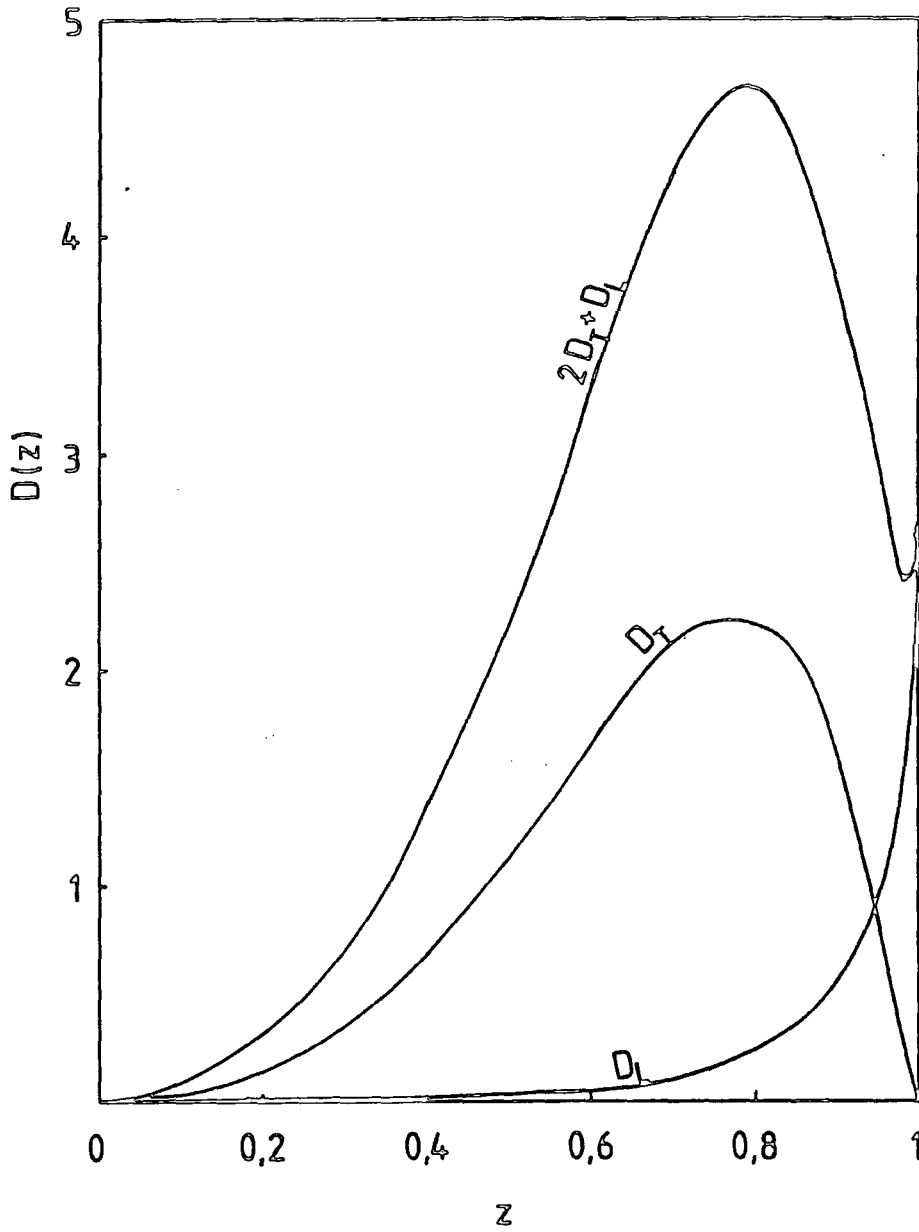
Figure (4.2) . *The same as figure (4.2) but for the case of bottom fragmentation.*
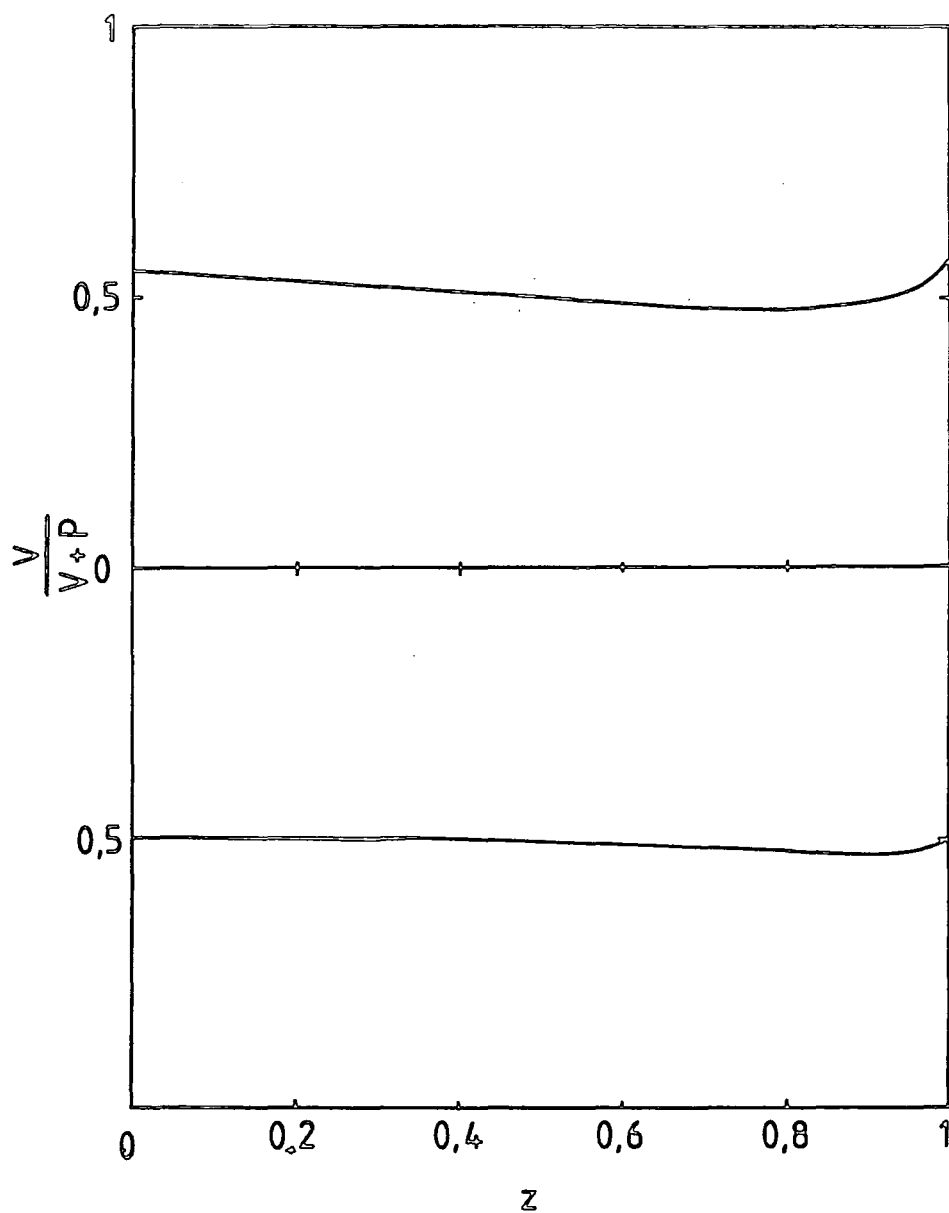
Figure (4.3) . *Prediction of the present model for the ratio of V/(V+P) for charm and bottom fragmenation.*
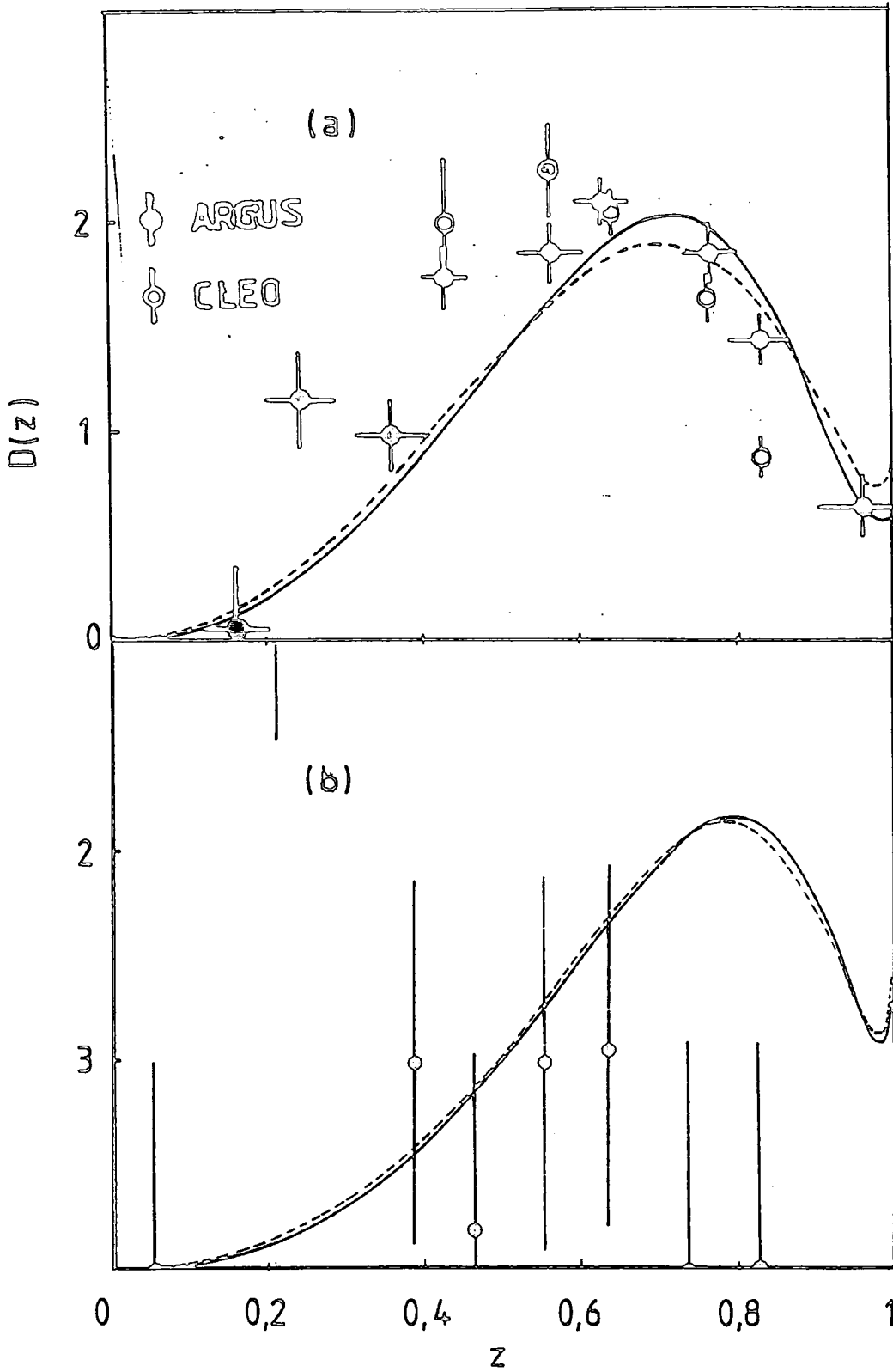
Figure (4.4) .*Comparison of charm and bottom quark fragmentation with data. The dashed and the solid lines shows the spectrum of a vector and a pseudoscalar fragmentation functions respectively* [28].

CHAPTER 5

WAVEFUNCTION APPROACH TO HEAVY
QUARK FRAGMENTATION

In this chapter we study the spin properties of heavy quark fragmentation in e^+e^- annihilation using a non-relativistic approach to the wavefunction of the final state hadron. We have chosen the method of the light-cone perturbation theory[58] (a brief review of this theory and Feynman rules are given in an appendix at the end of the thesis) and used the well established idea that the total amplitude for a process involving a bound state is a convolution of the hard scattering amplitude, which is calculated from the quark-gluon sub-process, together with the hadron's bound state wavefunction. We show that in this kind of calculation the final result is ultimately equivalent to multiplying the square of the transition amplitude by the bound-state wavefunction and integrating over the final state phase space.

The kinematics of the calculation are such that the fragmentation functions depend upon the transverse momentum of the process and that of the constituents inside the bound state. We demonstrate the effect of these transverse momenta explicitly.

We have compared our results with those of Suzuki, who has performed a similar calculation but used a delta function wavefunction to represent the distribution of the bound state constituents , and with the available experimental data on charm and bottom quark fragmentation. Our results give good agreement with the data for reasonable values for the transverse momenta. The fragmentation functions have the z dependence $\sim (1-z)^2$ in the limit $z \longrightarrow 1$

which is consistent with the behaviour expected in the phenomenological model due to Peterson, *et al.*

5.1 The Model

A typical diagram of the quark fragmentation in e^+e^--annihilation, to second order of perturbation theory, is shown in figure (5.1). There are three other topological possibilities of the same order but we assume that for the heavy quarks the dominant contribution to the probability amplitude comes from this diagram. To be more precise we assume that the probability of the light quark being produced by the heavy anti-quark catching up with the heavy quark to form the bound state, or the probability of heavy quarks being pair produced by the gluon, are considerably smaller.
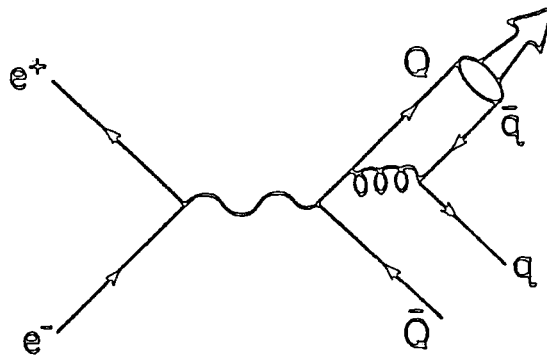
Figure (5.1) *Diagram for quark fragmentation in second order of perturbation theory. There are three other possible diagrams in the same order. The relevant four momenta are labelled.*

It is also assumed that whatever happens to the left of the gluon emission in figure (5.1), will not affect the energy-momentum partition between the final

84

state particles. This assumption was originally adopted by Peterson *et al.*, to derive their popular model.

Although these assumptions may not be valid for the production of light quarks, for the case of heavy quarks they seem quite reasonable. These approximations reduce the complexity of the final results considerably, particularly since we are interested in the analytical forms of the fragmentation functions.

We calculate the perturbative part of the diagram using light-cone perturbation theory. This choice of gauge is suitable for the case where the original heavy quark is off its mass shell. For the non-perturbative part we assume that the constituents of the bound state are effectively non-relativistic in the sense that gluon emission, higher order Fock states, and the retardation of the effective potential can be neglected [59]. The quark distribution is then controlled by the non-relativistic wavefunction for which we assume the following simple form[60]

$$\psi_M(x_i, q_{Ti}) = \frac{C}{x_1^2 x_2^2 \left[m_M^2 - \frac{(m_Q^2 + q_{TQ}^2)}{x_1} - \frac{(m_q^2 + q_{T\bar{q}}^2)}{x_2} \right]^2}, \qquad (5.1)$$

where m_M, m_Q and m_q are the masses of the meson, the heavy quark, and the light quark, respectively. The q_T's are the transverse momenta of the constituents with $\sum_{i=1}^{2} q_{Ti} = 0$, the x_i's are the light-cone momentum fractions satisfying $\sum_{i=1}^{2} x_i = 1$ and C is a normalisation factor. It can be shown that the above wavefunction is the solution of the Schrodinger equation with a Coulomb potential, which is the non-relativistic limit of the Bethe-Salpeter equation with a QCD kernel (for equal or unequal constituent masses[61]).

It is important to note that the wavefunction given in (5.1) is boost-invariant along the direction of motion of the bound state. We have sketched ψ_M against q_T in figure (5.2). The longitudinal momentum of the meson is

assumed to be partitioned between the consituents of the bound state according to their masses so that they stay together.
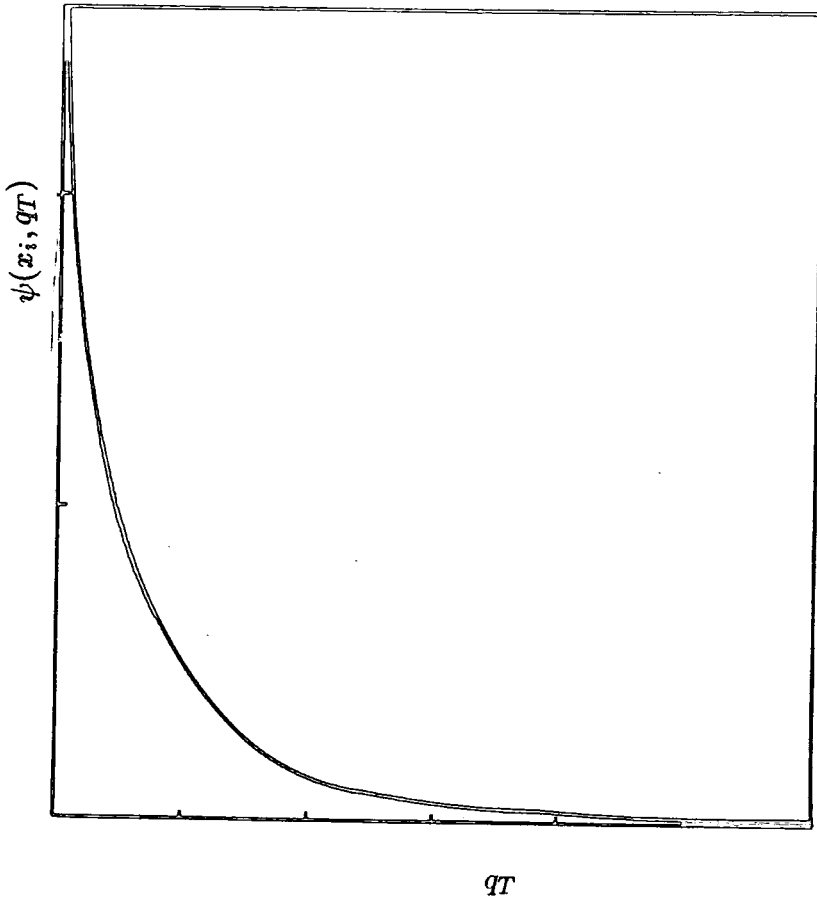
Figure (5.2) *Behaviour of (5.1) with respect to the transverse momenta for charmed meson. Note that $q_T^2 = q_{TQ}^2 = q_{T\bar{q}}^2$.*

5.2 The Kinematics

In light-cone perturbation theory all quanta are forward moving. So we write the relevant four-momenta as follows

$$\begin{cases} p_\mu = \left[(m_Q^2 + p^2)^{1/2}, \mathfrak{q}_T, \quad p_3 \right] \\[2mm] k_\mu = \left[(m_q^2 + k^2)^{1/2}, -\mathfrak{q}_T, \quad k_3 \right] \\[2mm] k'_\mu = \left[(m_q^2 + k'^2)^{1/2}, \mathfrak{k}_T, k_L \right] \\[2mm] p'_\mu = \left[\left[m_Q^2 + (p + k + k')^2\right]^{1/2}, \mathfrak{k}_T, k_L + (x_1 + x_2)P_3 \right], \end{cases} \qquad (5.2)$$

where P_3 refers to the longitudinal momentum of the meson. The three momentum configuration is shown in figure (5.3).
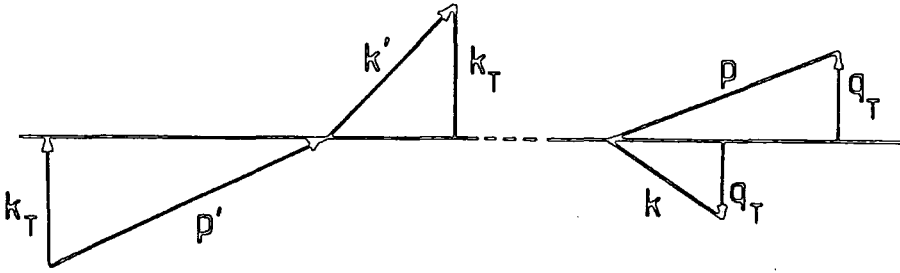
Figure (5.3) *Illustration of the kinematics in (5.2).*

We use the definition of the fragmentation parameter z as in (2.3), i.e.

$$z = \frac{(E + p_\parallel)_{hadron}}{(E + p_\parallel)_{beam}}. \qquad (5.3)$$

Here E and $p_\parallel$ refer to the energy and the longitudinal component of the relevant four momenta. To parametrise the four momenta of the quarks in terms of the fragmentation parameter, and the energy and momentum of the initial heavy quark, we write

$$\begin{cases} p^+ = x_1 P^+ \\[2mm] k^+ = x_2 P^+, \end{cases} \qquad (5.4)$$

where $p^+ \equiv p^0 + p^3$ and so on, and P refers to the momentum of the meson as before. This gives:

$$k^+ = \frac{x_2}{x_1} p^+. \qquad (5.5)$$

We can also write (5.3) in the following form

$$p^+ + k^+ = p'^+ z. \qquad (5.6)$$

Using (5.5) and (5.6) and energy momentum conservation we are led to the following parametrisation:

$$\begin{cases} p^+ = x_1 z p'^+ \\[2ex] k^+ = x_2 z p'^+ \\[2ex] k'^+ = (1-z) p'^+ \\[2ex] p'^+ = p'^+. \end{cases} \qquad (5.7)$$

In the light-cone notation the dot product of two four vectors p and k is given by

$$2p.k = (p^+ k^- + p^- k^+) - 2\mathbf{p}_T.\mathbf{k}_T, \qquad (5.8)$$

where $p^- \equiv p^0 - p^3$, etc. It is easily shown that

$$2p.k = \frac{p^+}{k^+}(k^2 + k_T^2) + \frac{k^+}{P^+}(p^2 + p_T^2) - 2\mathbf{p}_T.\mathbf{k}_T. \qquad (5.9)$$

We use (5.9) to replace the dot products in the calculation of the fragmentation functions.

5.3 Calculation of Fragmentation Functions

First we calculate the relative probability for a heavy quark Q and a light anti-quark $\bar{q}$ to form a spin singlet or triplet as in figure (5.1). In the light-cone gauge, using QCD factorisation, we write the probability amplitude for the production of a $^1S_0$ state meson as

$$T_0 = \frac{m_q m_Q g^2}{\sqrt{2}} \int_0^1 [dx] \int_0^\infty \frac{d^2 q_T}{16\pi^3} \psi(x_i, q_T i)$$

$$\times \left[\frac{\bar{u}_\uparrow(p)}{\sqrt{p^+}} \gamma^\mu \frac{u(p')}{\sqrt{p'^+}} \frac{\bar{u}(k')}{\sqrt{k'^+}} \gamma_\mu \frac{v_\downarrow(k)}{\sqrt{k^+}} + \frac{\bar{u}_\downarrow(p)}{\sqrt{p^+}} \gamma^\mu \frac{u(p')}{\sqrt{p'^+}} \frac{\bar{u}(k')}{\sqrt{k'^+}} \gamma_\mu \frac{v_\uparrow(k)}{\sqrt{k^+}} \right]$$

$$\times \frac{\overline{T}}{(k+k')^2 (p^- + k^- + k'^- - p'^-)}, \qquad (5.10)$$

where g is the strong coupling which represents the vertices in figure (5.2), and $[dx] \equiv \delta(x_1 + x_2 - 1) dx_1 dx_2$. In (5.10) $(\uparrow, \downarrow)$ refer to the helicities of the Q and $\bar{q}$ respectively and the u's and v's are Dirac spinors. The factor $(k+k')^{-2}$ is due to the gluon propagator and $d \equiv (p^- + k^- + k'^- - p'^-)^{-1}$ arises because the initial heavy quark is off mass shell. This second factor is often called the energy denominator. And finally $\overline{T}$ represents everything else that occurs in the left of the gluon-emission vertex in figure (5.1). Using longitudinal momentum conservation it is easily shown that the energy denominator in the light-cone gauge is the same as in the usual notation, i.e.

$$d = (p^\circ + k^\circ + k'^\circ - p'^\circ)^{-1}. \qquad (5.11)$$

Using (5.11) we can rewrite (5.10) as

$$T_0 = \frac{m_q m_Q g^2}{16\pi^3 \sqrt{2}} \int_0^1 [dx] \int_0^\infty \frac{d^2 q_T \psi(x_i, q_T)}{\left[p^+ p'^+ k^+ k'^+ \right]^{1/2}}$$

$$\times \left[\overline{u}(k')\gamma_\mu \left[v_\downarrow(k)\overline{u}_\uparrow(p) + v_\uparrow(k)u_\downarrow(p) \right] \gamma^\mu u(p') \right]$$

$$\times \frac{\overline{T}}{(k + k')^2 \left[p^\circ + k^\circ + k'^\circ - p'^\circ \right]}. \tag{5.12}$$

Employing the projection operators for fermions and antifermions, namely

$$u(p) = \frac{1}{\sqrt{2m_Q(p^\circ + m_Q)}}(\not{p} + m_Q)u(0), \tag{5.13}$$

and

$$v(k) = \frac{1}{\sqrt{2m_q(k^\circ + m_q)}}(\not{k} - m_q)u(0), \tag{5.14}$$

we can express (5.12) in the following form:

$$T_\circ = \frac{\sqrt{m_q m_Q}g^2}{32\pi^3\sqrt{2}} \int_0^1 [dx] \int_0^\infty \frac{d^2q_T\psi(x_i, q_T)}{\left[(k^\circ + m_q)(p^\circ + m_Q)p^+ p'^+ k^+ k'^+ \right]^{1/2}}$$

$$\times \left[\overline{u}(k')\gamma_\mu(\not{k} - m_q)\gamma^5(\not{p} + m_Q)\gamma^\mu u(p') \right]$$

$$\times \frac{\overline{T}}{(k + k')^2 \left[p^\circ + k^\circ + k'^\circ - p'^\circ \right]}. \tag{5.15}$$

The denominator of the wavefunction in equation (5.1) vanishes at

$$x_1 = \frac{m_Q}{m_q + m_Q}, \tag{5.16}$$

so for simplicity we replace the wavefunction by the following delta function

$$\psi_M \cong C'\delta\left[x_1 - \frac{m_Q}{m_q + m_Q} \right], \tag{5.17}$$

where C' is a constant which will be absorbed into the overall normalisation factor. Using (5.17), (5.15) simplifies to

$$T_0 = \frac{\sqrt{m_q m_Q}\, C' g^2}{32\pi^3 \sqrt{2}} \int_0^\infty \frac{d^2 q_T \times \overline{T}}{(k+k')^2 \left[p^\circ + k^\circ + k'^\circ - p'^\circ\right]}$$

$$\times \frac{\left[\bar{u}(k')\gamma_\mu(\slashed{k} - m_q)\gamma^5(\slashed{p} + m_Q)\gamma^\mu u(p')\right]}{\left[(k^\circ + m_q)(p^\circ + m_Q)p^+ p'^+ k^+ k'^+\right]^{1/2}}. \qquad (5.18)$$

By a similar procedure we obtain the corresponding amplitude for triplet state $(^3S_1)$ production as

$$T = \frac{\sqrt{m_q m_Q}\, C' g^2}{32\pi^3 \sqrt{2}} \int_0^\infty \frac{d^2 q_T \times \overline{T}}{(k+k')^2 \left[p^\circ + k^\circ + k'^\circ - p'^\circ\right]}$$

$$\times \frac{\left[\bar{u}(k')\gamma_\mu(\slashed{k} - m_q)\slashed{\epsilon}(\slashed{p} + m_Q)\gamma^\mu u(p')\right]}{\left[(k^\circ + m_q)(p^\circ + m_Q)p^+ p'^+ k^+ k'^+\right]^{1/2}} \qquad (5.19)$$

where ϵ is the polarisation vector for the vector meson which satisfies

$$\epsilon^{(T)\mu}.P_\mu = \epsilon^{(L)\mu}.P_\mu = 0$$

and

$$\epsilon^{(T)\mu}.\epsilon_\mu^T = \epsilon^{(L)\mu}.\epsilon_\mu^{(L)} = -1. \qquad (5.20)$$

Here P_μ is the momentum of the meson, and L and T refer to the longitudinal and transverse polarisations of the $Q\bar{q}$ bound state.

The fragmentation functions are obtained by integrating the square of the transition amplitudes (5.18) and (5.19) over the final state phase space

$$\int \left[dk_T\right]\left[dk^+\right]\delta^{(2)}(k_T)\delta(k^+), \qquad (5.21)$$

where $\left[dk_T\right] = d^2q_T d^2k_T d^2q_T'$ and $\left[dk^+\right] = dp^+ dk^+ dk'^+$. The fragmentation functions obtained from (5.18) and (5.19) in this way are

$$D_0(z) = \frac{N'g^4}{z(1-z)} \sum_{spin} \int_0^\infty \frac{d^2q_T d^2q_T' d^2k_T}{(k+k')^2(k_1+k')^2 p^{\circ2}(p^\circ + k^\circ + k'^\circ - p'^\circ)^2}$$

$$\times \left[(\not{p}'+m_Q)\gamma^\mu(\not{p}_1+m_Q)\gamma^5(\not{k}_1-m_q)\gamma_\mu(\not{k}'+m_q)\gamma_\nu(\not{k}-m_q)\gamma^5(\not{p}+m_Q)\gamma^\nu\right], \quad (5.22)$$

and

$$D_{T,L}(z) = \frac{N'g^4}{z(1-z)} \sum_{spin} \int_0^\infty \frac{d^2q_T d^2q_T' d^2k_T}{(k+k')^2(k_1+k')^2 p^{\circ2}(p^\circ + k^\circ + k'^\circ - p'^\circ)^2}$$

$$\times \left[(\not{p}'+m_Q)\gamma^\mu(\not{p}_1+m_Q)\gamma^\mu \not{\epsilon}(\not{k}_1-m_q)\gamma_\mu(\not{k}'+m_q)\gamma_\nu(\not{k}-m_q)\not{\epsilon}(\not{p}+m_Q)\gamma^\nu\right]. \quad (5.23)$$

where we have applied the parametrisation given in (5.7) to obtain the factor of $\frac{1}{z(1-z)}$. Next we perform the spin summation in (5.22) and (5.23) and replace the dot product by (5.9) using the parametrisation (5.7). We then perform the transverse momentum integrations by replacing the square of the transverse momenta by their average values for simplicity. We also replace the polarisation vectors for the meson bound state by

$$\epsilon_T = \mp(0,1,\pm i,0)/\sqrt{2} \quad (5.24)$$

$$\epsilon_L = (0,0,0,1). \quad (5.25)$$

Therefore the final forms of the fragmentation functions are

$$D_o(z) = \frac{N''g^4}{zF(z)} \left\{ \frac{M_{Tk}}{m_q m_Q} \left[10 + \frac{m_{Tq}}{m_q^2} \left[5 + \frac{m_{Tq}}{m_q^2} \right] + \frac{2\langle q_T^2 \rangle}{m_q^2} \left[1 + 5\frac{m_q}{m_Q} \right] \right] \right.$$

$$+ \frac{2(m_q + m_Q)}{m_q} \left[\left[1 + \frac{m_{Tq}}{m_q^2} \right] \left[\frac{qk_T}{m_q m_Q^2} - \frac{qk_T}{m_q^2 m_Q} - 2\frac{\langle q_T^2 \rangle}{m_q^2 m_Q} - \frac{m_{Tq}}{m_q^3} \right] \right.$$

$$\left. - \left[1 + \frac{3qkt}{m_q^2} \right] \right] \frac{1}{z} + \frac{(m_q + m_Q)^2}{m_q m_Q} \left[1 + \frac{m_{Tq}}{m_q^2} \right]^2 \frac{1}{z^2} - 2 \left[6 + 5 \left[1 + \frac{m_{Tq}}{m_q^2} \right] \right.$$

$$+ \frac{2}{m_q m_Q} \left[\langle k_T^2 \rangle + 5\langle q_T^2 \rangle + 4qk_T \right] + \frac{1}{m_q m_Q} \left[1 + \frac{m_{Tq}}{m_q^2} \right]$$

$$\times \left[3\langle k_T^2 \rangle + 4\langle q_T^2 \rangle + 4qk_T \right] + \frac{2qk_T}{m_q m_Q} \left[4\frac{m_q}{m_Q} + \frac{\langle q_T^2 \rangle}{m_q m_Q} - \frac{3qkt}{m_q m_Q} \right] \right]$$

$$\times \frac{1}{1-z} + \frac{2(m_q + m_Q)}{m_Q} \left[3 + \frac{m_{Tq}}{m_q^2} \left[4 + \frac{m_{Tq}}{m_q^2} - \frac{2qk_T}{m_q^2} - \frac{2qk_T}{m_q^2} \right. \right.$$

$$\left. + \frac{2\langle q_T^2 \rangle + qk_T}{m_q m_Q} \left[1 + \frac{m_{Tq}}{m_q^2} \right] \right] \frac{1}{z(1-z)} + \frac{M_{Tk}}{(m_q + m_Q)m_Q}$$

$$\times \left[3 + \frac{m_{Tq}}{m_q^2} + \frac{2\langle q_T^2 \rangle}{m_q m_Q} - \frac{2qk_T}{m_q^2} \right] \frac{z}{1-z} + \frac{qk_T}{m_q m_Q} \left[7 + 5\frac{m_{Tq}}{m_q^2} - \frac{2qk_T}{m_q(m_q + m_Q)} \right.$$

$$\left. + \left[1 + \frac{m_{Tq}}{m_q^2} \right]^2 + \frac{2\langle q_T^2 \rangle}{m_q m_Q} \left[5 + 2\frac{m_{Tq}}{m_q^2} \right] \right] \frac{1}{(1-z)^2} - \frac{2m_{Tk}}{m_q(m_q + m_Q)}$$

$$\times \left[6 + \frac{2m_{Tq}}{m_q^2} + \frac{4\langle q_T^2 \rangle}{m_q m_Q} + \frac{q k_T}{m_q m_Q} \right] \frac{z}{(1-z)^2} + \left[\frac{4m_{Tk} M_{Tk}}{m_q m_Q (m_q + m_Q)^2} \right] \frac{z^2}{(1-z)^2} \right\} \quad (5.26)$$

$$D_T(z) = \frac{N'' g^4}{z F(z)} \left\{ \frac{4 M_{Tk}}{m_q m_Q} \left[1 + \frac{\langle q_T^2 \rangle}{m_q m_Q} \right] - \frac{2 q k_T (m_q + m_Q)}{m_q^2 m_Q} \left[2 + \frac{m_q}{m_Q} \right. \right.$$

$$+ \frac{2 \langle q_T^2 \rangle}{m_q m_Q} + \frac{m_{Tq}}{m_q m_Q} \left] \frac{1}{z} - \frac{(m_q + m_Q)^2}{m_q m_Q} \left[1 - \frac{m_{Tq}}{m_q^2} \left[1 + \frac{\langle q_T^2 \rangle}{m_q m_Q} \right] \right] \frac{1}{z^2} \right.$$

$$-2 \left[3 + \frac{m_{Tq}}{m_q^2} + \frac{2 \langle q_T^2 \rangle}{m_q m_Q} + \frac{2 q k_T^2}{m_q^3 m_Q} \left[2 + \frac{m_{Tq}}{m_q m_Q} \right] \right] \frac{1}{1-z} + \frac{4 q k_T (m_q + m_Q)}{m_q^2 m_Q}$$

$$\times \left[1 + \frac{m_{Tq}}{m_q m_Q} \left[1 + \frac{m_Q}{m_q} + \frac{m_{Tq}}{2 m_q^2} + \frac{\langle q_T^2 \rangle}{m_q m_Q} - \frac{m_q}{m_Q} \right] \frac{1}{z(1-z)}$$

$$+ \frac{2 q k_T M_{Tk}}{m_q m_Q^2 (m_q + m_Q)} \left[1 + 4 \frac{m_Q}{m_q} + \frac{m_{Tq}}{m_q^2} + \frac{2 \langle q_T^2 \rangle}{m_q m_Q} \right] \frac{z}{1-z}$$

$$+ \frac{m_{Tk}}{m_q m_Q} \left[1 + \frac{2 \langle q_T^2 \rangle}{m_q m_Q} + \frac{2 m_{Tq}}{m_q^2} \left[1 + \frac{m_{Tq}}{2 m_q^2} + \frac{\langle q_T^2 \rangle}{m_q m_Q} \right] \right] \frac{1}{(1-z)^2}$$

$$- \frac{2 m_{Tk} q k_T}{m_q m_Q^2 (m_q + m_Q)} \left[3 + m_{Tk} \frac{m_Q}{m_q^3} + \frac{2 \langle q_T^2 \rangle}{m_q^2} \right] \frac{z}{(1-z)^2}$$

$$- \frac{m_{Tk} M_{Tk}}{m_q m_Q (m_q + m_Q)^2} \left[1 - \frac{m_{Tq}}{m_q^2} - \frac{2 \langle q_T^2 \rangle}{m_q m_Q} \right] \frac{z^2}{(1-z)^2} \right\}, \quad (5.27)$$

$$D_L(z) = \frac{N''g^4}{zF(z)}\left\{\frac{M_{Tk}}{m_q m_Q}\left[1 - \frac{m_{Tq}}{m_q^2} + \frac{2\langle q_T^2\rangle}{m_q m_Q}\right]\right.$$

$$-\frac{2qk_T(m_q + m_Q)}{m_q^2 m_Q}\left[2 + \frac{m_q}{m_q} + \frac{m_{Tq}}{m_q m_Q} + \frac{2\langle q_T^2\rangle}{m_q m_Q}\right]\frac{1}{z}$$

$$+\frac{(m_q + m_Q)^2}{m_q m_Q}\left[1 + \frac{2\langle q_T^2\rangle}{m_q m_Q} + \frac{2m_{Tq}}{m_q^2}\left[1 + \frac{\langle q_T^2\rangle}{m_q m_Q}\right]\right]\frac{1}{z^2}$$

$$-2\left[3 + \frac{m_{Tq}}{m_q^2} + \frac{2}{m_q m_Q}(\langle q_T^2\rangle + 2\langle k_T^2\rangle) + \frac{\langle q_T^2\rangle\langle k_T^2\rangle}{m_q^2 m_Q^2}\left[2 + \frac{m_Q}{m_q}\right]\right.$$

$$+\frac{2qkt^2}{m_q^3 m_Q}\left[2 + \frac{m_q^2}{m_Q^2} + \frac{m_{Tq}}{m_q m_Q} + \frac{2\langle q_T^2\rangle}{m_Q^2}\right]\left.\right]\frac{1}{1-z} + \frac{4(m_q + m_Q)qkt}{m_q^2 m_Q}$$

$$\times\left[1 + \frac{m_{Tq}}{m_q m_Q}\left[1 + \frac{m_Q}{m_q} + \frac{m_{Tq}}{2m_q^2} + \frac{\langle q_T^2\rangle}{m_q m_Q}\right] - \frac{m_q}{2m_Q}\right]\frac{1}{z(1-z)}$$

$$+\frac{2qktM_{Tk}}{m_q(m_q + m_Q)m_Q^2}\left[1 + 4\frac{m_Q}{m_q} + \frac{m_{Tq}}{m_q^2} + \frac{2\langle q_T^2\rangle}{m_q m_Q}\right]\frac{z}{1-z}$$

$$-\frac{m_{Tk}}{m_q m_Q}\left[2 - \frac{m_{Tq}}{m_q^2}\left[1 + \frac{m_{Tq}}{m_q^2} + \frac{2\langle q_T^2\rangle}{m_q m_Q}\right]\right]\frac{1}{(1-z)^2}$$

$$-\frac{2m_{Tk}qk_T}{m_q^2(m_q + m_Q)m_Q}\left[1 + 2\frac{m_q}{m_Q} + \frac{m_{Tq}}{m_q^2} + \frac{2\langle q_T^2\rangle}{m_q m_Q}\right]\frac{z}{(1-z)^2}$$

$$+\frac{2m_{Tk}M_{Tk}}{m_q m_Q(m_q + m_Q)^2}\left[1 + \frac{m_{Tq}}{m_q^2} + \frac{2\langle q_T^2\rangle}{m_q m_Q}\right]\frac{z^2}{(1-z)^2}\right\}, \qquad (5.28)$$

where N'' is a normalisation constant and

$$F(z) \equiv \left[\frac{2(m_q + m_Q)(m_q^2 - qk_T)}{m_q m_Q^2} + \frac{zm_{Tk}}{M^2(1-z)} + \frac{m_{Tq}(m_q + m_Q)^2(1-z)}{zm_q^2 m_Q^2} \right]^4,$$

(5.28)

and

$$\begin{cases} m_{Tk} \equiv m_q^2 + \langle k_T^2 \rangle \\[2mm] M_{Tk} \equiv m_Q^2 + \langle k_T^2 \rangle \\[2mm] m_{Tq} \equiv m_q^2 + \langle q_T^2 \rangle \\[2mm] M_{Tq} \equiv m_Q^2 + \langle q_T^2 \rangle \end{cases}$$

(5.29)

We have taken $D_o(z)$ and $2D_T(z) + D_L(z)$ to represent the pseudoscalar and the vector meson fragmentations respectively. If we set the transverse momentum to zero in (5.25), (5.26) and (5.27) then we are led directly to the fragmentation functions given by Suzuki.

5.4 Charm Quark Fragmentation

We have used numerical methods to evaluate the functions (5.26), (5.27) and (5.28) for the prediction of the fragmentation of a charm quark into a charmed meson. Figure (5.4) shows the behaviour of $D_o(z)$ and $2D_T(z) + D_L(z)$ in terms of $\langle q_T^2 \rangle = 0$ and $\langle k_T^2 \rangle = 1$ GeV^2 for the charm quark. These curves are identical to those from the Suzuki model. We have normalised all the fragmentation functions to one. The behavior of the singlet and the triplet fragmentation functions for different values of the transverse momenta $\langle k_T^2 \rangle$ at $\langle q_T^2 \rangle = 0$ are shown in figures (5.5) and (5.6).

It is seen that as $\langle k_T^2 \rangle$ increases, we get softer fragmentations as expected.

To see the effect of the constituent transverse momentum, we have drawn the same curves with $\langle k_T^2 \rangle = 1$ GeV^2 and different values of $\langle q_T^2 \rangle$ in figures.(5.7) and (5.8). We find that this effect is almost the same as the effect of the beam transverse momentum but, as is clear from figure (5.6), the peak of the spectrum moves towards higher values of z as $\langle q_T^2 \rangle$ increases. High values of $\langle q_T^2 \rangle$ are not expected because a bound state with constituents flying apart with high momentum is improbable. We show the comparison of our results for $\langle k_T^2 \rangle = 1$ GeV^2 and $\langle q_T^2 \rangle = 0.3$GeV^2 with a compilation of data (figure (2.5)) for D^* fragmentation. Although the agreement with data looks poor, neverthless comparison of figures (5.9) and (5.4) showss the effect of the constituent transverse momentum on the present model for $\langle q_T^2 \rangle = 0.3$GeV^2.

5.5 Bottom and Heavier Quark Fragmentation

For heavier quarks we notice that in (5.26), (5.27), and (5.28) k_T, q_T and m_q are of the same order of magnitude and we can simply ignore the terms which contain higher orders of the ratio of these quantities with the heavy quark mass. Being careful at the limit $z \to 1$ where terms involving powers $(1 - z)^{-1}$ become large, we obtain

$$
D_0(z) = \frac{N'' g^4}{zF(z)} \left\{ \frac{m_Q}{m_q} \left[10 + \frac{m_{Tq}}{m_q^2} \left[5 + \frac{m_{Tq}}{m_q^2} \right] + \frac{2\langle q_T^2 \rangle}{m_q^2} \right] - \frac{2m_Q}{m_q} \right.
$$

$$
\times \left[\left[1 + \frac{m_{Tq}}{m_q^2} \right] \left[\frac{m_{Tk}}{m_q^2} + \frac{2\langle q_T^2 \rangle}{m_q m_Q} + \frac{qkt}{m_q m_Q} \right] + \left[1 + \frac{3m_{Tq}}{m_q^2} \right] \right] \frac{1}{z}
$$

$$
+ \frac{m_Q}{m_q} \left[1 + \frac{m_{Tq}}{m_q^2} \right]^2 \frac{1}{z^2} - 2 \left[6 + 5 \left[1 + \frac{m_{Tq}}{m_q^2} \right] \right] \frac{1}{1-z} + 2 \left[3 + \frac{m_{Tq}}{m_q^2} \right.
$$

$$
\times \left[4 + \frac{m_{Tq}}{m_q^2} - \frac{2qkt}{m_q^2} \right] - \frac{2qkt}{m_q^2} \right] \frac{1}{z(1-z)} + \left[3 + \frac{m_{Tq}}{m_q^2} - \frac{2qkt}{m_q^2} \right] \frac{z}{1-z}
$$

$$+ \frac{m_{Tk}}{m_q m_Q}\left[7 + 5\frac{m_{Tq}}{m_q^2} + \left[1 + \frac{m_{Tq}}{m_q}\right]^2\right]\frac{1}{(1-z)^2}$$

$$-\frac{2T_1}{m_q m_Q}\left[6 + 2\frac{m_{Tq}}{m_q^2}\right]\frac{z}{(1-z)^2} + \frac{4m_{Tk}}{m_q m_Q}\frac{z^2}{(1-z)^2}\Bigg\}, \qquad (5.30)$$

$$D_T(z) = \frac{N'' g^4}{zF(z)}\Bigg\{ 4\frac{m_Q}{m_q} - 4\frac{qkt}{m_q^2}\frac{1}{z} - \frac{m_Q}{m_q}\left[1 - \frac{m_{Tq}}{m_q}\right]\frac{1}{z^2} - \left[3 + \frac{m_{Tq}}{m_q^2}\right]\frac{1}{1-z}$$

$$+4\frac{qkt}{m_q^2}\left[1 + \frac{Q_1}{m_q^2}\right]\frac{1}{z(1-z)} + \frac{2qkt}{m_q m_Q}\left[1 + 4\frac{m_Q}{m_q} + \frac{m_{Tq}}{m_q^2}\right]\frac{z}{1-z} + \frac{m_{Tq}}{m_q m_Q}$$

$$\times\left[1 + \frac{2m_{Tq}}{m_q^2}\left[1 + \frac{m_{Tq}}{2m_q^2}\right]\right]\frac{1}{(1-z)^2} - \frac{m_{Tk}}{m_q m_Q}\left[1 - \frac{m_{Tk}}{m_q^2}\right]\frac{z^2}{(1-z)^2}\Bigg\}, \qquad (5.31)$$

and

$$D_T(z) = \frac{N'' g^4}{zF(z)}\Bigg\{ \frac{m_Q}{m_q}\left[1 - \frac{m_{Tq}}{m_q^2} - \frac{4qkt}{m_q^2}\frac{1}{z} + \frac{m_Q}{m_q}\left[1 + 2\frac{\langle q_T^2\rangle}{m_q m_Q}\right.\right.$$

$$+\frac{2m_{Tq}}{m_q^2}\left[1 + \frac{\langle q_T^2\rangle}{m_q m_Q}\right]\right]\frac{1}{z^2} - 2\left[3 + \frac{m_{Tq}}{m_q^2}\right]\frac{1}{1-z} + \frac{4qkt}{m_q^2}\left[1 + \frac{m_{Tq}}{m_q^2}\right]\frac{1}{z(1-z)}$$

$$+8\frac{qkt}{m_q^2}\frac{z}{1-z} - \frac{T_1}{m_q m_Q}\left[2 - \frac{m_{Tq}}{m_q^2}\left[1 + \frac{m_{Tq}}{m_q^2}\right]\right]\frac{1}{(1-z)^2}\frac{2T_1}{m_q m_Q}\left[1 + \frac{Q_1}{m_q^2}\right]\frac{z^2}{(1-z)^2}\Bigg\}.$$
$$(5.32)$$

We have examined these functions for different values of $\langle k_T^2 \rangle$ and $\langle q_T^2 \rangle$ in a similar way to the charm quark case. We checked the validity of the approximation from which we obtained these functions. We found that the effect of constituent transverse momentum is much smaller than in the case of charm fragmentation. Finally we compared the prediction of (5.30), (5.31) and (5.32) for production of the B and B^* mesons with the experimental data in figure (5.9) in terms of $\langle k_T^2 \rangle = 1$ GeV^2 and $\langle q_T^2 \rangle = 0.3$ GeV^2.

As the quark mass increases even further, in the absence of constituent transverse momentum which becomes negligible, all the fragmentation functions approach a common limiting form of

$$D(z) = \frac{N'' g^4}{z F(z)} \left\{ \left[1 - \frac{m_q}{m_Q} \frac{1}{1-z} \right]^2 + \frac{\langle k_T^2 \rangle}{m_q^2} \frac{1}{(1-z)^2} \right\}. \tag{5.33}$$

5.6 Remarks and Conclusions

The model introduced in this chapter is obtained in certain approximations which are still quite removed from the real world. We have considered the process of fragmentation through the emission of a vector gluon, which is a perturbative feature and have treated the bound state non-relativistically to obtain the non-perturbative momentum smearing. The transverse momentum of the constituent quarks is introduced in a way which is only applicable for $L = 0$ bound states.

Nevertheless this model gives a clear picture of the spin components of the heavy quark fragmentation function. It shows the effect of the transverse momenta in the different spin components of the fragmentation functions and serves to demonstrate their behaviour for different values of the transverse momentum of both the process and the constituents of the bound state.
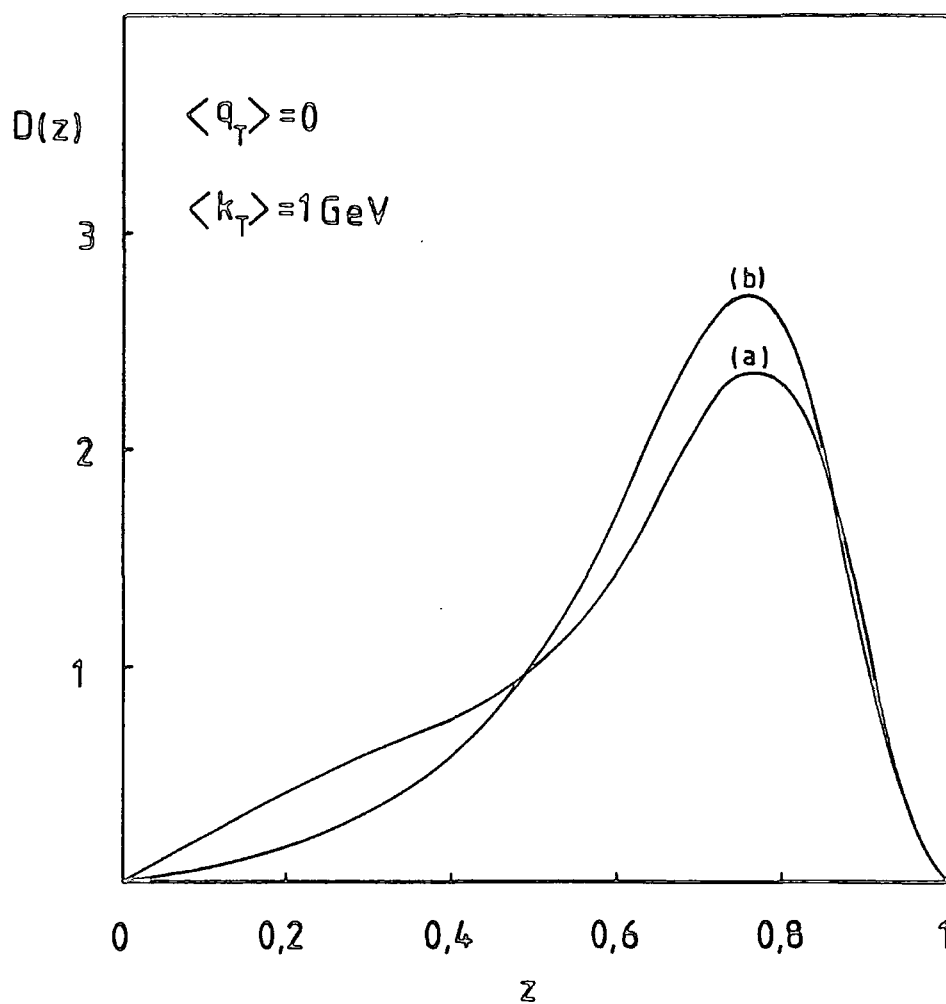
Figure (5.4) . *a) the singlet and b) the triplet fragmentation functions using (5.26), (5.27) and (5.28) in the absence of the constituent transverse momentum.*
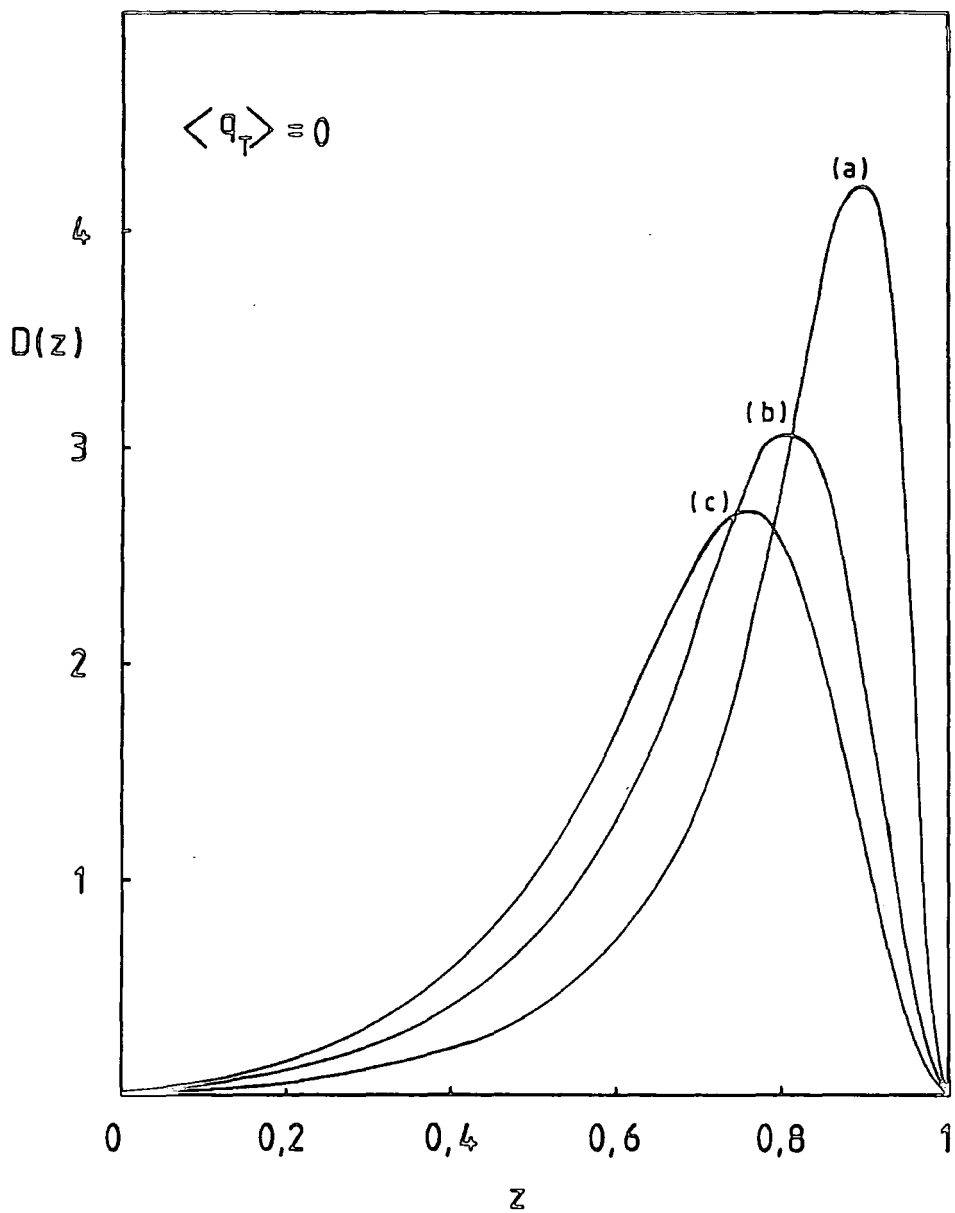
Figure (5.5) . *The effect of the transverse momentum in the case of the singlet fragmentation function (5.26) for charm fragmentation with a) $\langle k_T^2 \rangle = 0.2$ GeV^2, b) $\langle k_T^2 \rangle = 0.6$ GeV^2 and c) $\langle k_T^2 \rangle = 1$ GeV^2.*
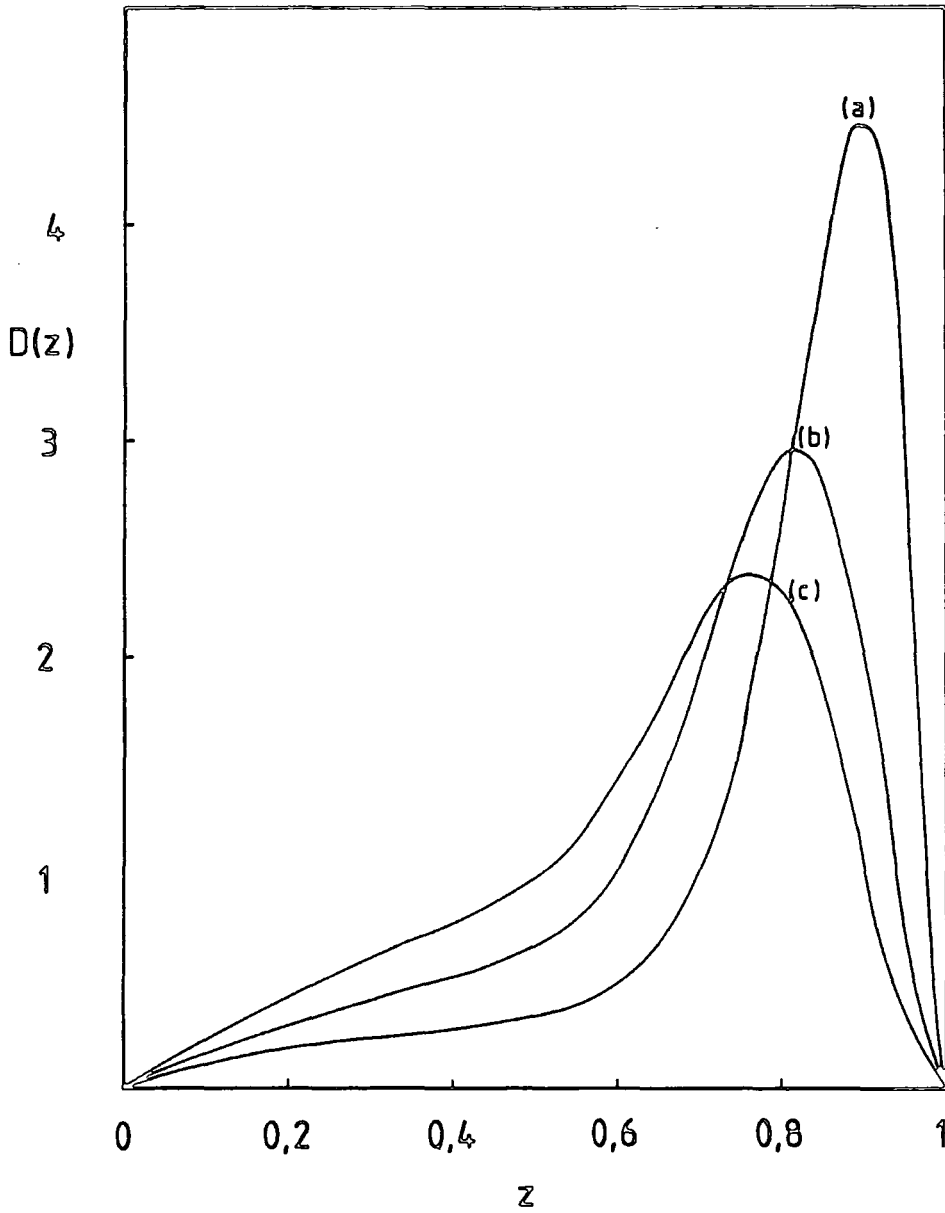
Figure (5.6) . *The same as figure (5.5) for triplet fragmentation using (5.27) and (5.28).*
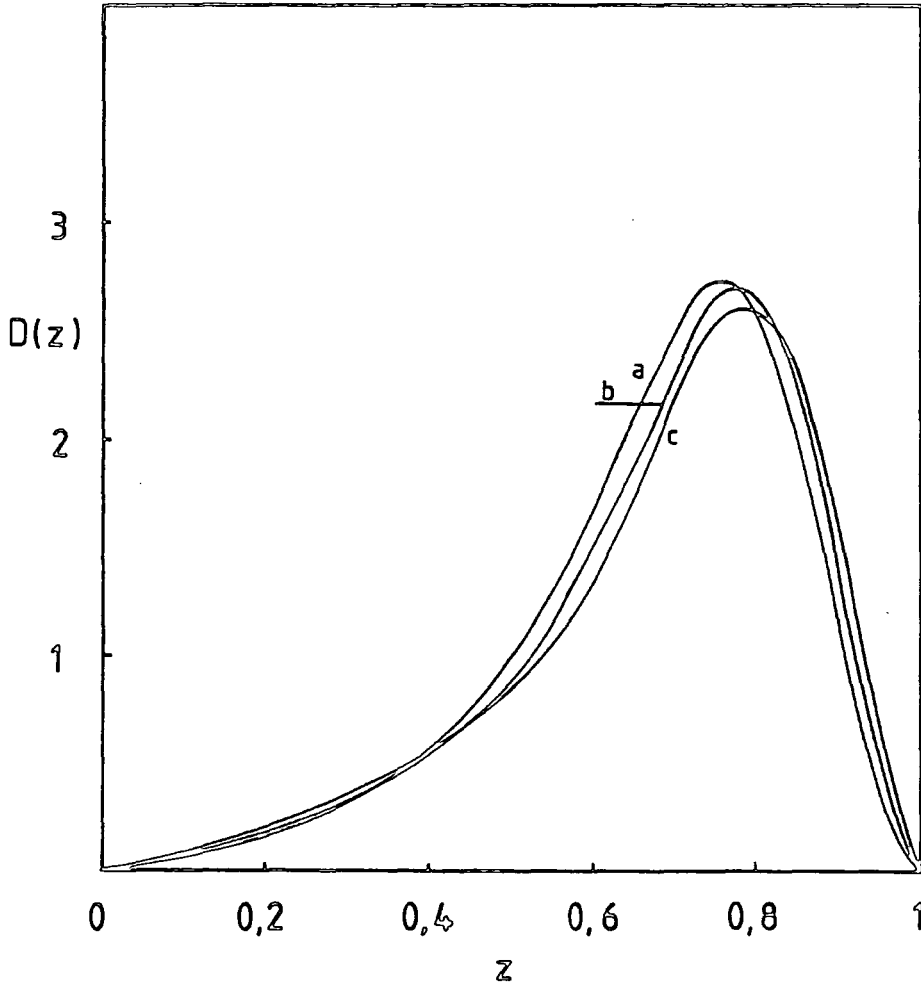
Figure (5.7) . *The effect of the constituent transverse momentum in the bound state on the singlet fragmentation function (5.26) for charm quark fragmentation. $\langle k_T^2 \rangle$ is fixed at 1 GeV with a) $\langle q_T^2 \rangle = 0$ GeV^2, $\langle q_T^2 \rangle = 0.1$ GeV^2 and $\langle q_T^2 \rangle = 0.3$ GeV^2.*
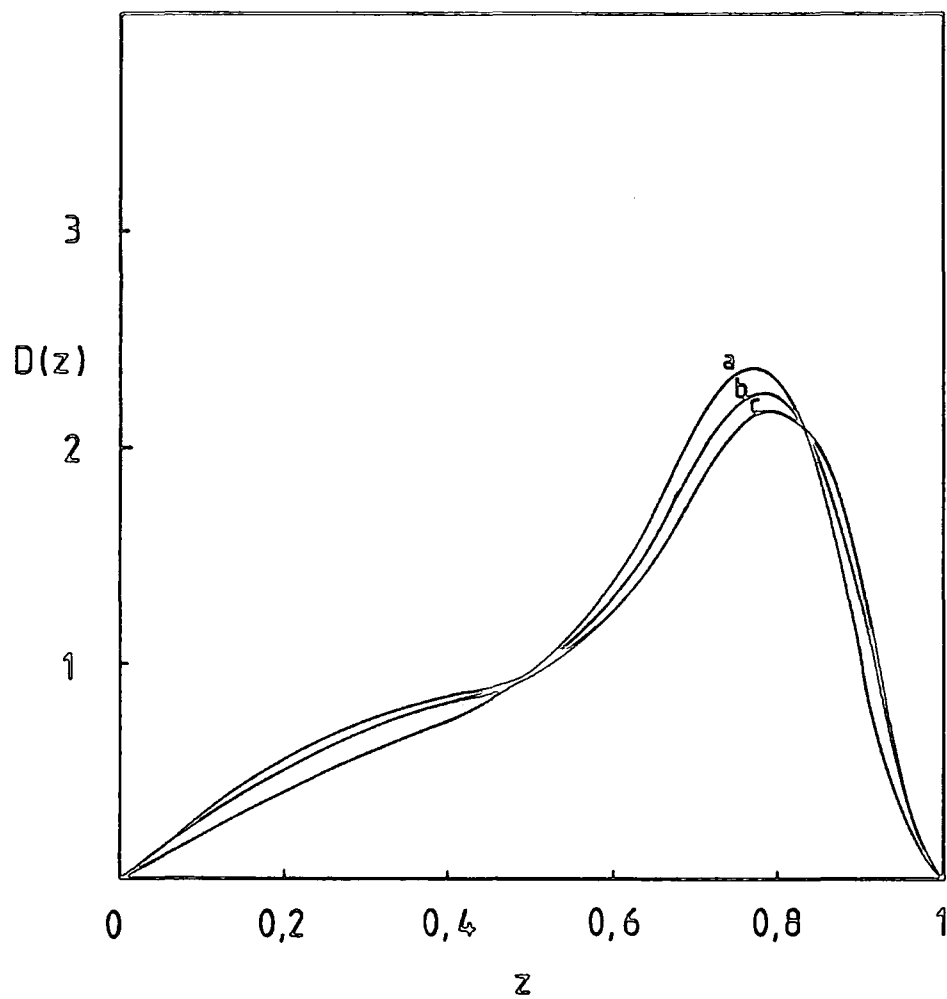
Figure (5.8) . *The same as figure (5.7) for triplet fragmentation from (5.27) and (5.28) .*
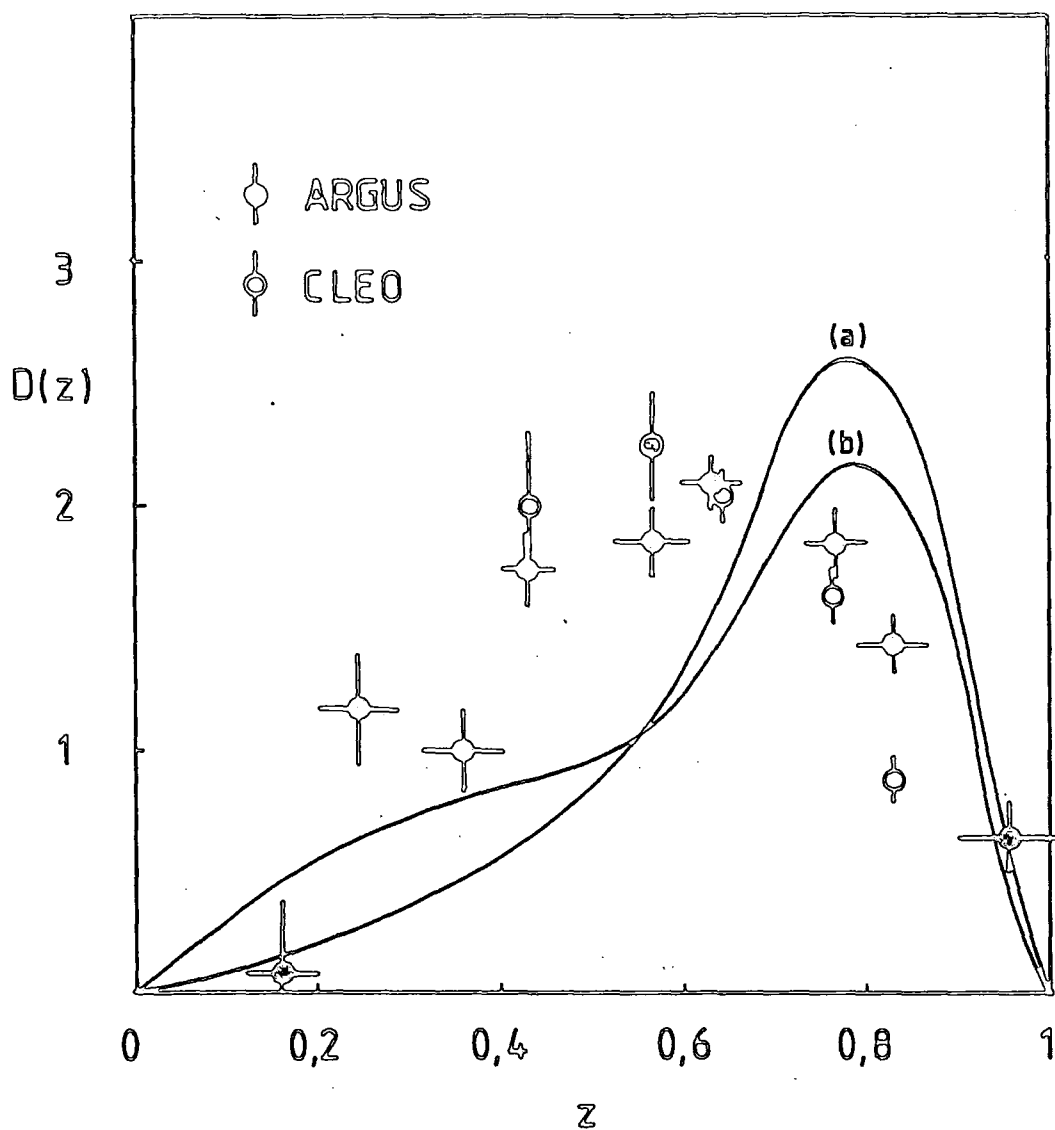
Figure (5.9) . *a) singlet and b) triplet fragmentation functions with* $\langle q_T^2 \rangle = 1$ GeV^2 *and* $\langle q_T^2 \rangle = 0.3$ GeV^2 *compared with data on* D^* *fragmentation*[23].
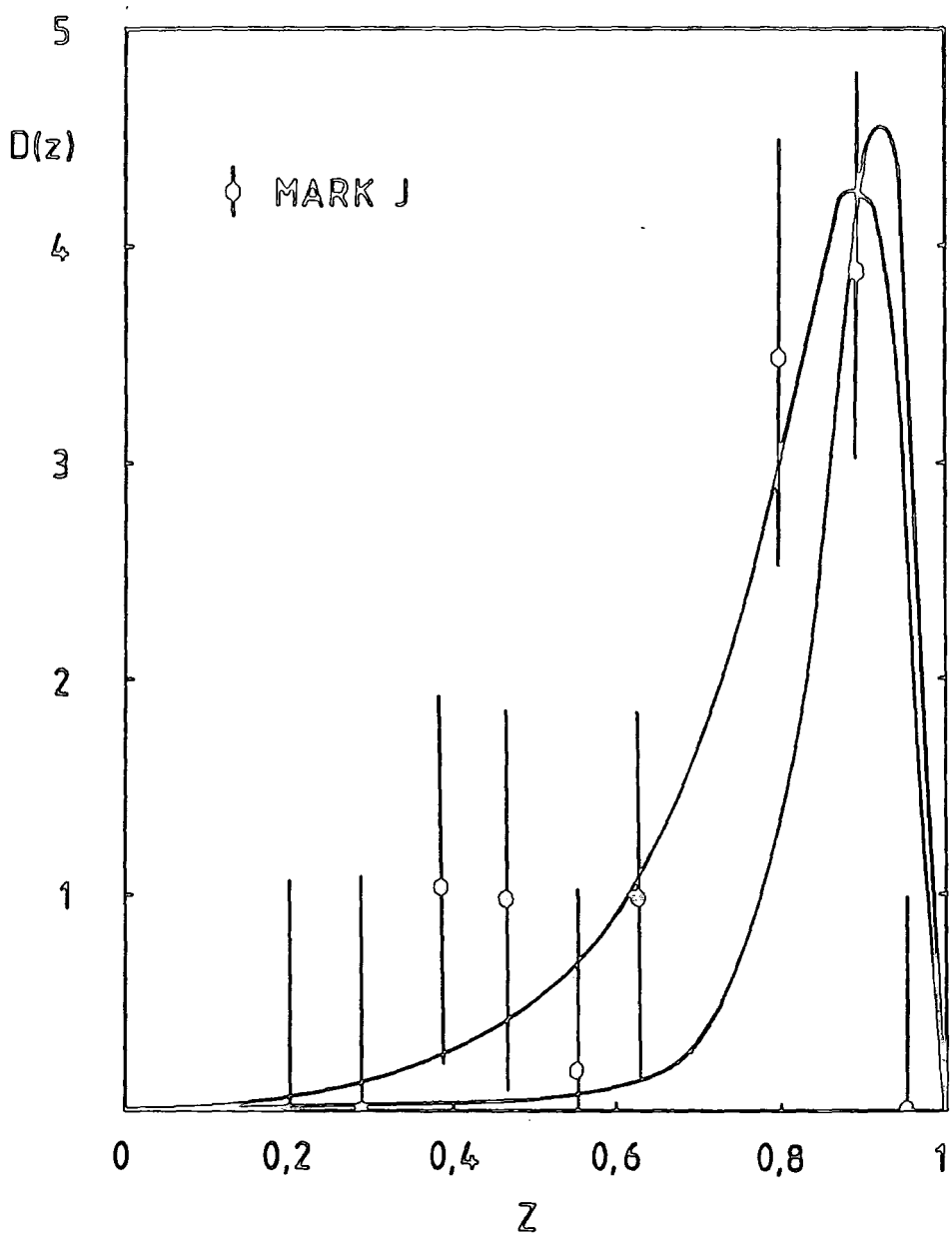
Figure (5.10) . *The same as (5.9) for b quark fragmentation.*

CHAPTER 6

HEAVY MESON PRODUCTION AND THEIR
SEMILEPTONIC DECAYS

We have studied different models for the process of heavy flavour fragmentation in some detail. However, this is only a part of the complicated sequence of events which happens in the real world of particle collisions. Once a heavy quark is produced in a collision, it will fragment into a heavy hadron and then reveal itself by the final state leptons which are produced when it decays. Figure (6.1) shows these stages in a $p\bar{p}$ collision.

In this chapter we are interested in the effect of the various fragmentation models on the momentum distributions of the heavy mesons that are produced in such collisions and of the final state leptons which result from their semileptonic decays. We are not particularly concerned with the study of heavy flavour production, so we have adopted the so called perturbative QCD fusion mechanism, namely $q\bar{q} \rightarrow Q\overline{Q}$ and $gg \rightarrow Q\overline{Q}$, in order to calculate the production cross-section of heavy quarks in our Monte Carlo study. (It is thought that the diffractive mechanism may also be significant for the production of very heavy quarks in multi-TeV range.) We include processes of order α_s^2 and α_s^3 in our calculations. Although there is some evidence of cancellation in the sum $O(\alpha_s^2) + O(\alpha_s^3)$, we simply add the contributions of these orders together to obtain the required results. We then add in the later processes, like the fragmentation of the heavy quark and the decay of heavy mesons, using appropriate calculations.
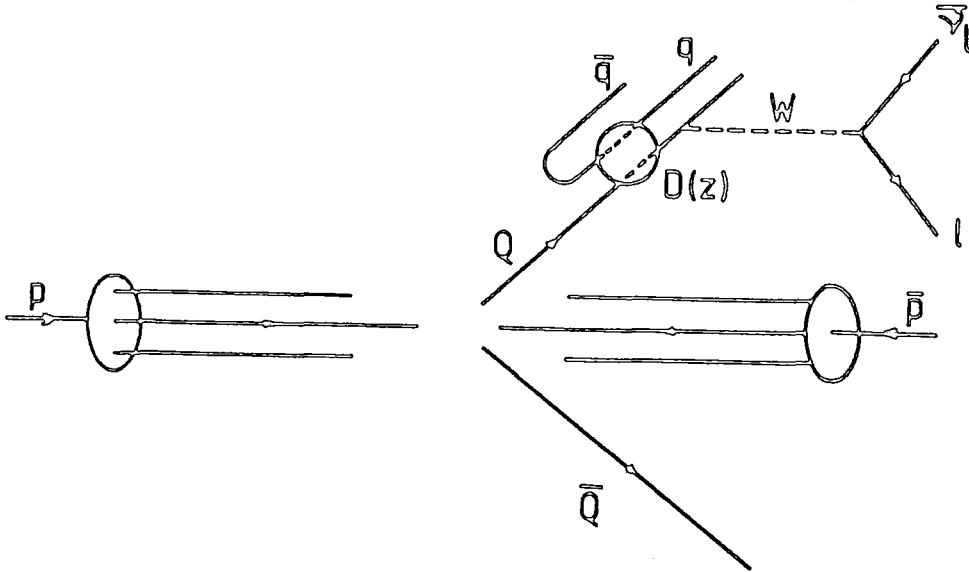
Figure (6.1) *The production, fragmentation and decay of a heavy quark Q in a $p\bar{p}$ collision. The heavy quark Q is produced with energy E_Q. Then Q fragments into a heavy hadron H of energy $E_H = zE_Q$ with probability of $D_Q^H(z)$. The hadron H subsequently decays into leptonic products and the lepton momentum reflects the z of the primary hadron H.*

6.1 Heavy Quark Production

Reliable specification of the dynamics of heavy flavour production in hadron collisions is an important challenge for several reasons. From a theoretical perspective, heavy flavour production offers an opportunity to develop and test perturbative quantum chromodynamics (QCD). There has also been a good deal of interest over the past few years in the cross-section for top quark production at $p\bar{p}$ colliders. The main points of interest are:

1) what is the most effective signature for heavy flavour production-specially top? and

2) what sort of event rates should one expect?

The best way to look for heavy flavour events is to look for large p_T electrons

and muons resulting from their semileptonic decay.

The lowest order Born diagrams for heavy flavour production in perturbative quantum chromodynamics are sketched in Figure (6.2). These are two-parton to two-parton subprocesses (i.e. 2 to 2) in which either two gluons fuse (gg) or a light quark (q) annihilates with a light antiquark $(\bar{q})$ to produce a heavy quark (Q) and heavy antiquark $(\overline{Q})$ in the final state.
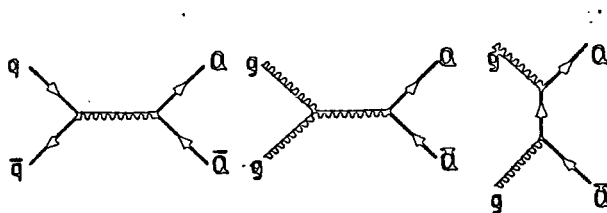
Figure (6.2) *Feynman diagrams for the lowest order perturbative QCD processes for heavy flavour production.*

The cross section $\sigma(p\bar{p} \to QX)$ can be obtained by convoluting the subprocess cross section $\sigma(ab \to Q\overline{Q})$ given by the above Born diagrams with appropriate proton and anti-proton structure functions

$$\sigma(s) = \int dx_1 dx_2 \sum_{a,b} \left[F_{a/p}(x_1, \mathcal{Q}^2) F_{b/\bar{p}}(x_2, \mathcal{Q}^2) + a \leftrightarrow b \right] \sigma(x_1, x_2, s), \qquad (6.1)$$

where $F_{a,b}$ are the structure functions, x_a and x_b are momentum fractions of partons which participate in the reaction and finally $\sigma(x_1, x_2, s)$ is the same as $\sigma(ab \to Q\overline{Q})$ calculated in terms of x_1 and x_2 and the center of mass energy s. So the cross section $\sigma(s)$ depends on the structure functions, the center of mass energy, the quark masses and the value of $\alpha_s(\mathcal{Q}^2)$.

Equation (6.1) emphasises the important assumption of parton model factorisation. The integrand is a product of three separate factors: a subprocess

cross section, $\sigma(ab \rightarrow Q\overline{Q})$ and two probability densities which are assumed to be universal, process independent, properties of the incident hadrons.

Using (6.1), the following values, which are calculated at $\Lambda=0.2$ [62], give an idea of heavy flavour production cross section at the CERN $p\overline{p}$ collider energy ($\sqrt{s} = 630$ GeV and $m_t = 40$ GeV).

$$\begin{cases} \sigma(p\overline{p} \rightarrow cX) \cong 58\mu b, \\\\ \sigma(p\overline{p} \rightarrow bX) \cong 13\mu b, \\\\ \sigma(p\overline{p} \rightarrow tX) \cong 1.4nb. \end{cases} \qquad (6.2)$$

Of course, due to the various heavy flavour triggers which involve transverse momentum cuts, and the limited geometrical acceptance of the detectors, only a small fraction of the cross sections (6.2) are actually measurable.

It has been established that the $O(\alpha_s^3)$ corrections to heavy flavour production are significant. The order of $\alpha_s^2(\mathcal{Q}^2)$ $2 \rightarrow 2$ subprocesses yield $Q\overline{Q}$ pairs in which the quark Q is back to back with the antiquark $\overline{Q}$ in the parton-parton center of mass frame. The next-to-leading order $\alpha_s^3(\mathcal{Q}^2)$ contributions to $\sigma(p\overline{p} \rightarrow QX)$ provide a new phase space configuration. The $2 \rightarrow 3$ Born diagrams are shown in figure(6.3).

Since the virtual corrections to the $2 \rightarrow 2$ diagrams of figure (6.2) are not yet available, the $O(\alpha_s^3)$ contribution of the $2 \rightarrow 2$ processes are not considered. The dominant contribution to $O(\alpha_s^3)$ is due to the process [63]

$$g + g \rightarrow g + g^* \rightarrow Q\overline{Q} \qquad (6.3)$$

which is really an $O(\alpha_s)$ correction to the gluon-gluon fusion process $g + g \rightarrow g + g$ and leads to 3-jet production.

The $2 \rightarrow 3$ processes shown in figure (6.3) belong to the three general
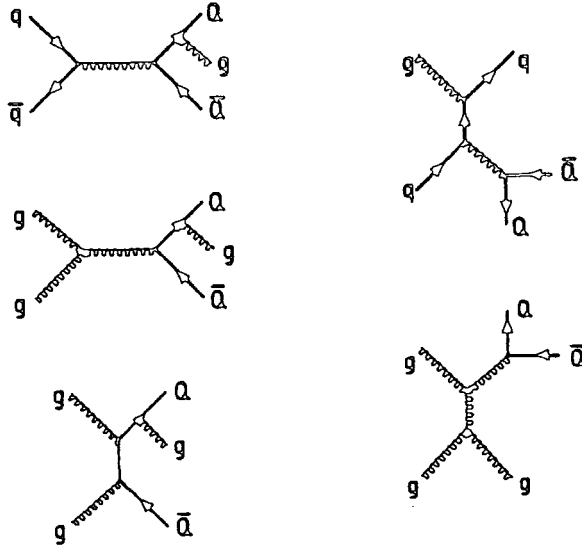
Figure (6.3) *Next-to-leading order perturbative QCD processes at the Born level for heavy flavour production in hadron-hadron collisions.*

classes given below:

$$\begin{cases} q + \overline{q} \to g + Q + \overline{Q}, \\ \\ g + g \to g + Q + \overline{Q}, \\ \\ q + g \to q + Q + \overline{Q}, \end{cases} \quad (6.4)$$

where only the contribution of the light quarks in the initial state are included. We have not considered the so called flavour excitation contributions [64]

$$g + Q \to g + Q, \quad (6.5)$$

which may be important in diffractive production.

In our calculation of heavy quark production we have used the $2 \to 2$ and $2 \to 3$ matrix elements with $m_Q \neq 0$ derived by Ellis and Sexton[65]. Although the cross-section to $O(\alpha_s^2)$ is integrable down to $p_T = 0$, their $O(\alpha_s^3)$

counterparts $gg \rightarrow g\ Q\overline{Q}$, i.e. the processes (6.4), require an infra-red cut-off (to avoid E_q, $E_g \rightarrow 0$ singularities) as well as a collinearity cut-off (to avoid singularities from the initial state). To control these singularities we have imposed a cut-off on the recoil momentum of the additional gluon or light quark against the heavy quark. We use $p_T^{cut} = 5$ GeV as a reasonable value for this cut-off because experimentally it turns out to be very difficult to reconstruct jets with energies less than about 5 GeV. Theoretically, the $2 \rightarrow 3$ cross-section should be integrated for $p_t^{q,g} < p_T^{cut}$ and added to the cross-section for $2 \rightarrow 2$ processes to define the effective $2 \rightarrow 2$ heavy quark pair production cross-section in $O(\alpha_s^3)$.

The QCD calculations presented in this work are based on the choice of the Eichten et al. [66] parametrisation for the structure functions with $\Lambda = 0.3$ GeV for valence and sea quarks. The argument of $\alpha_s(Q^2)$ is fixed at $Q^2 = m_Q^2$.

We have done a Monte Carlo calculation with the above requirements to obtain the transverse momentum distribution of the heavy quarks which are produced up to the order of $\alpha_s^3(Q^2)$. We use the following definition of the rapidity

$$\eta = \frac{1}{2}\log\left\{\frac{E + p_\parallel}{E - p_\parallel}\right\}, \qquad (6.6)$$

where E is the energy and $p_\parallel$ represents the longitudinal momentum of the produced particle. The rapidities of the produced heavy quarks are restricted by the cut $|\eta^Q| < 2.5$ which is consistent with recent experiments at CERN and FNAL. In figure (6.4) and (6.5) we show the differential cross-sections for $d\sigma/dp_T^Q$ for $p + \overline{p} \rightarrow Q + X$, where $Q = c, b$ and t. The cross-section $p + \overline{p} \rightarrow t + X$ increases by approximately one order of magnitude between $\sqrt{s} = 0.63$ and $\sqrt{s} = 1.8$ TeV. They are consistent with similar calculations using the EUROJET Monte Carlo[67].
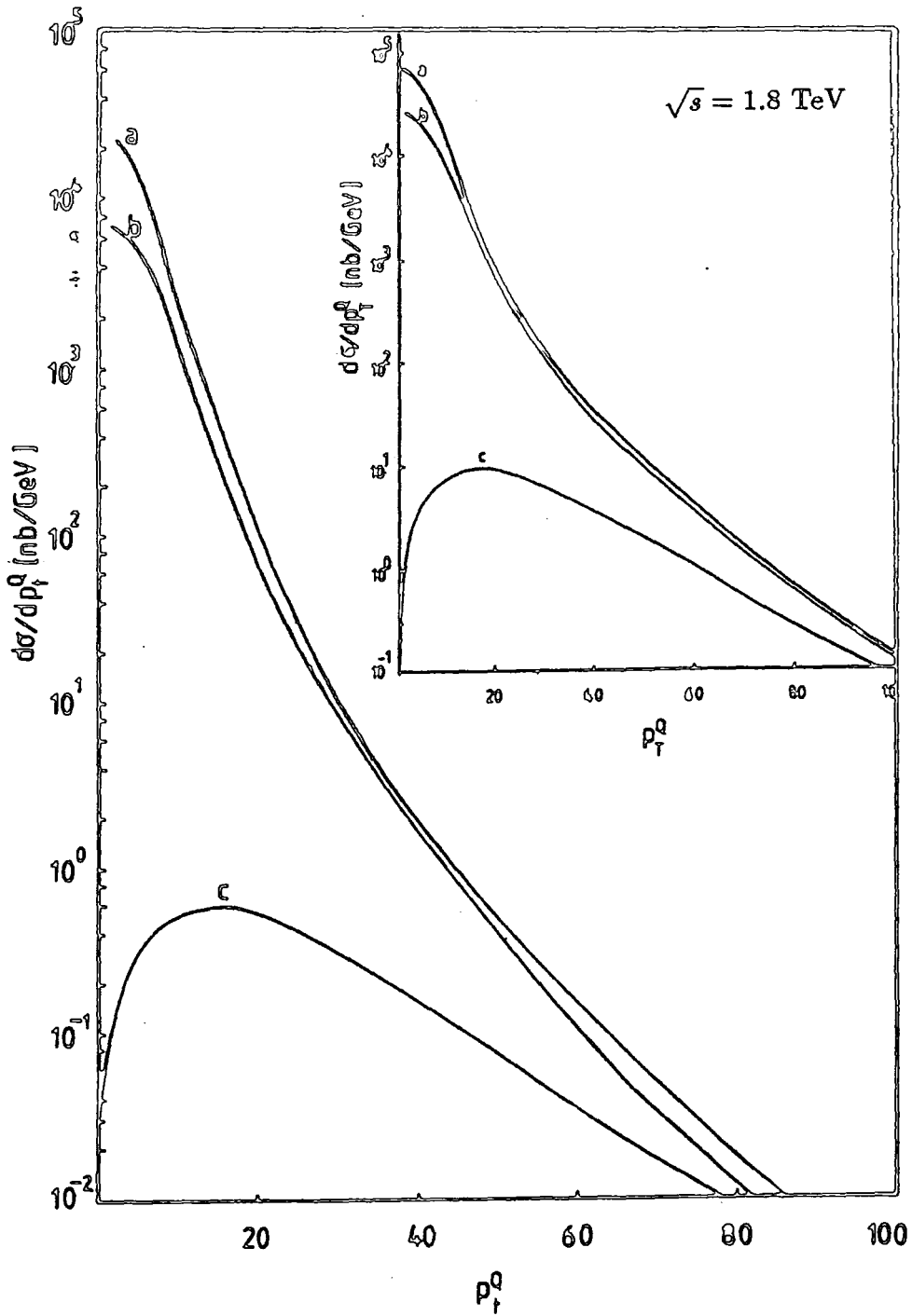
Figure (6.4) *The inclusive heavy quark transverse momentum distribution* $d\sigma/dp_T^Q$ *for charm, bottom and top quarks represented by a, b, and c respectively for* $\sqrt{s} = 0.63$ *and* $\sqrt{s} = 1.8$ *TeV. The rapidity is restricted to* $|\eta^Q| < 2.5$. *The heavy quark masses are taken to be* $m_c = 1.65$, $m_b = 5.0$ *and* $m_t = 40$ *GeV.*
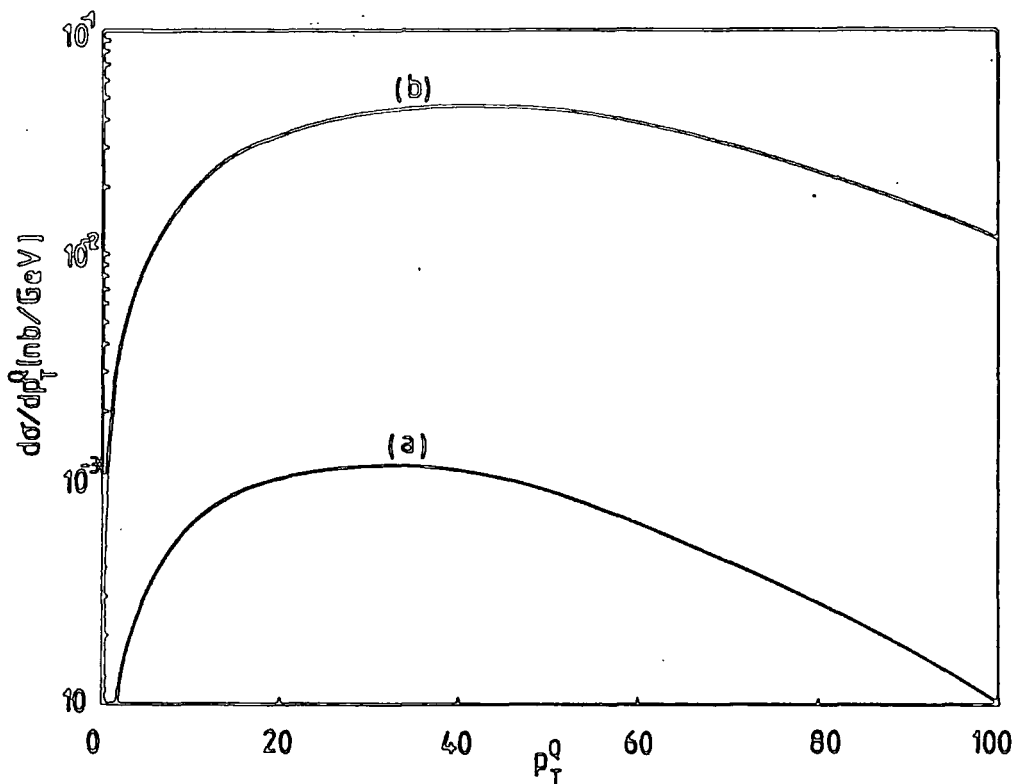
Figure (6.5) *Production of a top quark of mass 100 GeV at a)* $\sqrt{s} = 0.63$ *and b)* $\sqrt{s} = 1.8$ *TeV.*

6.2 Heavy Meson Production

We now employ the various fragmentation functions of interest to us in the Monte Carlo program to obtain the inclusive heavy hadron p_T distribution $d\sigma(p\bar{p} \rightarrow HX)/dp_T^H$ where H is a heavy meson. The p_T and the rapidity cuts are the same as in the case of quark production.

Among the phenomenological fragmentation models which we discussed in previous chapters, we choose the Collins-Spiller, Scott and Suzuki models along with Peterson's to demonstrate the effect on p_T distributions of D, B and

114

T meson production. This choice was made because in typical Monte Carlo studies there are various other theoretical uncertainties which mean that spin effects in the fragmentation process and the internal motion of the constituent quarks in the bound state (which we discussed in the chapters 4 and 5) are less important.

We have shown our results for D, B and T meson production at CERN and FNAL energies in figures (6.6), (6.7), (6.8) and (6.9). These results are obtained using $\epsilon_c = 0.1$, $\epsilon_b = 0.011$ and $\epsilon_t = 0.0001$ in the Peterson model, $\langle k_T^2 \rangle = 0.2$ GeV^2 and $\kappa = 0.5$ in the Collins-Spiller model and $\langle k_T^2 \rangle = 1$ GeV^2 for the Suzuki fragmentation functions. As would be expected from our comparison of the fragmentation functions in chapter 3, for charmed mesons the results of the different models are very close to each other. However differing results are obtained in the case of B and T meson production. The Scott model shown in figures (6.8) and (6.9) is very different. For top meson production the prediction of the Suzuki model is very close to the result obtained using the Peterson fragmentation function and is not shown in the figures.

6.3-The weak Decay of Heavy Hadrons

The time scale of the strong interaction is typically $\gtrsim 10^{-22}$ seconds or so. The particles that survive longer than this generally decay electromagnetically or weakly. In the case of c and b quark production, the produced heavy flavour states typically decay via the weak interaction after about $10^{-13} - 10^{-12}$ seconds.

The weak and electromagnetic interactions are well described by the SU(2)×U(1) gauge theory of Weinberg, Salam and Glashow. In this model the chiral left-handed components of the fundamental fermions are grouped into iso-doublets, as shown below:
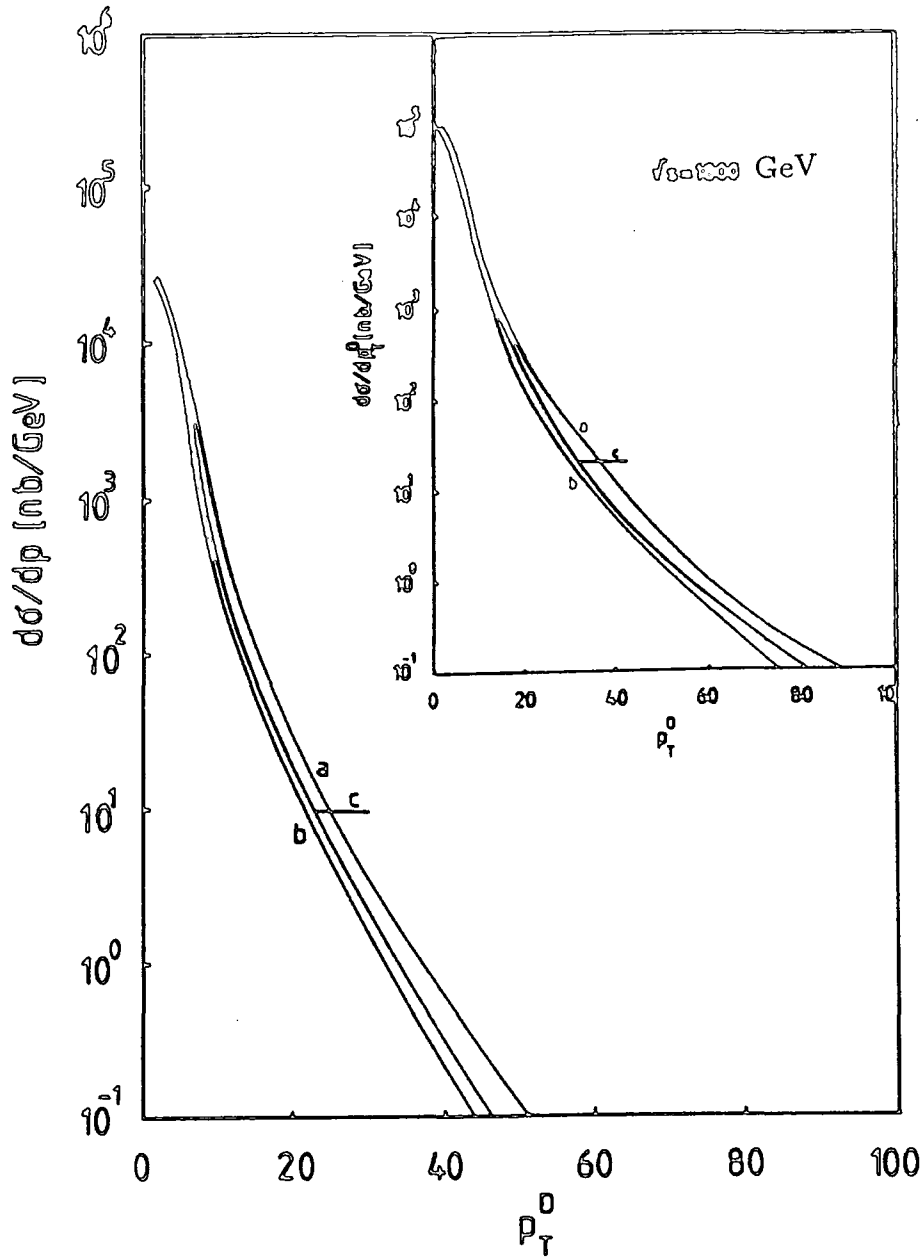
Figure (6.6) *The inclusive D meson transverse momentum distribution* $d\sigma/dp_T^D$ *at* $\sqrt{s} = 0.63$ *and* $\sqrt{s} = 1.8$ *TeV with the rapidity cut off* $|\eta^Q| < 2.5$ *as predicted by a) the Suzuki, b) the Collins-Spiller and c) the Peterson fragmentation functions.*

116
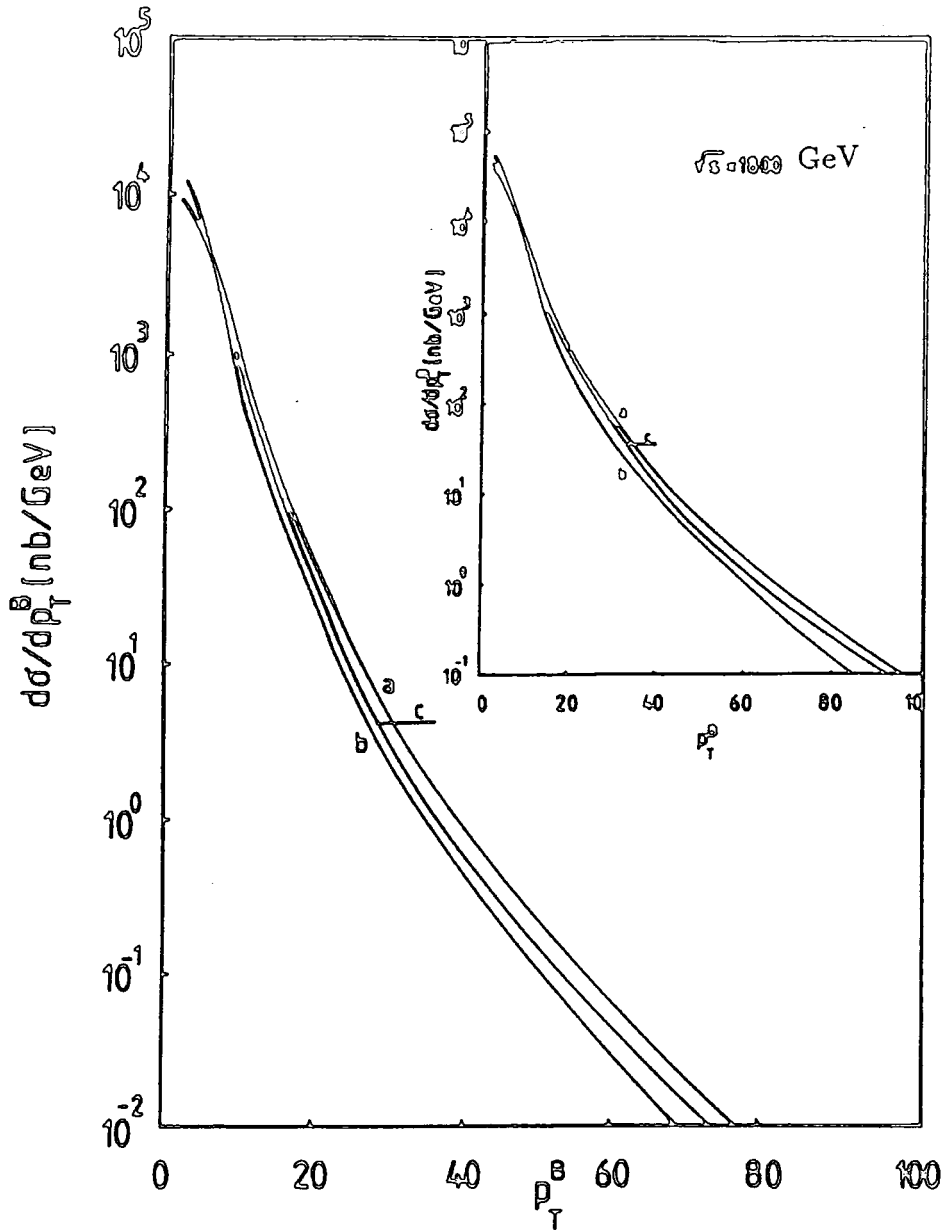
Figure (6.7) *The same as (6.6) for B meson production with $m_b = 5$ GeV.*
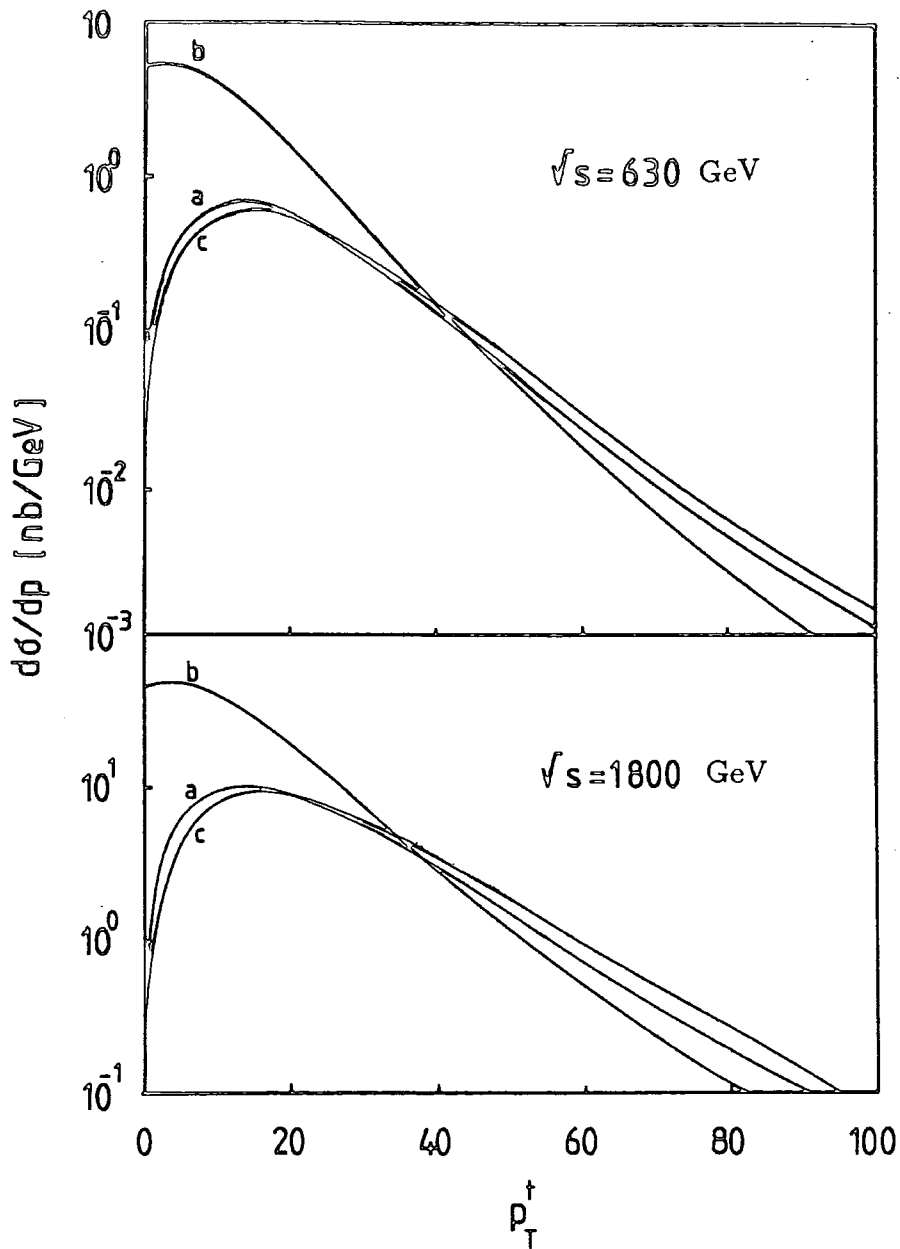
Figure (6.8) *T meson production with $m_t = 40$ GeV at $\sqrt{s} = 0.63$ and $\sqrt{s} = 1.8$ TeV using a) the Collins-Spiller and b) the Scott fragmentation functions compared with c) the Peterson model.*
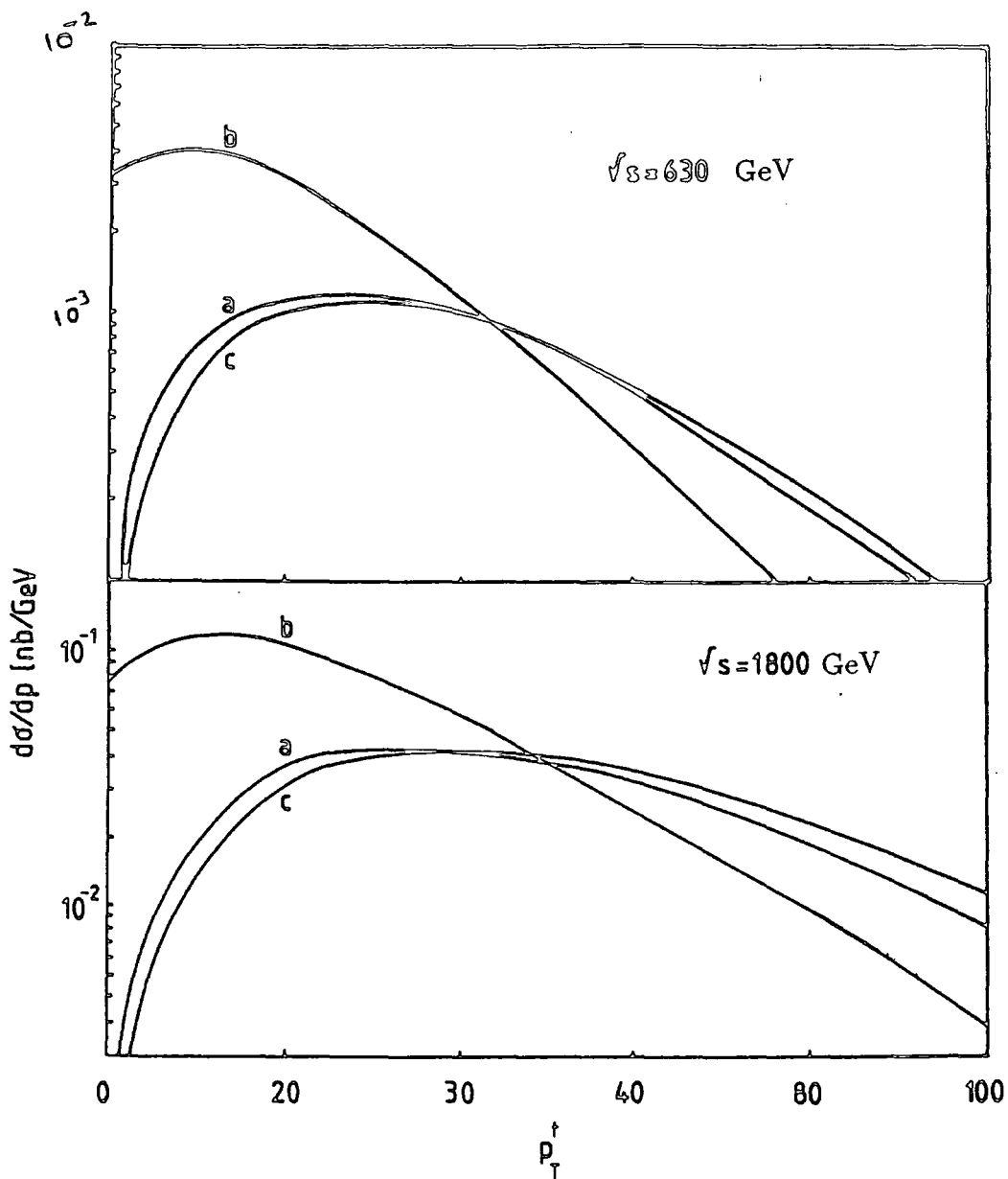
Figure (6.9) *The same as (6.8) with $m_t = 100$ GeV.*

$$\begin{pmatrix} \nu_e \\ e \end{pmatrix} \begin{pmatrix} \nu_\mu \\ \mu \end{pmatrix} \begin{pmatrix} \nu_\tau \\ \tau \end{pmatrix}$$
$$\begin{pmatrix} u \\ d \end{pmatrix} \begin{pmatrix} c \\ s \end{pmatrix} \begin{pmatrix} t \\ b \end{pmatrix}, \quad (6.7)$$

where the hypothetical top quark is required to complete the bottom quark doublet. The standard model does not constrain the number of generations but only requires the given arrangment of paired doublets. The right handed components of each massive fermion are weak iso-singlets. Since the weak interaction does not conserve flavour, the quarks that appear in the weak doublets are not eigenstates of the strong interactions. The mixing matrix that describes these weak transitions is by convention defined so that the weak iso-doublet d', s' and b' quarks are each a linear combination of the down, strange and bottom mass eigenstates,

$$\begin{pmatrix} d' \\ s' \\ b' \end{pmatrix} = V \begin{pmatrix} d \\ s \\ b \end{pmatrix}. \quad (6.7a)$$

This KM matrix was parametrised by Kobayashi and Maskawa in terms of angles analogous to the well known Cabbibo angles[68], and it has been relatively well determined by experiment[69]. The accepted range of the experimental values of its elements are as follows

$$V = \begin{pmatrix} V_{ud} & V_{us} & V_{ub} \\ V_{cd} & V_{cs} & V_{cb} \\ V_{td} & V_{ts} & V_{tb} \end{pmatrix}$$
$$= \begin{pmatrix} 0.974 - 0.976 & 0.218 - 0.222 & 0.000 - 0.012 \\ 0.183 - 0.231 & 0.81 - 1.0 & 0.035 - 0.049 \\ 0.000 - 0.022 & 0.032 - 0.050 & 0.998 - 0.999 \end{pmatrix} \quad (6.8)$$

It is clear from the above matrix that the dominant weak decay chain is $t \to b \to c \to s \to u$.

A simple model of the mechanism of heavy hadron weak decays is based on muon decay (Figure (6.10)). Unlike the decay of a bottom or charm meson,

muon decay is a purely leptonic process. However the spectator quark model [70], shown in figure (6.10b), has been found to provide useful as a first guess for lifetime calculations. In the free quark spectator model the light quark in the heavy meson is regarded as a mere spectator and the heavy meson decay is approximated as the decay of a free heavy quark into its semileptonic products just like muon decay.

The semileptonic decays of heavy hadrons are the main source of prompt leptons in hadronic events. A consequence of the large mass difference between bottom and charm quarks is that the leptons from their decays populate very different regions of transverse momentum(p_T), measured with respect to the quark jet axis.

6.4 Leptons From Heavy Mesons

Observation of the leptons from the semileptonic decays of heavy hadrons is the main way of detecting such hadrons. For example the B meson decays are thought to proceed by decay of the b quark into either a c or a u quark and a virtual W boson which then disintegrates into an electron and an antineutrino as in figure (6.10b). The detection of these electrons, and muons and also di-muons has received special attention in last few years.

To demonstrate the effect of quark fragmentation, we choose the case of D and B meson decays into electrons. (Since electrons and muons are both treated as massless particles in this kind of calculations, our results will apply for both cases). These processes have been investigated experimentally by different collaborations and the branching ratios for the different decay modes are now available[71]. We list some of these results, which we have used in our calculation, in table (6.1). We now consider these processes in greater analytical detail.   121
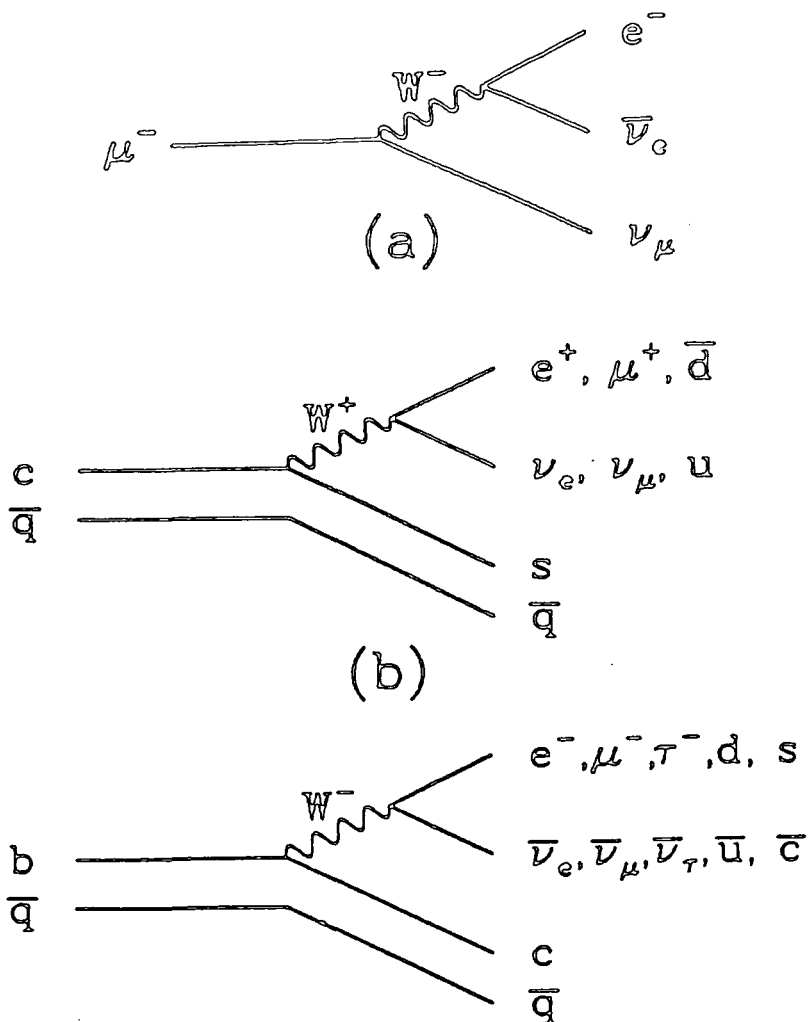
Figure (6.10) *Weak decays: muon decay and the spectator diagrams for D and B meson decay.*

Table(6.1)Semileptonic branching ratios of heavy quarks.

	Ref.	$BR(c \to e\nu_e X)\%$	$BR(b \to e\nu_e X)\%$
TASSO	[72]	$9.2 \pm 2.2 \pm 4.0$	$11.1 \pm 3.4 \pm 4.0$
CELLO	[73]	–	$14.1 \pm 5.8 \pm 3.0$
MARK-II	[74]	$6.6 \pm 1.4 \pm 2.8$	$13.5 \pm 2.6 \pm 2.0$
TPC	[75]	$9.1 \pm 0.9 \pm 1.3$	$11.0 \pm 1.8 \pm 1.0$
CLEO	[76]	–	$12.0 \pm 0.7 \pm 0.5$
MARK-III	[77]	$11.7 \pm 1.0 \pm 0.5$	–
CUSB	[78]	–	$13.2 \pm 0.8 \pm 1.4$
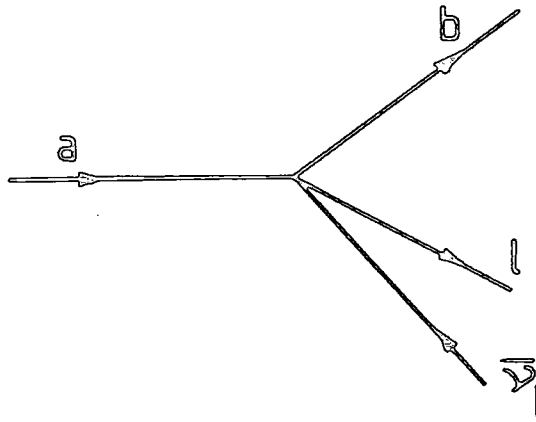
Figure (6.11) *Feynman diagram for the semileptonic decay* $a \to b\, l\, \bar{\nu}$ *by a contact interaction.*

The decay of a quark a into a quark b and lepton l and its neutrino $\bar{\nu}$ is shown in figure (6.11). In this process the emission of the highly virtual intermediate W boson is treated as a contact interaction. The Feynman amplitude $\mathcal{M}$ for the decay process is

$$\mathcal{M} = \frac{G_F}{\sqrt{2}} \big\{ \overline{u}(b)\gamma^\alpha(1-\gamma_5)u(a)\overline{u}(l)\gamma_\alpha(1-\gamma_5)v(\overline{\nu}) \big\}, \tag{6.9}$$

where a, b, l and $\overline{\nu}$ represent the four momenta of the relevant particles. Since this is a general calculation, we have not included the relevant KM matrix elements. Taking the square over spins, and replacing the spinor products by projection operators, we find:

$$\sum |\mathcal{M}|^2 = \frac{1}{2}G_F^2 tr\big\{ \gamma^\alpha(1-\gamma_5)(\not{a}+m_a)\gamma^\beta(1-\gamma_5)(\not{b}+m_b) \big\}$$

$$\times tr\big\{ \gamma_\alpha(1-\gamma_5)\not{\overline{\nu}}\gamma_\beta(1-\gamma_5)(\not{l}+m_l) \big\}.$$

$$= 128 G_F^2 (a.\overline{\nu})(b.l), \tag{6.10}$$

for (V+A)-(V+A) interaction.

For a (V+A) coupling at $a \to b$ vertex and a (V-A) coupling at $l\,\overline{\nu}$ vertex we find a similar expression

$$\sum |\mathcal{M}|^2 = 128 G_F^2 (a.l)(b.\overline{\nu}). \tag{6.11}$$

Now given the fact that the quark-quark and lepton-neutrino interaction vertices are (V+A)-(V+A) for c and t quarks and (V+A)-(V-A) in the case of the b quark, we may write

$$c \to s\, e^+\, \nu_e \qquad \sum |\mathcal{M}|^2 \sim (c.e^+)(s.\nu_e), \tag{6.12}$$

$$b \to c\, e^-\, \overline{\nu}_e \qquad \sum |\mathcal{M}|^2 \sim (b.\overline{\nu}_e)(c.e^-), \tag{6.13}$$

$$t \to b \, e^+ \, \bar{\nu}_e \qquad \sum |\mathcal{M}|^2 \sim (t.e^+)(b.\nu_e). \qquad (6.14)$$

For the charm and bottom quarks the decay products will be almost collinear with the decaying c or b quark at sufficiently high energies. For the case of a top quark with $m_t < m_W$, we will use the expression given by (6.14). If $m_t > m_W$ then the decay mode changes and one has to consider separately the decay of a top quark into a bottom quark and a real W boson and the subsequent decay of the W particle into a lepton and its neutrino .

6.5 The Collinear Approximation

To obtain the momentum distribution of the final state electrons one should incorporate the contributions of the Feynman diagrams for the sequence of the processes $p\bar{p} \to$ heavy quark $\to$ heavy hadron $\to$ electrons. However at sufficiently high energies we can consider the electrons from the decay of charm and bottom quarks to be moving collinearly with the original heavy quark[79]. For the range of energies available at CERN and FNAL this approximation is only useful in the case of c and b quarks but not for heavier ones. (For a hypothetical top quark of mass 40 GeV for example, the transverse momentum is not by any means negligible).

In the collinear approximation one calculates the probability function for a heavy quark to decay into an electron which is collinear with the original heavy quark. This function is $\frac{1}{\Gamma_{tot}}\frac{d\Gamma}{dy}$, where Γ is the partial decay width, Γ_{tot} is the total decay width and y represents the fraction of the momentum of the original quark taken by the lepton. The calculation of the so-called *Decay Functions* is similar to the kind of calculations presented in chapters 4 and 5. The results for D and B meson decay in the spectator model are as follows:

$$D_{l+/D}(y) = 2(1 - 3y^2 + 2y^3), \tag{6.15}$$

$$D_{l-/B}(y) = (5 - 9y^2 + 4y^3)/3, \tag{6.16}$$

where y is defined as

$$y = \frac{(E + p_\parallel)_l}{(E + p_\parallel)_M}. \tag{6.17}$$

Now if we consider the fragmentation function $D_{M/Q}(z)$ and define

$$x = \frac{(E + p_\parallel)_l}{(E + p_\parallel)_Q}, \tag{6.18}$$

then we can write the total probability of obtaining the lepton l from a heavy meson M as:

$$D_{l/Q}(x) = \int_0^1 dz \int_0^1 dy D_{M/Q}(z) D_{l/M}(y) \delta(x - yz). \tag{6.19}$$

Performing the delta function integration in favour of z, we obtain

$$D_{l/Q}(x) = \int_x^1 \frac{dy}{y} D_{M/Q}(x/y) D_{l/M}(y). \tag{6.20}$$

We have used (6.20) to obtain the lepton spectrum from D and B mesons in the spectator model. The rapidity condition which we have use here is $|\eta^{l\pm}| <$ 1.5. The results are shown in figures (6.12) and (6.13) for two collider energies. The effect of the different fragmentation functions is more or less the same as for meson production but the range of transverse momenta is different.

Muon and di-muon data from UA1 collaboration at CERN [80] are the only large p_T lepton spectra from $p\bar{p}$ collisions available at present. This data is for $p\bar{p} \rightarrow \mu + X$ and includes the contributions from all possible QCD processes. We have shown this in figure (6.14). Our results in (6.12) and (6.13) are consistent with this data.

126
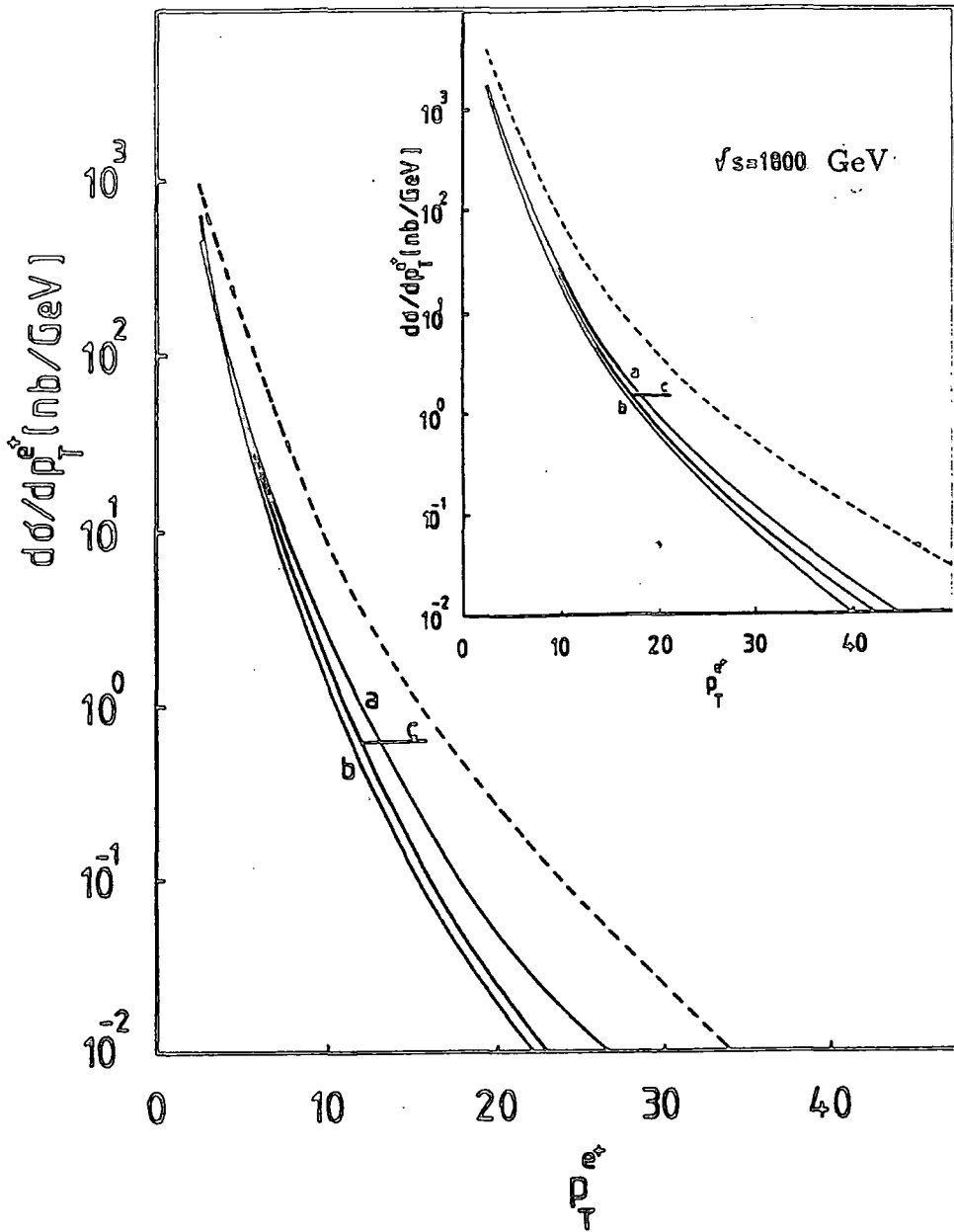
Figure (6.12) *The positron spectrum from D meson in $p\bar{p}$ collisions at $\sqrt{s} = 0.63$ and $\sqrt{s} = 1.8$ TeV using a) the Suzuki, b) Collins-Spiller and c) the Peterson fragmentation function in the collinear approximation. The rapidity of the positrons is restricted to $|\eta^{l^+}| < 1.5$. The dashed line is the same spectrum from the corresponding heavy quark.*

127
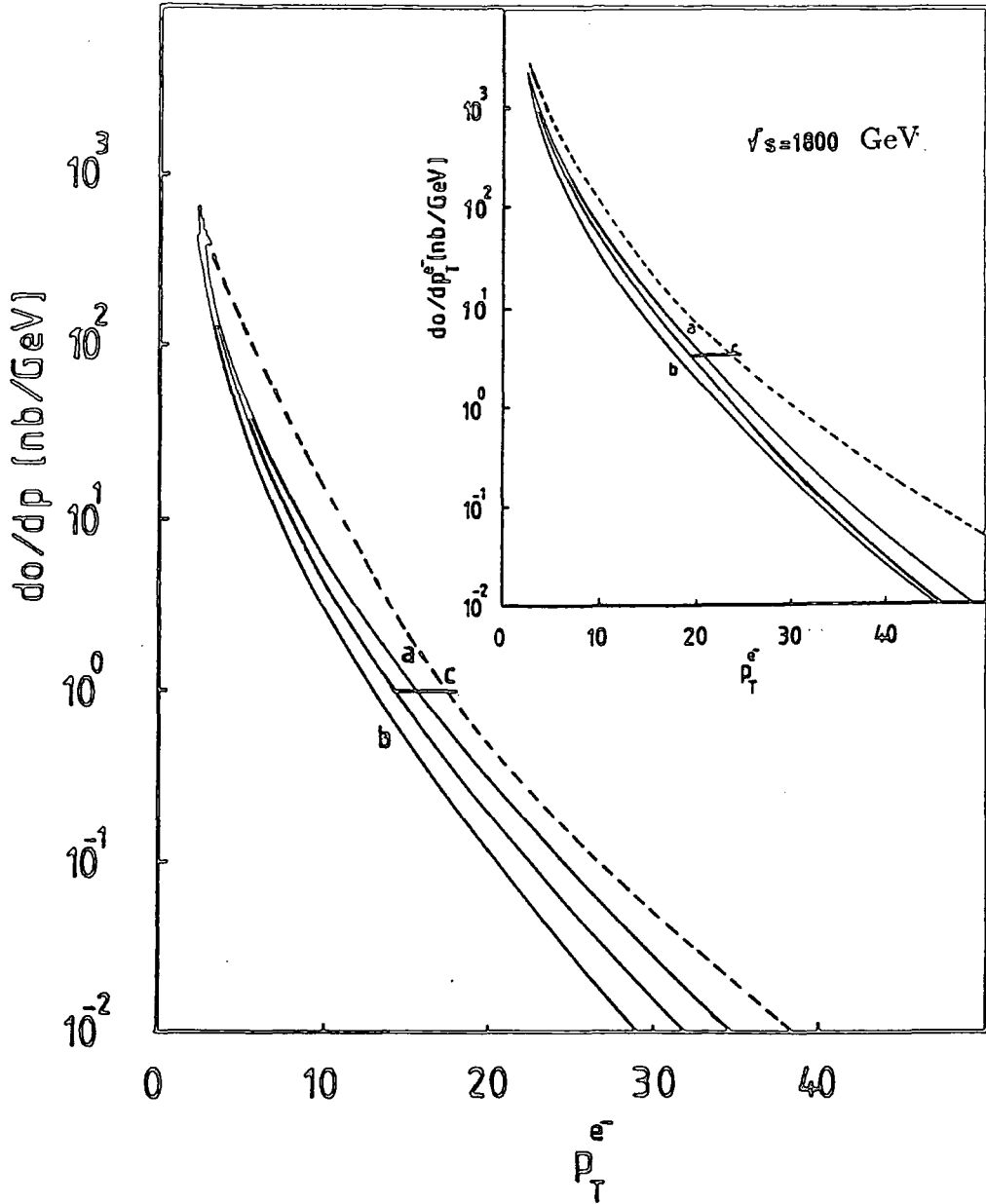
Figure (6.13) *The same as (6.12) for electrons from B mesons.*
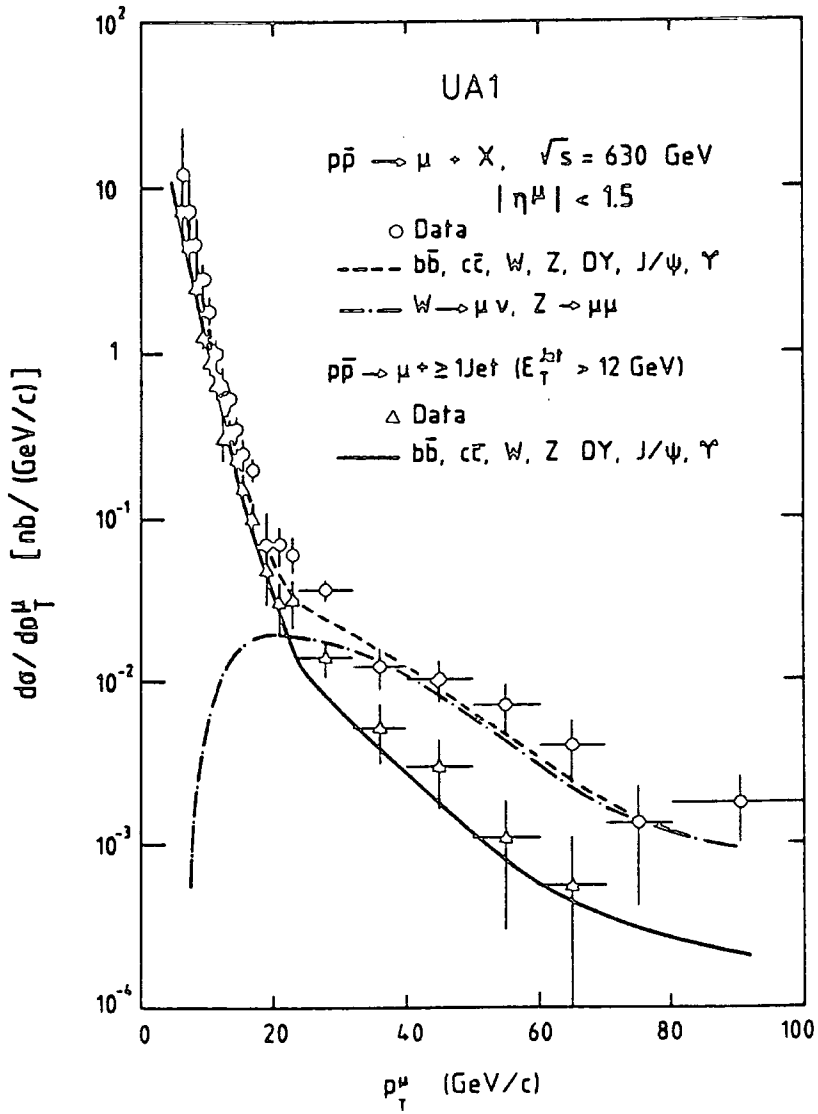
Figure (6.14) *The inclusive muon spectrum for all events and for events with at least one jet with $E_T > 12$ GeV. The curves show the sum of the ISAJET predictions.*

6.6 Top Quark Decay with $m_t > m_W$

A top quark with mass $m_t > m_W + m_b$ will decay into a real W boson and a lighter quark as illustrated in figure (6.15)
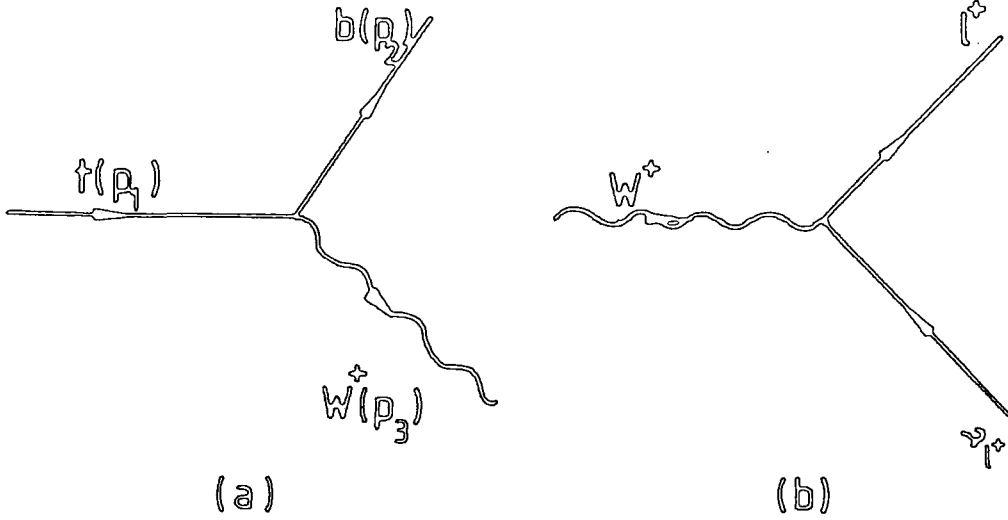
Figure (6.15) *a) Top quark decay into a real W boson and a bottom quark and b) the subsequent decay of W into a lepton and its neutrino. The four momenta are labelled.*

The matrix element for this decay is

$$\mathcal{M} = \frac{g}{2\sqrt{2}} V_{tb} \left\{ \overline{u}(p_2) \gamma^\alpha (1 - \gamma_5) u(p_1) \epsilon_\alpha(p_3) \right\}. \tag{6.21}$$

where g is the coupling constant and V_{tb} is the KM matrix element for top quark to decay into a bottom quark and a W. Using the amplitude (6.21), the total decay width for the diagram (a) in figure (6.15) is found to be [81]

$$\Gamma_t = \frac{G_F m_t^3}{8\pi\sqrt{2}} |V_{tb}|^2 \left(1 - \frac{m_W^2}{m_t^2}\right)^2 \left(1 + \frac{2m_W^2}{m_t^2}\right), \tag{6.22}$$

where

$$G_F = \frac{g^2 \sqrt{2}}{8m_W^2}.$$ (6.23)

Similarly the total decay width for the diagram (b) in the same figure is found to be [82]

$$\Gamma_W = \frac{G_F m_W^3}{6\pi \sqrt{2}}.$$ (6.24)

While the decay of such a top quark into a W boson and a lighter quark is almost certain, for the subsequent W decay into $l\overline{\nu_l}$ we attribute a branching ratio of 10% [83]. Using (6.22) and (6.24) we have obtained the differential cross-section for electron production from T meson decays in $p\overline{p}$ collisions. The results of our calculations are displayed in figures (6.16) and (6.17) for the two different modes of top decay. We have considered the CERN and the FNAL energies and $m_t = 40$, 100 and 150 GeV . The results of applying the different fragmentation models are shown. As the mass of the top quark increases, the Peterson and the Suzuki fragmentation functions approach the form of a delta function at $z = 1$. In these circumstances the only significantly different result comes from the Collins-Spiller model. The result of the Scott model is very different and we do not include it in figure (6.17). We have applied the final result of our calculation in chapter 4 (i.e. $D = 2D_T + D_L$ using (4.19) and (4.20). The effect of such a fragmentation model is to reduce the production rate even further. This is shown in figures (6.16) and (6.17).

6.7 Conclusions

We have applied a perturbative approach to the production of heavy quarks in order to investigate the effect of quark fragmentation on the momentum distribution of heavy mesons and the electrons which are their semileptonic decay products. We chose the so called 'spectator model' to represent the decay of the heavy meson.
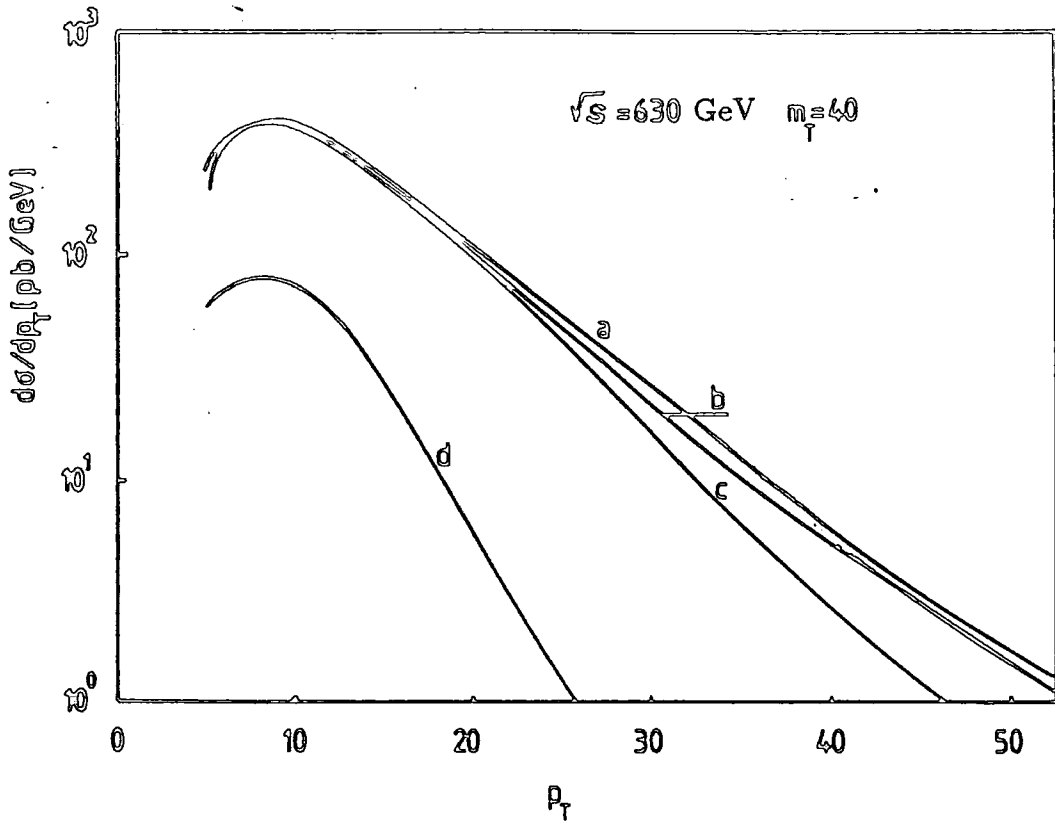
Figure (6.16) *The transverse momentum distribution of electrons from top decay in p$\bar{p}$ collisions (m$_t$ = 40 GeV). a) The spectrum from the top quark, b) the same spectrum from top mesons which fragment according to the Peterson model before decay and c) and d) show the same distributions using the Collins-Spiller and the Scott models respectively.*

For heavy meson production the effect of the different fragmentation models is more or less similar to that of the fragmentation functions given in chapter 3. The Scott and the Collins-Spiller model predict softer spectrums of mesons compared to the Peterson model. A larger population of higher momentum mesons is predicted by the Suzuki and Amiri models. This effect is most pro-
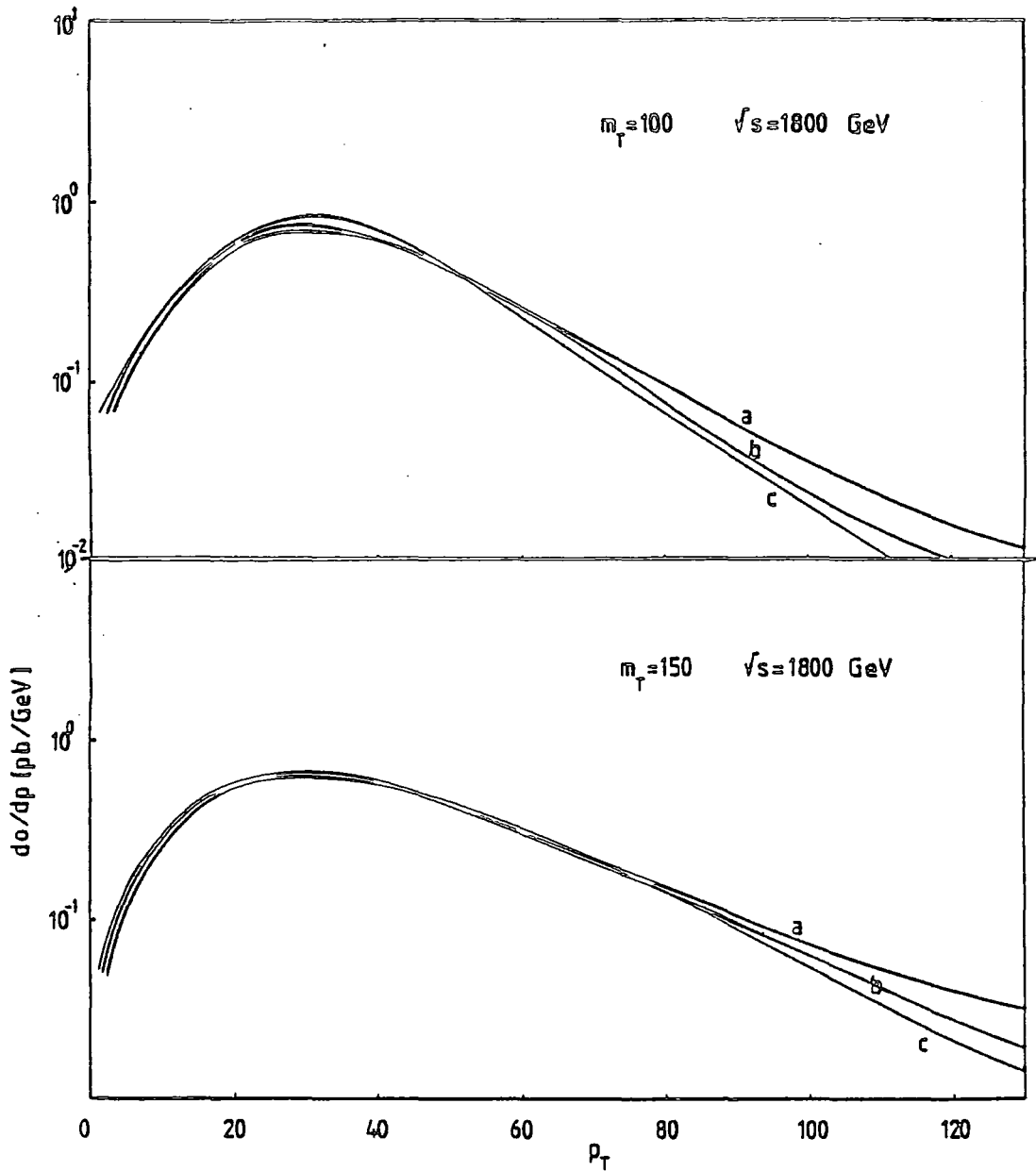
Figure (6.17) *The same as figure (6.15) but for $m_t = 100$ and $m_t = 150$ GeV at $\sqrt{s} = 1800$ GeV. a) and b) show the effect of the Peterson and the Collins-Spiller models and c is due to the model devaloped in chapter 4.*

nounced in the case of top meson production.

Investigations of the effect of quark fragmentation on the electron, and equivalently the muon, momentum distributions through the application of the so called 'collinear approximation' (which proves to be a good approximation at CERN and FNAL energies) show that the regions of momenta for electrons are distinctly different to that of the mesons. This is also clear for the spectrum obtained from D and B mesons. The fragmentation models have the same effect as described above. For the top meson the effect of the Suzuki and the Peterson models approch to a delta function at $z = 1$ and the only significant effect is in the Collins-Spiller model which makes the spectrum softer for large momentum electron production. Although there are no strong theoretical grounds for prefering any of these models, figures (6.16) and (6.17) demonstrate that heavy quark fragmentation may make quite a significant difference to the predicted rate of very high p_T leptons resulting from t decay at hadron colliders. This difference becomes more important in the case of the model which we developed in Chapter 4.

CHAPTER 7

SUMMARY

Our aim in this work has been (a) to study the process of heavy quark fragmentation, to compare some of the present models and present new models to try and improve our understanding of the dynamical details, and (b) to investigate the effect of these models on the momentum spectrum of the final state heavy mesons and the leptons produced by their decays in $p\bar{p}$ collisions in the CERN and FNAL colliders.

1) After summarising our knowledge of confinement, jets and fragmentation, we have put the known fragmentation models into three main categories, the independent jet models, the QCD shower models and the colour string models. We have classified quarks into light and heavy by comparing their mass with the mass scale of strong interactions. Following the early work of Suzuki and Bjorken we have explained how the statistical behaviour of light quark fragmentation changes into a hard process for heavy quarks. The dimensional counting rules are discussed and their importance for heavy quark fragmentation is emphasised.

2) We have considered five models, due to Scott, Peterson, Collins-Spiller, Suzuki and Amiri respectively, in our comparison of heavy quark fragmentation models. We put these models in two classes according to their behaviour with respect to large values of the fragmentation parameter. The models which agree with the dimensional counting rules, $\sim (1 - z)$ i.e. the Scott and Collins-Spiller models, exhibit softer fragmentation than the others which have a harder behaviour $\sim (1 - z)^2$. This difference is quite dramatic for the hypothetical top quark. Although the Peterson model is popular both among theorists and ex-

perimentalists, the Collins-Spiller, Suzuki and the Amiri models try to include more of the dynamical details.

3) To study the spin properties of fragmentation, we repeated the calculations of the Collins-Spiller model for different spin states and so obtain fragmentation functions for the different polarisation states which are consistent with the behaviour of the pion structure function calculated by Gunion et al. The agreement with experimental data for charm and bottom fragmentation looks satisfactory without needing to introduce the idea of secondary fragmentation as in the original model. As required by reciprocity, the transverse fragmentation function behaves like $\sim (1 - z)^2$ as $z \to 1$ while the longitudinal one $\to$ a constant. In fact the latter is an increasing function which takes its maximum value at $z = 1$.

4) For reasonable values of the transverse momentum and the other parameters, the prediction of the phenomenological heavy quark fragmentation models are harder than we expect to observe for charm and bottom fragmentations. There are several reasons for this. One is that not all the D mesons, for example, arise directly from the fragmentation of a charm quark: some of them will be the result of hadronic decays like $D^* \to D\pi$. This is included in the Collins-Spiller model.

The second reason is the possible radiation of gluons by the quark before the hadronisation process. There is experimental evidence of single and double gluon radiation by heavy quarks. By explicit calculation we have evaluated single gluon radiation and obtained its effect on the D meson fragmentation function in the Peterson model.

The third possiblity which may make the fragmentation softer is bound state effects. We have studied them by using a non-relativistic wavefunction,

136

but disregarding the orbital angular momentum of the constituents. The fragmentation functions for different polarisation states are calculated using the wavefunction.

5) We have adopted a perturbative QCD approach to evaluate the consequences of the quark fragmentation on the heavy meson and lepton spectra in $p\bar{p}$ collision experiments. Our calculations are up to order α_s^3 and the total result is evaluated by adding $O(\alpha_s^2)$ and $O(\alpha_s^3)$ contributions. The results of our programs are consistent with the similar results obtained with the ISAJET Monte Carlo.

We have obtained the momentum distribution of the final state mesons by incorporating the required fragmentation functions in the production calculation. It is found that the production rate of a heavy quark and the production rate for a heavy meson may be significantly different at large transverse momenta. In particular the Collins-Spiller and the Scott models give rise to lower production rates. For the top quark the Amiri, Suzuki are similar while the Collins-Spiller and the Scott models still predict a lower rate.

To obtain the spectrum of leptons from semi-leptonic charmed and bottom hadron decays, we adopted the so-called collinear approximation in the quark spectator model. The results are similar to those for mesons but, obviously, the leptons occupy lower momenta regions compared to the mesons. In the case of top quark decay we have distinguished between the cases where the top quark mass is less than or greater than the W boson mass since the mode of the decay changes. Again, soft models like the Collins-Spiller model predict a significant reduction in the large p_T lepton production rate because of the fragmentation.

APPENDIX

Light-Cone Perturbation Theory

One of the most convenient formalisms for processes with large transverse momentum is light-cone quantisation, or its equivalent, time-ordered perturbation theory in the infinite-momentum frame [84]. Defining $P^{\pm} = p^0 \pm p^3$, we can parametrise a particle's momentum as

$$p^{\mu} = (p^+, \ p^-, \ \mathbf{p}_T) = \left(p^+, \ \frac{m^2 + p_T^2}{p^+}, \ \mathbf{p}_T\right)$$

where $p^2 = p^+ p^- - p_T^2 = m^2$. (note that in general we may write the dot product of p and k as $2p.k = (p^+k^- + p^-k^+ - \mathbf{p}_T.\mathbf{k}_T.)$ These variables naturally distinguish between a particle's longitudinal and transverse degrees of freedom and when used in an appropriate frame lead to much simplification. This is particularly true in any analysis of collinear singularities which appear as divergences only in integrations over the transverse momentum, k_T.

For each time ordered graph, the rules of light-cone perturbation theory are the following

(R1) Assign a momentum k_{μ} to each line such that (a) k^+, k_T are conserved at each vertex, and (b) $k^2 = m^2$; i.e. $k_- = (k_T^2 + m^2)/k^+$ and k_{μ} is on mass shell.

(R2) All quanta are forward moving ($k_3 > 0$) in the infinite-momentum frame.

(R3) The gluon-fermion vertices are

$$\frac{\overline{u}(k)}{(k^+)^{1/2}} \gamma^{\mu} \frac{u(l)}{(l^+)^{1/2}}, \qquad \frac{\overline{u}(k)}{(k^+)^{1/2}} \gamma^{\mu} \frac{u(l)}{(l^+)^{1/2}}$$

$$-\frac{\overline{v}(k)}{(k^+)^{1/2}}\gamma^\mu\frac{u(l)}{(l^+)^{1/2}}, \qquad -\frac{\overline{v}(k)}{(k^+)^{1/2}}\gamma^\mu\frac{u(l)}{(l^+)^{1/2}}$$

The factors $1/(k^+)^{1/2}$, $1/(l^+)^{1/2}$ are omited for external fermions in a scattering amplitude.

(R4) For each intermediate state there is a factor

$$\frac{1}{\sum_{inc}k^- - \sum_{inter}k^- + i\epsilon},$$

where the sums in the 'energy denominator' are over the light-cone 'energies,' k^-, of the incident (inc) and intermediate ($inter$) particles.

(R5) Integrate $\int_0^\infty dk^+ \int d^2k_T/16\pi^3$ over each independent k and sum over internal spins and polarisations.

(R6) In amplitudes with an external line off-shell (which have momentum q^μ, $q^2 \neq m^2$), the energy denominator for intermediate states which follow the vertex with the virtual external line are notified by the replacement $\sum_{inc}k^- \longrightarrow \sum_{inc}k^- + q^-$ where the light-cone energy $q^- = (q^2 + q_T^2)/q^+$ is specified by momentum conservation (and not by on-shell kinematics as is usual). This is equivalent to treating the external virtual particles as on-shell particles but with mass q^2 rather than m^2.

(R7) A scattering amplitude involving a bound state wave function ψ is given by

$$T = \int_0^1 [dx] \int_0^\infty \frac{d^2k_T}{16\pi^3}\mathcal{M}\psi(x_i, k_T; p),$$

where $\mathcal{M}$ is the amplitude with the bound state replaced by its constituents.

REFRENCES

1. E. Fermi and C.N. Yang: Phys. Rev. **76**, 1739 (1949)

2. S. Sakata: Prog. Theor. Phys. **16**, 686, (1956)

3. M. Gell-Mann: '*The Eightfold Way; a Theory of Strong Interaction Symmetry*', CIT Rept. CTSL-20, (1961)

4. Y. Ne'emann: Nucl. Phys. **26**, 222, (1961)

5. M. Gell-Mann: Phys. Lett. **8**, 214, (1964)

6. G. Zweig: '*Model of Strong Interaction Symmetry and its Breaking*', CERN Rept. No. 8182/TH401, (1964)

7. See for example P.D.B. Collins and A.D. Martin: *Hadron Interactions*, Adam Hilger 1984

8. S.J. Brodsky and G.R. Farrar: Phys. Rev. Lett. **31**, 1153, (1973)

9. R.D. Field and R.P. Feynman: Nucl. Phys. **B136**, 1 (1978)

10. P. Hoyer *et al.*: Nucl. Phys. **B161**, 349, (1979)

11. A. Ali *et al.*: Phys. Lett. **B93**, 155, (1980)

12. X. Artru and G. Mennessier: Nucl. Phys. **B70**, 93, (1978); X. Artru: Phys. Rep. **97**, 147, (1983)

13. B. Andersson *et al.*: Z. Phys. **C1**, 105, (1979)

14. HRS Collaboration, M. Derrick *et al.*: Phys. Lett. **B158**, 519, (1985); CELLO Collaboration, H.J. Behrend *et al.*: Z. Phys. **C20**, 207, (1983)

15. HRS-collaboration, R. Brandelik *et al.*: Phys.Lett. **B117**, 135, 237 (1985)

16. J.D. Bjorken: Phys. Rev. **D17**, 171, (1977)

17. M. Suzuki: Phys. Lett. **B71**, 139, (1977)

18. See refrences[16] and [17]

19. B. Anderson *et al.*: Phys. Rep. **97**, 33 (1983); Z. Phys C-Particles and

fields 20, 317 (1983)

20. C. Peterson *et al.*: Phys. Rev. D27, 105 (1983)

21. P.C. Rowson *et al.*: Phys. Rev. Lett. 54, 2580 (1985); see also P.C. Rowson, Lawrence Berkely Laboratory, LBL-20463

22. J. Chrin: DESY preprint, DESY 87-040

23. W. Bartel *et al.*: Phys. Lett. B146, 121 (1984).

24. JADE Collab. W.Bartel *et al.*: Phys. Lett. 114, 7 (1987); R. Marshall: Z. Phys. C-Particles and fields 29, 175 (1984); see also Ref. [23].

25. Crystal Ball Collaboration, K. Wachs *et al.*: DESY preprint, DESY 88-111, SLAC-PUB-4691

26. JADE collab. W. Bartel *et al.*: Z. Phys. C-particles and Fields 33, 339 (1987)

27. S. Bethke: Z. Phys. C-particles and Fields 29, 175 (1985)

28. P. Matting: DESY preprint, DESY 88-125 (1988)

29. B. Anderson *et al.* Phys. Rep. 97, 33 (1983); T. Sjostrand: Comp. Phys. Commun. 27, 243 (1982); ibid. 28 229 (1983)

30. TASSO Collab. M. Althoff *et al.*: Z. Phys. C-Particles and Fields 22, 219 (1984)

31. TASSO Collab. M. Althoff *et al.*: Phys. Lett. B146, 443 (1984)

32. MARK-J Collab. B.Adeva *et al.*: Phys. Rev. Lett. 51, 443 (1983)

33. See Ref. [26]

34. NAC Collab. C. Fernandez *et al.*: Phys. Rev. Lett. 50, 2054 (1983)

35. MARK-II Collab. M.E. Nelson *et al.*: Phys. Rev. Lett. 50, 1542 (1983)

36. MARK-II Collab. P.C. Rowson *et al.*: Phys. Rev. Lett. 45 2580 (1985)

37. HRS Collab. P. Keston *et al.*: Phys. Lett. B161, 412 (1985)

38. DELCO Collab. D.E. Koop *et al.*: Phys. Rev. Lett. 52, 970 (1983)

39. TPC Collab. H.Aihara *et al.*: Phys. Rev. D37, 2719 (1985)

40. See Ref. 39 and CLEO Collab. M. Pohl DESY Preprint DESY 84-054 ; HRS Collab. M. Derrik et al. Phys. Lett. 146 261 (1984).; JADE Collab. W. Bartel et al. Phys. Lett. 146B, 121, (1984); H. Aihara *et al.*: Z. Physics C-Particles and Fields 43, 1945 (1986)

41. P. Matting: DESY preprint, DESY 88-125

42. D.M. Scott: Phys. Rev. D18, 210(1978)

43. See Ref. [20]

44. P.D.B. Collins and T.P. Spiller: J. Phys. G: Nucl. Phys 11, 1289-1298 (1985)

45. M. Suzuki: Phys. Rev. D33, 676 (1986)

46. F. Amiri and C.R. Ji: SLAC preprint SLAC-PUB-4023

47. See Ref. [42]

48. P.V. Landshoff and D.M. Scott: Nucl. Phys. B131, 172 (1977)

49. S.J. Brodsky and G.R. Farrar: Phys. Rev. Lett. 31, 1153 (1973)

50. See for example M. Chaichian and N.F. Nelipa: *Introduction to Gauge Field Theories*, Springer-Verlag (1984)

51. JADE collab., W. Bartel *et al.*: Z. Phys. C-Particles and Field 33, 339-349 (1987)

52. V.N. Gribov and L.N. Lipatov: Phys. Lett. B37 78 (1971).

53. J.F. Gunion and W. Frazer: Phys. Rev. D20, 147, (1979).

54. P.D.B. Collins and T.P. Spiller: DTP/84/26

55. J.F. Gunion *et al.*: Phys. Rev. 29, 2491 (1984)

56. See for example P.D.B. Collins: *Introduction to Regge Theory and High Energy Physics* , Cambrige University Press (1977)

57. T.P. Spiller: Ph.D. Thesis, University of Durham (1984)

58. J.D. Bjorken *et al.*: Phys. Rev. D3 1382 (1971)

59. J. Brodsky and C.R. Ji: Phys. Rev. Lett. 55, 2257 (1985)

60. F. Amiri and B.C. Harms: Phys. Rev. D32, 2982 (1985)

61. See for example Ref.[59]

62. E. Eichten *et al.*: Rev. Mod. Phys. 56 (1984) 579

63. F. Halzen and P.Hoyer: Phys. Lett. B154 (1985) 324; V.Barger and R.J.N. Phillips: Phys. Rev. D31 (1985) 215; G. Koepp, J.H. Kuhn and P.M. Zerwas: Phys. Lett. 153B (1985) 315;A. Ali and G. Ingelman: Phys. Lett. 156 (1985) 111; E.W.N. Glover, K. Hagiwara and A.D. Martin: Phys. Lett. 168 (1986) 289, F. Halzen: Proc. 21st Int. Conf. on High Energy Physics, Paris, France (1982)

64. F. Halzen: Proc. 21st Int. Conf. on High Energy Physics, Paris, France (1982)

65. R.K. Ellis and J.C. Sexton: Nucl.Phys. 269 (1986)

66. See Ref. 62.

67. A. Ali: Nucl. Phys. 292 (1987) 1-58

68. M. Kobayashi and T. Moskawa: Prog. Theor. Phys. 49, 652, (1973)

69. Stanley Wojcicki in Proceeding of the Twelfth SLAC Summer Institute on Particle Physics, SLAC-Report 281, edited by Patrica M. McDonough, Stanford CA,175 (1984)

70. G. Altarelli *et al.*: Nucl. Phys. B208 (1982) 381

71. See for example Cruystal Ball Collab.: DESY Preprint, DESY-88-111, SLAC-PUB-4691 (1988); JADE Collab.: Z. Phys. C-Particles and Fields 33-349 (1987); JADE Collab.: DESY Preprint, DESY 86-129 (1986)

72. TASSO Collab., M. Althoff *et al.*: Phys. Lett. B146 443 (1984)

73. CELLO Collab. H.J. Behrend *et al.*: Z. Phys. C- Particles and Fields

19, 291 (1983)

74. N. Lockyer: 'Proceedings of the 11th SLAC Summer Institute on Particle Physics', Stanford, Californa, (1983); SLAC Report No. 267 p.689, SLAC-3245 (1983)

75. TPC Collab., H. Aihara : Z. Phys. C 27 (1985) 39

76. CLEO Collab. K. Chadwick *et al.*, Phys. Rev. D27 (1983) 475

77. MARK III Collab., R.M. Baltrusaitis *et al.* Phys. Rev, Lett. 54 (1985) 1976

78. CUBS Collab., C. Klopfenstein *et al.* Phys. Lett. 130 (1983) 444

79. See for example Ref. [63]

80. UA1 Collaboration: Z. Phys. C 37 (1985) 489-503.

81. V.D. Barger and R.J.N. Phillips: *'Collider Physics'*, Addison-Wesley Publishing Company(1987)

82. F. Mandl and G. Shaw: *'Quantum Field Theory'*, John Wiley and Sons(1984)

83. See for example Ref. [81]

84. See especially J.B. Kogut and D.E. Soper, Phys. Rev. D1, 2901 (1970), and J.B. Bjorken, J.B. Kogut, and D.E. Soper, *ibid.* 1382 (1971). For earlier references and developments see S. Weinberg, Phys. Rev. 150, 1313 (1966); L. Susskind and H. Frye, *ibid.* 165, 1535 (1968); S.D. Drell, D. Levy and T.M. Yan, it ibid. 187, 2159 (1969): Phys. Rev. D1, 1617 (1970); 1, 1035 (1970). Renormalisation is discussed in S.J. Brodsky, R. Roskies and R.S. Suoya, Phys. Rev. D8, 4574 (1973).